UNIVERSITY OF CALIFORNIA, SAN DIEGO

The sclerochronology of *Donax gouldii* and *Chione undatella*: Environmental archives of the past and present Southern California Bight

A dissertation submitted in partial satisfaction of the
requirements for the degree Doctor of Philosophy

in

Oceanography

by

Marco B.A. Hatch

Committee in Charge:

Professor Paul K. Dayton, Chair
Professor Christopher D. Charles
Professor David M. Checkley, Jr.
Professor Richard D. Norris
Professor Stephen A. Schellenberg
Professor David S. Woodruff

2012

The Dissertation of Marco B.A. Hatch is approved, and it is acceptable in quality and in form for publication on microfilm and electronically:

Chair

University of California, San Diego

2012

DEDICATION

This dissertation is dedicated to my long time friends and mentors, Ken Hansen and Russel Barsh. I owe my success to involvement in hands-on research as part of a program created by Ken and Russel to increase Native American representation in natural sciences. I hope to honor their vision throughout my career. Hy'Shqa dear friends.

TABLE OF CONTENTS

LIST OF FIGURES

Chapter 2

Chapter 3

Chapter 4

Chapter 5

LIST OF TABLES

Chapter 3

Chapter 5

ACKNOWLEDGMENT

Be well do good work and keep in touch.

Garrison Keillor

Many people have contributed to the successful completion of my dissertation and the text that follows is my feeble attempt to thank them. My thanks will begin with my thesis advisor, Dr. Paul Dayton. One of the most important lessons Paul has imparted is, that like art, good science requires creativity, dedication, and unwavering dedication to the craft. However, unlike art, good science comes from joy. This is not to say all aspects of science are fun, but to say that to do good work you need to be fascinated with nature and be driven by the desire to learn from nature.

The rest of my committee also deserves thanks for their patience, dedication, and support. Dr. Stephen Schellenberg provided a second home to me and devoted an enormous amount of time to better this research. His mentorship provided a window into balancing professional and personal life. Thank you for opening your lab and home to me. Dr. David Checkley taught me to think about the ocean from a mechanistic stand point, to explain phenomena from first principles. His guidance had led me to realize how variable marine systems are and how understanding this variability is the most fundamental question in marine ecology. Dr. Chris Charles has offered unwavering support during my foray into stable isotopes, without his guidance I surely would have been lost. Dr. Richard Norris provided constant support and teaching me about the geology of the Southwest and Baja. Thank you, Dr. David Woodruff for having a clear vision of the issues at hand and providing a navigable path through tumultuous waters.

There are many past mentors who helped shape me a scientist and guided me down this path. I would truly not be here if it were not for Dr. Russel Barsh and Chairman Ken Hansen. Russel and Ken had a vision to create an environmental research center staffed by Native Americans, pursuing research important to Native people. I cannot express how grateful I am that they took a chance on a college flunky waiter and turned me into a thoughtful marine scientist. Dr. Sandy Wyllie-Echeverria was one the first true blue marine ecologists I met and through my career at UW he made sure I always had a small research project and he insisted that I attend and present at a number of conferences. Dr. Kerry Naish took me under her wing during my second quarter at UW, her guidance and mentorship is what pushed me toward pursuing a PhD.

To my fellow Ritter 330 occupants over the years, thank you Tonya Huff for initiating me into the Dayton and thank you for the continued support with course development. Miriam Goldstein, thanks for great discussions and founding the Friday lab meeting. Damien Cie has been huge help getting me ready of the professional world and has been very accommodating as I have expanded to 75% of the office.

A very special thanks to the entire 2005 Biological Oceanography cohort, you are what makes Scripps the special place that it is. I look forward to maintaining our bond formed from countless hours studying and playing together. To Andrew Thurber, Geoff Cook, Talina Konotchick, Megan McKenna, and Elizabeth Henderson thank you for all the fond memories.

To my parents for taking me outside, I don't know where I would be if it were not for enumerable camping trips, the most memorable of which were to Hoods Canal and the San Juan Islands. To my father, Mike, for teaching me that I don't want to dig ditches for a living, and that no matter how bad things seen at work it beats digging ditches. For teaching me that

to succeed you need to take risks, you need to bite off more than you can chew and then finish the job. To my mother, Lisa, thank you for your continuous love and support.

To my loving partner, Renee, thank you for your support over the past seven years from the moment I let you know that I had to pack my bags and head to San Diego while you were still in Seattle planning our wedding and selling our home to your recent round the clock support, you have been a pillar of support bearing immeasurable weight. To Marin, I know I have not been around the last few weeks but know that if we only saw each other for a few minutes a day it was the highlight of my day and what kept me going.

Finally, the research presented in this dissertation was made possible by funding provided by National Science Foundation Pre-Doctoral Research Fellowship, Ford Foundation, National Science Foundation IGERT, Eugene Cota-Robles Fellowship, Summan Fellowship, Moore Fellowship, Mia Tegner Research Grant and the generous donations by Russ and Eloise Duff, who also brought me into their home and treated my like family.

A special thanks to Old King Neptune for providing the waves in this dissertation.

Chapter 2, in full, is currently being prepared for submission for publication of the material, Hatch, Marco B.A, Schellenberg, S.A. The dissertation author was the primary investigator and author of this material.

Chapter 3, in full, is a reprint of the material as it appears in Palaeogeography, Palaeoclimatology, Palaeoecology 2012. Hatch, Marco B.A, Schellenberg, S.A., Carter, M.L. The dissertation author was the primary investigator and author of this paper.

Chapter 4, in part, is currently being prepared for submission for publication of the material. Hatch, Marco B.A. The dissertation author was the primary investigator and author of this paper.

Chapter 5, in part, is currently being prepared for submission for publication of the material. Hatch, Marco B.A. The dissertation author was the primary investigator and author of this paper.

VITA

2005 Bachelor of Science Magna Cum Laude, University of Washington, Seattle, WA

2007 Master of Science, University of California, San Diego

2012 Doctor of Philosophy, University of California, San Diego

PUBLICATIONS

Hatch, M.B.A., S.A. Schellenberg, M. Carter. 2012 Utilization cross-dated sub-annul growth increments to date Ba/Ca variations in the modern intertidal bean clam *Donax gouldii*. Palaeogeography, Palaeoclimatology, Palaeoecology.

Winter, R.N, M.B.A. Hatch, 2010. Investigating the parasitism of Southern California bean clams (*Donax gouldii*) by the trematode *Postmonorchis donacis*. Bulletin: Southern California Academy of Sciences. 109(3) 144-152

Braje, T.J., J.M. Erlandson, T.C. Rick, P.K. Dayton, M.B.A. Hatch. 2009. Fishing from Past to Present: Continuity and Resilience of Red Abalone Fisheries on the Channel Islands, California. *Ecological Applications*. 19(4)906-919.

.

ABSTRACT OF THE DISSERTATION

The sclerochronology of *Donax gouldii* and *Chione undatella*:

Environmental archives of the past and present Southern California Bight

by

Marco B.A. Hatch

Doctor of Philosophy in Oceanography

University of California, San Diego, 2012

Professor Paul K. Dayton, Chair

High resolution archives of environmental conditions determined from the chemistry and growth increments of bivalves provide a unique opportunity to examine relationships between climate-induced environmental change and biological productivity in the Southern California Bight. However, before bivalves can be used as high resolution biorecorders of environmental change, the record of interest (e.g. $\delta^{18}O$, $\delta^{13}C$, Sr/Ca, Ba/Ca or growth increments) must first be calibrated to known environmental conditions. For *Donax gouldii*

this was accomplished by comparing $\delta^{18}O$, $\delta^{13}C$ and Sr/Ca to well-constrained environmental records. *D. gouldii* Ba/Ca was investigated by assigning an exact date to each laser ablation Ba/Ca determination by cross-dating tidal growth increments and then comparing the dated Ba/Ca values to local biological and physical parameters. The timing of growth increments and temperature of thermally induced growth shut down in *Chione undatella* was determined by a mark-recapture study. To obtain historic context, *C. undatella* from over 6,000 years were analyzed for growth, age, and size at harvest. Calibrations of *D. gouldii* provide the context necessary to utilize *D. gouldii* as a paleothermometer and Ba/Ca may have utility as an upwelling indictor. Additionally, the technique of cross-dating was applied to tidal growth increments, providing a new level of accuracy to shell dating. *C. undatella* have a lower thermal limit for growth of 17 °C and form winter growth increments with decreasing growth with age. Archaeological *C. undatella* show a remarkably stable growth rate and size at harvest through the Middle and Late Holocene. This research presents a greater understanding of how environmental variables are recorded in bivalves and the utility of these proxies for paleoecological and paleoclimite studies.

CHAPTER 1

1. Introduction

"*The purpura [a gastropod in the Mediterranean Sea] lives about six years, and every year its growth is clearly observable from the intervals in the shell of the spiral*" Aristotle (translation by Peck, 1968)

A major barrier to implementing marine conservation is forming a consensus that marine populations have been negatively impacted by human activity. Given that individual perception of ecosystem state is often limited to personal experience, a true baseline must be found to evaluate the current status marine ecosystems. The limitation of personal experience to evaluate the true state of marine populations relative to virgin conditions is known as the shifting baselines syndrome (Pauly 1995). The shifting baseline syndrome has arisen because each generation of fishers and fishery scientists sets their baseline of what a system should look like and how much productively they expect from that system to their first experience with that system. As generations and generations of scientists and fishers have been working in a system slowing declining, each generation expects less and less from that system and over time the true baseline – the true potential – for these systems has been lost from view. One striking example of lowered expectation from shifting baselines syndrome is the reduction in size of catch in recreational charter boats in

Key West, Florida (McClenachan 2009). By analyzing charter boat catch photos from over 50 years at the exact same location a massive, previously unrecognized, reduction in catch was found (McClenachan 2009).

1.1. Climate variability

While the identification of shifted baselines helps create a holistic picture of historic environmental change, identification alone is not sufficient to mechanistically understand how marine populations have changed. Fishing is an often visible impact on the marine organisms but the effects of climate, habitat loss, changes in productivity, and reductions in carrying capacity must also be considered. Separating the intertwined impacts of climate variability, habitat alteration, and fishing is one the great challenges in marine management. The sardine collapse of 1940s left fishery managers confounded about the contribution of fishing and climate variability to the dramatic decline of sardine population off the American West Coast. To understand what led to the sardine collapse and how to avoid future such collapse the California Cooperative Oceanic Fisheries Investigations (CalCOFI) was formed, bridging multiple disciplines to better understand how physical oceanography and climate related to biological productivity in the Eastern Pacific. One paradigm-altering discovery from this consortium was at times the inverse productivity of sardine and anchovies for nearly two thousand years (Baumgartner et al 1992). Based on anchovy and sardine scales in sediment cores from the anoxic Santa Barbara basin it was found that one species would dominate for 60 years while the other remained low, and then the dominance would flip, all in the absence of commercial fishing (Baumgartner et al 1992).

1.2. Archaeological contributions to ecology

Archaeological mollusks from coastal shell middens can be used as a window into the past providing information on the productivity and resilience of marine ecosystems. Abalone, *Haliotis* spp., have a long and complex history of human harvest in California. Throughout the Holocene, Native Americans harvested abalone for food and used the shells for a variety of purposes. During the early explorer and fur trader time periods the two major abalone predators, otters and Native Americans, were removed the system. Native American populations were depressed from diseases and otters were effectively removed from the system through hunting, leaving abalone without its two major predators. During this period black abalone (*Haliotis cracherodii*) grew to sizes not seen in 10,000 years of archaeological records (Braje and Erlandson 2007). To determine resilience of red abalone populations in the northern Channel Islands, Braje et al. (2009) compared the percentage of red abalone (*H. rufescens)* in shell middens to commercial harvest. Braje et al. (2009) found that catches have been highest at San Miguel Island for the past 8,000 years. The modern implication of these data is that despite all of the climate variability in the past 8,000 years, San Miguel has always had higher populations of red abalone and it would be expected that this population would recover first.

In modern and ancient marine, estuary and freshwater systems mollusk shells have been used as recorders of environmental and climate change. For more

than seventy years growth increments and shell chemistry has been used as archives of past environmental conditions (Davenport 1938; Epstein et al. 1953; Clark 1968). Mollusks calcify shells through an incremental process, resulting in growth bands. Because these growth rates are influenced by environmental variables, temperature, food, oxygen levels, and other variables (Dettman et al. 2004; Schöne et al. 2006), variation in growth increments can provide information about past environments. This approach is particularly useful when paired with geochemical analysis.

However, while these proxies can be extremely useful, they must first be calibrated in modern systems due to species and location-specific differences in growth increment formation and shell chemistry – environmental relationships. For example the timing of "winter" annual bands can vary depending on where the species is in its range. For example species with a wide biogeographic range such as *Chione undatella* may produce an annual band when temperature drops below its growth threshold in the winter in cooler regions and in warmer regions it may produce an annual band during the summer when temperature are above its threshold. Also, in areas of large temperature ranges bivalves can produce two "winter" bands, such as in the northern Gulf of California where *Chione cortezi* produces both a winter and summer band (Goodwin et al. 2001). This plasticity necessitates verification of the periodicity and season of growth increment formation

If higher frequency growth increments are used to estimate bivalve year class, then the periodicity of increment formation also requires verification. Intertidal mollusks often form a growth increment when exposed at low tide, but the

frequency of growth formation may depend on the tidal position of the organism, tidal height, type of tide and tidal cycle. Other bivalves follow a solar periodicity, such as the giant clam (*Tridacna gigas*) with photosynthetic symbionts.

Once the periodicity of growth increments has been verified error must not be introduced in counting the often hard-to-delineate growth increments, particularly when working with large numbers of increments. Provided there is temporal overlap between specimens, then growth increments can be cross-dated. Cross-dating is a technique widely used in dendrochronology with allows growth increments between samples to be statistically correlated into a common time-series. This not only greatly increases the accuracy of date assignment to individual growth increments but also reduces error in growth increment – environmental correlations.

1.3. Shell Chemistry

Shell chemistry has been used as a proxy for a variety of biological and physical variables, often with a specific shell-environmental relationship changing between species and location. For example, Ba/Ca has been reported to be a proxy for salinity, temperature, diatoms, and upwelling (Gillikin et al. 2006). The relationship between Mg/Ca and temperature has also been shown to vary between species of the genus. Stable oxygen isotopes are the mostly widely used temperature proxy in carbonates however, the exact thermo-dynamic relationship between seawater and shell oxygen isotopes vary between taxon.

In this thesis, I explore the utility and reliability of using bivalves as environmental records to further our understanding climate-driven biological

variability in the Southern California Bight. In Chapter 2, the $\delta^{13}C$, $\delta^{18}O$ and elemental (Sr/Ca) variations in *Donax gouldii* are evaluated as environmental proxies. Chapter 3 brings new data to the complicated relationship of Ba/Ca to environmental variables through the technique of cross-dating and utilizing phytoplankton community data. In Chapter 4 the growth increments and thermal tolerances of *Chione undatella* is quantified. Chapter 5 utilizes 6,000 years of *C. undatella* growth rates to investigate environmental change.

Dissertation Outline

Chapter 2: Assessing the reliability of intraskeletal stable-isotopic ($\delta^{13}C$ and $\delta^{18}O$) and elemental (Sr/Ca) variations within the intertidal bivalve *Donax gouldii* as an environmental proxy

In chapter 2, I test the relationships between *D. gouldii* shell chemistry and environmental variables with the goal quantifying the utility of *D. gouldii* proxies for palaeoecological research. A statistical model is used with a variety to environmental data including seawater and weather variables to best describe the observed patterns in *D. gouldii* shell chemistry.

Aims and Objectives

2.1 To determine and variables and conditions that best predict *D. gouldii* shell $\delta^{13}C$, $\delta^{18}O$ and Sr/Ca

2.2 To evaluate shell chemistry variability in the light of micro-habitat variability

Hypotheses

2.1 *D. gouldii* shell $\delta^{18}O$ is statistically dependant on seawater $\delta^{18}O$ and seawater temperature

2.2 *D. gouldii* shell $\delta^{13}C$ remains enigmatic

2.3 *D. gouldii* Sr/Ca is most related to growth rate or ontogenetic effects

Chapter 3: Ba/Ca variations in the modern intertidal bean clam *Donax gouldii*: An upwelling proxy?

In Chapter 3, I utilize the dendrochronology tool of cross-dating to date daily growth increments of *D. gouldii*, and then relate laser ablation-determined Ba/Ca to environmental parameters. This research questions widely accepted assumptions on the drivers of shell Ba/Ca and presents an important examples why high frequency local phytoplankton counts are needed to determine if phytoplankton blooms are reflected in shell chemistry.

Aims and Objectives

3.1 To determine if daily growth increments can be cross-dated

3.2 Evaluate the relationship between peak Ba/Ca and environmental conditions

Hypotheses

3.1 Once dated, laser ablation determined Ba/Ca will show a common population level peak

3.2 Chlorophyll *a* and diatom abundance will not be related

3.3 Ba/Ca peaks will be related to seawater barium concentrations

Chapter 4: Growth increment formation and minimum temperature threshold in *Chione undatella*

In Chapter 4, I complete a mark capture study with *C. undatella* to determine frequency of growth increment formation and temperature related growth shutdown.

Aims and Objectives

4.1 To determine season of increment formation

4.2 To determine thermal shutdown

Hypotheses

4.1 *C. undatella* have winter shutdown

4.2 *C. undatella* will have a lower shutdown temperature but not an upper

Chapter 5: Age and growth of archaeological *Chione undatella* from a Southern California Lagoon

Chapter 5 explores the growth rate, age and size at harvest of *C. undatella* collected from 6,000 years and uses the results to evaluate ancient climate variability. This research provides a new framework to interpret archaeological hypothesis.

Aims and Objectives

5.1 Determine the size distributions of harvested *C. undatella* from archaeological shell middens

5.2 Use the growth rate and age at harvest of *C. undatella* as proxies for environmental variation

Hypotheses

5.1 Are the environmental and social changes reported by archaeologist reflected in the growth rate and size of harvested *C. undatella*?

5.2 Do the observed changes in total *Chione* shell occur with changes in *C. udatella* growth rates?

References

Baumgartner, T. R., Soutar, A., and Ferreira-Bartrina V. (1992) Reconstruction of the history of Pacific sardine and Northern Pacific anchovy populations over the past two millennia from sediments of the Santa Barbara basin. CalCOFI Report, 33: 24-40.

Davenport CB (1938) Growth lines in fossil pectens as indicators of past climates. J Paleontol 12:514–515

Peck, A.L. 1968: *De partibus animalium* (English and Greek). Harvard: Harvard University Press.

Braje TJ, Erlandson JM (2007) Measuring subsistence specialization: Comparing historic and prehistoric abalone middens on San Miguel Island, California. Journal of Anthropological Archaeology **26**:474-485

Braje TJ, Erlandson JM, Rick TC, Dayton PK, Hatch MBA (2009) Fishing from past to present: continuity and resilience of red abalone fisheries on the Channel Islands, California. Ecological Applications **19**:906-919

Clark GR, II (1968) Mollusk Shell: Daily Growth Lines. Science **161**:800-802

Dettman DL, Flessa KW, Roopnarine PD, Schöne BR, Goodwin DH (2004) The use of oxygen isotope variation in shells of estuarine mollusks as a quantitative

record of seasonal and annual Colorado river discharge. Geochimica et Cosmochimica Acta **68**:1253-1263

Epstein S, Buchsbaum R, Lowenstam HA, Urey HC (1953) Revised Carbonate-Water Isotopic Temperature Scale. Geological Society of America Bulletin **64**:1315-1326

Gillikin DP, Dehairs F, Lorrain A, Steenmans D, Baeyens W, André L (2006) Barium uptake into the shells of the common mussel (*Mytilus edulis*) and the potential for estuarine paleo-chemistry reconstruction. Geochimica et Cosmochimica Acta **70**:395-407

Goodwin DH, Flessa KW, Schone BR, Dettman DL (2001) Cross-Calibration of Daily Growth Increments, Stable Isotope Variation, and Temperature in the Gulf of California Bivalve Mollusk *Chione cortezi*: Implications for Paleoenvironmental Analysis. Palaios **16**:387-398

McClenachan L (2009) Documenting Loss of Large Trophy Fish from the Florida Keys with Historical Photographs

Documentación de la Pérdida de Peces de Trofeo en los Cayos de Florida con Fotografías Históricas. Conservation Biology **23**:636-643

Pauly D (1995) Anecdotes and the shifting baseline syndrome of fisheries. Trends in Ecology and Evolution **10**:430

Schöne BR, Rodland DL, Fiebig J, Oschmann W, Goodwin D, Flessa KW, Dettman D (2006) Reliability of multitaxon, multiproxy reconstructions of environmental conditions from accretionary biogenic skeletons. J Geol **114**:267-285

CHAPTER 2

Assessing the reliability of intraskeletal stable-isotopic ($\delta^{13}C$ and $\delta^{18}O$) and elemental (Sr/Ca) variations within the intertidal bivalve *Donax gouldii* as an environmental proxy

Marco B.A. Hatch[1], Stephen A. Schellenberg[2],

[1]Scripps Institution of Oceanography, University of California, San Diego,

La Jolla, California 92093-0208 USA

[2] Department of Geological Sciences, San Diego State University,

San Diego, California 92182-1020 USA

Abstract

The bean clam, *Donax gouldii*, is a common intertidal bivalve mollusk found in sandy beaches from Point Conception USA to Acapulco Mexico and lives to a maximum age of three years (length <25 mm). The distinct growth bands and narrow intertidal distribution of this bivalve could provide an ideal bio-recorder of high frequency environmental variability provided that shell $\delta^{18}O$, $\delta^{13}C$, and Sr/Ca are strongly correlated with ambient environmental conditions. To assess the relationship between environmental variables and shell chemistry, stepwise forward regressions were used with environmental variables related to ambient seawater (i.e., $\delta^{18}O_{SW}$, $\delta^{13}C_{DIC}$, salinity, temperature), weather (i.e., air temperature, solar radiation, wind speed), tides (% submergence at tidal levels 0.3, 0.2, 0.1 MLLW) and specimen size. A *D. gouldii* specific paleotemperature equation was created based on $\delta^{18}O_{SW}$ and seawater temperature. $\delta^{13}C_{Donax}$ was significantly related to shell size and air temperature. $\delta^{13}C_{Donax}$ was not significantly related to seawater $\delta^{13}C_{DIC}$ ($p>0.36$). Sr/Ca was only significantly related to shell size with a low goodness of fit ($r^2=0.19$). To evaluate potential ontogenic controls on Sr/Ca, umbo-to-commissure profiles of Sr/Ca were created by LA-ICP-MS. These data show maximal Sr/Ca values near the umbo, suggesting ontogenetic or calcification-rate control.. These data highlight the need to calibrate chemical variations in biogenic carbonate to known ambient environmental conditions as the relationship between $\delta^{18}O_{carbonate}$ and Sr/Ca to temperature and $\delta^{13}C_{carbonate}$ to $\delta^{13}C_{DIC}$ have been shown to be variable between species and locations.

1. Introduction

Paleoclimate records are a primary means for discriminating natural variability within the climate system from the effects of anthropogenic forcing. Faced with relatively short instrumental records, especially for the oceans, natural archives (e.g., corals, sclerosponges, forams, and mollusks) have been examined through various proxies (e.g., growth banding, stable isotopes, elemental ratios) to reconstruct ambient environmental conditions (e.g., temperature, salinity, upwelling) (Cobb et al. 2003; Rosenheim et al. 2005b; Field et al. 2006; Black et al. 2009). Oxygen isotopic ($\delta^{18}O$) variations within the shell carbonate of mollusks, particularly bivalves, have been used extensively to reconstruct coastal temperatures (Carre et al. 2005; Jones et al. 2005), but this proxy suffers from its dual sensitivity to the ambient temperature and oxygen isotopic value of seawater ($\delta^{18}O_{SW}$) (Epstein et al. 1953a), where the latter can vary due to global (i.e., ice volume) and local (i.e., evaporation and precipitation) factors and is often poorly constrained for paleoclimate studies. To circumvent this problem, $\delta^{18}O$-independent elemental-ratio-based temperature proxies, such as Mg/Ca in calcite and Sr/Ca in aragonite (Klein et al. 1996; Sosdian et al. 2006), have been developed and often paired with specimen $\delta^{18}O$ variations to constrain past $\delta^{18}O_{SW}$ values. However, many studies have determined that elemental ratios can be sensitive to additional temperature-dependent or -independent factors (e.g., metabolic processes, calcification rates, intertidal exposure, specimen age) (Weber 1972; de Villiers et al. 1994; de Villiers et al. 1995; Purton et al. 1999; Surge and Walker 2006). Such

complexities highlight the need for species-specific calibration studies to assess the scalability and universality of such isotopic- and elemental-based proxies.

In addition to ambient temperature, proxies for coastal upwelling have been developed to provide an environmental context for observed variations in ecological data ranging from intraspecific population demographics to paleocommunity assemblage changes (Dietl and Flessa 2011). Such upwelling proxies are necessary to create a more complete context for understanding both paleoclimate and paleoecology. For example, the carbon isotopic composition of dissolved inorganic carbon ($\delta^{13}C_{DIC}$) often decreases precipitously within a upper few hundred meters of the ocean as a result of the sinking and remineralization of isotopically-light organic matter from the euphotic zone (Kroopnick et al. 1970). This nutrient-like profile for $\delta^{13}C_{DIC}$, coupled with the assumption that ambient $\delta^{13}C_{DIC}$ is reflected in shell $\delta^{13}C_{carbonate}$, led researchers to interpret relative minima in shallow marine shell $\delta^{13}C_{carbonate}$ as a proxy for upwelling (Killingley and Berger 1979). However, additional controls on $\delta^{13}C_{carbonate}$ often exist, such as temperature (Grossman and Ku 1986), kinetics (McConnaughey 1989a), and metabolism and reproduction (McConnaughey 1989b).

Given the above potentials and complexities, this field-based study assesses the utility of isotopic ($\delta^{18}O$ and $\delta^{13}C$) and elemental (Sr/Ca) variations within the aragonitic shells of *Donax gouldii* as proxies for sea surface temperature (SST) and upwelling. *D. gouldii* is a relatively small (< 25mm) and short-lived (< 3 years) bivalve that inhabits the surf zone of sandy open coast beaches from Point Conception, California to Acapulco, Mexico (Coe 1955). The species is an ideal candidate for such

assessment given its distinct tidal growth bands (Hatch et al. *in press*), narrow sub- to intertidal habitat, and prevalence within late Holocene Native American middens as well as wave-cut terrace deposits from oxygen isotope stages 5a (~85 ka) and 5e (~125 ka) (Valentine 1960; Gallegos 2002). The purpose of this study is to independently test environmental-shell chemistry relationships in *D. gouldii* and assess the use of these correlations for paleo-climate studies.

2. Methods and Location

2.1. Oceanographic context

The Southern California Bight is typified as a seasonally stratified oceanographic regime with Ekman-transport-driven upwelling delivering dissolved nutrients from below the mixed layer. While such upwelling relates to productivity in many nearshore systems, it is not the major source of physical forcing of primary production for the waters surrounding the Scripps Institution of Oceanography (SIO) Pier based on the poor correlation between chlorophyll and an index of upwelling (Bakun Index, (Bakun 1973)), SST and salinity (Kim et al. 2009). Given the *a priori* knowledge that offshore buoy or satellite measurements are not a substitute for local records all physical and biological records come from SIO pier which was < 100m from were *D. gouldii* were collected.

2.2. D. gouldii collection

Every two weeks during lower low tides (<0.2 m mean lower low water (MLLW)) from August 2007 to September 2008 (n=27), 10-15 *D. gouldii* were haphazardly collected from the Scripps Coastal Reserve (<100 m from SIO pier)

(Figure 2.1). Unlike other species of this genus, *D. gouldii* does not migrate with the tide, and their greatest local population densities consistently occur within 0.1-0.3 m MLLW at the sand surface (Morris et al. 1980; Ellers 1995).

Collected *D. gouldii* were euthanized, cleaned, rinsed in deionized water, and dried in a 30 °C oven. Strongly modal size-distributions throughout the study allowed each specimen to be assigned to one of three cohorts (A, B, or C) based on their anterior-posterior valve length (Figure 2.2). Cohort A specimens (n=7) were relatively large and occurred in sample populations at the start of the study (i.e., August 2007). Cohort B specimens (n=123) persisted throughout the study and showed a general size increase from Fall 2007 through Spring 2008 followed by relatively stable sizes through the remainder of the study. Cohort C specimens (n=15) were relatively small and first occurred in August 2008 with generally increasing size through the short remainder of the study. This distribution of valve sizes is consistent with the presence of three distinct generations of *D. gouldii* given the species' strongly seasonal reproductive strategy (Coe 1955).

2.3. Environmental monitoring

From September 2007 through October 2008, SST at -0.8 m MLLW was recorded every ten minutes by a HOBO pendent submersible logger attached to the SIO pier. At this depth, the logger was just below the tidal height of the lowest tide of the year (-0.6 m MLLW). To obtain logger-location-equivalent SST for August 2007, the daily average SST from Hobo loggers for September 2007-Decemember 2008 were correlated with daily measured SST from the Shore Station Program

(http://shorestation.ucsd.edu) at SIO pier (i.e., $T_{Hobo} = 0.99* T_{ShoreStation} + 0.016$ (r^2=0.94), and this slightly non-unity relationship was applied to the August 2007 Shore Station SST. The Shore Station Program daily SIO pier salinity values were used for the study interval (Figure 2.3).

Weather data (i.e., air temperature, difference between SST and air temperature, solar radiation, and wind speed) were obtained from the California Nevada Applications Program (CNAP) and the California Climate Change Center (CCCC) (http://meteora.ucsd.edu/cap/) from the weather station located on the SIO Pier. Six minute verified tidal height was obtained for the SIO Pier (station ID 9410230) from NOAA Center for Operational Oceanographic Products and Services.

Intertidal organisms offer a unique challenge in attempting to quantify their habitat, while SST is relativity easy to constrain, the temperatures experienced during subaerial exposure are much harder to constrain. To assess the temperature variability experienced by subaerially exposed *D. gouldii*, transects of sand temperature were taken perpendicular to the shore every three meters starting near the seawall to the water using a SBE 39 logger. The 2.5 cm thermal probe was inserted into the sand and temperature was taken every 3 seconds for a total of 30-60 seconds with an accuracy of ±0.002 °C. Air temperature was also measured with the SBE 39 two meters above the sand surface for 60 seconds. Seawater temperature was measured by immersing the SBE 39 in 0.3-1.0 m of water for a minimum of 60 seconds.

2.4. Seawater isotopes

During each *D. gouldii* collection, seawater samples for $\delta^{18}O_{SW}$ and $\delta^{13}C_{DIC}$ were taken from the surfzone, filtered through a 0.22 μm filter (Millex CP), poisoned with 2-3 drops of 10% zephiran chloride, and stored in vials capped with CO_2-impermeable septa (Wheaton 224186). $\delta^{18}O_{SW}$ and $\delta^{13}C_{DIC}$ values were determined using a Gas Bench II headspace sampling interface coupled to a ThermoFinningan Delta Plus XP isotope ratio mass spectrometer (IRMS) at the University of California, Santa Cruz, Stable Isotope Laboratory. $\delta^{18}O_{SW}$ values were determined by equilibrium exchange of the water sample with 0.3% CO_2 gas in a predominantly helium headspace environment. Analytical precision of internationally calibrated in-house standards was better than 0.06‰ for $\delta^{18}O_{SW}$ and values are reported relative to the VPDB international standard. $\delta^{13}C_{DIC}$ values were determined by injecting 0.7 ml of a water sample into a helium-flushed 12 cc Labco Exetainer vials containing 1 ml of supersaturated phosphoric acid (specific gravity 1.91 g/cm^3). DIC-derived CO_2 was allowed to evolve from the acidified water into the headspace over a period of at least six hours. After this equilibration period, the headspace gas was entrained into a He stream and passed through two Nafion dryers and a PoraPlot Q gas chromatographic (GC) column. During analysis, calibrated in-house $NaHCO_3$ standards and a second calibrated laboratory standard with a low $\delta^{13}C$ (-25‰) were run to correct for source-stretching effects. Standards were prepared daily from $NaHCO_3$ by dissolving bulk powders in water that has been stripped of DIC by sonication under a weak vacuum for one hour. These laboratory standards, which are selected to be compositionally

similar to the samples being analyzed, have been previously calibrated against NIST Standard Reference Materials (NBS-19, NBS-18, and LSVEC). Analytical precision was typically better than 0.06 ‰ (±1 σ) for $\delta^{13}C_{SWDIC}$ and values are reported relative to VPDB international standard (Figure 2.3).

2.5. D. gouldii shell sampling

For along-commissure (i.e., growth edge) sampling of each specimen, the umbo of each left valve was mounted to a glass slide using UV-activated epoxy. Valves were milled ~1,000 μm along the commissure and 150μm from the growing edge, staying in the aragonitic prismatic layer (Figure 2.2 inset). The resulting ~300 μg of aragonite powder was split for stable-isotopic ($\delta^{18}O$, $\delta^{13}C$) and elemental-ratio (Sr/Ca) determinations. Based on growth increment analysis, milled sections (~150 μm) represent between four and seven days of growth (Hatch et al. *in press*).

2.5. Stable isotope determination

For $\delta^{18}O$ and $\delta^{13}C$ values, a minimum of 75μg of aragonite powder was analyzed at the University of California, Santa Cruz, Stable Isotope Laboratory on a Micromass PRISM or OPTIMA mass spectrometer with common acid bath carbonate preparation system using 100% H_3PO_4 at 90°C or at the University of California, Davis, Stable Isotope Lab using a GV OPTIMA. For both laboratories, long-term reproducibility based on in-house standards tied to NBS standards averaged better than ±0.04‰ for $\delta^{18}O$ and ±0.06‰ for $\delta^{13}C$. All values are reported relative to the VPDB standard.

2.6. Sr/Ca determination

For elemental ratio determinations, a minimum of 125 μg of aragonite powder was placed in an acid-cleaned 2 mL polypropylene microcentrifuge tube, acidified with 1 ml trace-metal-grade 0.5 N HNO_3 to produce a ~1-4 mM Ca solution, and analyzed on a Perkin Elmer 4300 Dual View Inductively Coupled Plasma-Optical Emission Spectrometer (ICP-OES) at the San Diego State University Ecology Analytical Laboratory. Based on preliminary analyses designed to constrain the expected range of elemental ratios within the sample population, a calibration matrix comprised of four ratios (i.e., nominal Sr/Ca ratios of 0.00, 0.46, 1.83, and 5.49 mmol/mol) at three different concentrations (i.e., 1.31, 2.61, and 5.22 mM Ca) were analyzed multiple times within each analytical session. Calibrations for each analytical session were based on linear regressions between the nominal molar ratios for the four standards and their determined intensity ratios at the three different concentrations (Wara et al. 2003). In addition to these calibration standards, a liquid consistency standard produced from bulk sampling and dissolution of a *D. gouldii* shell (2.25 mM Ca) was routinely analyzed within and between analytical sessions and produced a grand average of 1.50 ± 0.04 Sr/Ca mmol/mol (2.73% RSD). Multiple blanks of 1 mL trace-metal-grade 0.5 N HNO_3 were routinely analyzed within analytical sessions and revealed no significant biases from background noise, sample carry over, or metal leaching for plastic.

2.7. Laser Ablation Preparation and Analyses

Four *D. gouldii* specimens collected on 8 July 2008 were prepared for laser ablation analyses by embedding in epoxy, thin-sectioning along their maximum growth axis with a Buehler IsoMet 5000 Linear Precision Saw, and hand-polishing to a final thickness of ~1 mm with 3M WetorDry Sandpaper (320, 600, 800, 1000 grit) using a duct-tape manipulator (Carpenter 1998). The resulting polished sections were analyzed using a New Wave UP-213 laser ablation system coupled to a Finnigan MAT Element2 Sector Inductively Coupled Plasma Mass Spectrometer (ICP-MS) at the University of California, Santa Barbara. Ablation paths followed the central portion of observable growth lines within the prismatic layer from the umbo to the commissure, and were spaced every 300 μm for Specimens A and B and every 900 μm for Specimens C and D. All ablation spots were ~70 μm by ~100 μm and analyses were calibrated against an in-house liquid standard 6.15 ± 0.02 Sr/Ca mmol/mol; 0.38% RSD) specifically designed for carbonate analyses in order to assess and correct any instrumental drift as well as the NIST 612 glass standard (0.39 ± 0.01 Sr/Ca mmol/mol; 2.37% RSD) and the USGS MACS3 standard (7.66 ± 0.07 Sr/Ca mmol/mol ;0.90% RSD). All ablations were continuous scans covering 100μm using a 70 μm spot taken parallel to growth-increments, representing roughly one lunar day of biomineralization. The laser was operated at a repetition rate of 10 Hz with an RF power of 1200 watts. The nebulizer flow rate of argon was 0.8 L min^{-1} and 0.5ml min^{-1} through the sample chamber.

2.8. Statistical analysis

Stepwise forward regression analysis was used to determine which environmental factors are significantly related ($p<0.001$) to the isotopic and minor element ratios in *D. gouldii*. The amount of time represented by milling in 150 μm from the commissure was estimated to be between four and seven days based on analysis of daily growth increments (Hatch et al. in press). To match the sample window between shell chemistry and environmental data, all environmental data was averaged over seven days, by averaging from the day of collection to six days prior. Separate analyses were run for each independent variable (i.e., $\delta^{18}O_{Donax}$, $\delta^{13}C_{Donax}$ and Sr/Ca) using the following suite of dependent variables: shell size, collection-date $\delta^{18}O_{SW}$, collection-date $\delta^{13}C_{DIC}$, and seven day averages for seawater temperature, seawater salinity, air temperature, sea-air temperature difference, solar radiation, wind speed, and % submergence at tidal levels 0.3, 0.2, and 0.1 MLLW. The stepwise forward regressions attempt to create the best model to describe the dependant variable by selecting models based on the lowest AIC and optimizing for the fewest number of variables (Burnham and Anderson 2002).

3. Results

3.1. Oxygen isotopes

$\delta^{18}O_{Donax}$ ranged from -1.85 to 1.00 and averaged -0.46‰ (±0.63; n=145), with more negative values during the summer and fall and more positive values during the winter (Figure 2.4). Stepwise multiple regressions with $\delta^{18}O_{Donax}$ as the dependent variable and 13 independent variables resulted in seven-day temperature and $\delta^{18}O_{SW}$

being significant ($p<0.01$) in the following model: $\delta^{18}O_{Donax} = 3.42 – (0.19 * SST) + (1.44 * \delta^{18}O_{SW})$ ($r^2 = 0.78$). This $\delta^{18}O_{Donax}$ predictive model independently verifies seawater temperature and $\delta^{18}O_{SW}$ as being the parameters needed to estimate $\delta^{18}O_{Donax}$. While, it is expected that $\delta^{18}O_{Donax}$ is related to seawater temperature and $\delta^{18}O_{SW}$ this method also produces the best parameter coefficients for *D. gouldii* at this location (Figure 2.4).

The pairwise difference between $\delta^{18}O_{Donax}$ and regression-predicted $\delta^{18}O$ ($\delta^{18}O_{predicted}$) for the entire study was 0.08 ‰ (±0.29), with $\delta^{18}O_{Donax}$ being more positive than $\delta^{18}O_{predicted}$. Six of the 27 collections had pairwise differences greater than one standard deviation from the study mean and in five of the six $\delta^{18}O_{Donax}$ was more positive than $\delta^{18}O_{predicted}$ (i.e., 11/5/07, 0.32‰; 12/12/07, 0.44‰; 1/4/08, 0.40‰; 7/21/08, 0.36‰; 8/4/08, 0.40‰; 9/21/08, -0.17‰). In general, $\delta^{18}O_{Donax}$ between 11/5/07 and 1/4/08 was more positive than $\delta^{18}O_{predicted}$.

When comparing the *D. gouldii* specific paleotemperature equation to those presented in Grossman and Ku (1986) and Bohm et al. (2000), the *D. gouldii* paleotemperature equation predicts more negative $\delta^{18}O$ for a given temperature, with a steeper slope (Figure 2.5). The difference between the *D. gouldii* paleotemperature equation and the others is less at higher temperatures and greater at lower temperature. The Grossman and Ku (1986) equation derived from aragonite mollusks and foraminifera best approximated the *D. gouldii* paleotemperature equation, while the Grossman and Ku (1986) mollusk only equation was the most offset. The

paleotemperature equation presented in Bohm et al. (2000) was more positive than the *D. gouldii* specific equation and is between the two Grossman and Ku (1986) equations.

3.2. Carbon isotopes

$\delta^{13}C_{Donax}$ averaged 1.08‰ (±0.44) (n=145) ranging from -0.54 to 1.91 with more positive values in the winter and more negative values in the summer and fall (Figure 2.6). The stepwise regression for $\delta^{13}C_{Donax}$ resulting in the following model: $\delta^{13}C_{Donax} = 3.05 – (0.12 * \text{air temperature}) + (0.02 * \text{length } \textit{D. gouldii})$ ($r^2 = 0.56$), with factors being significant at $p < 0.01$. Cohort C $\delta^{13}C_{Donax}$ was consistently more negative than predicted. Within a given collection, smaller individuals tended to be more negative $\delta^{13}C_{Donax}$ than larger specimens, with small cohort C specimens having the most negative $\delta^{13}C_{Donax}$ (Figure 2.6). $\delta^{13}C_{DIC}$ values are within the range of other regionally measured $\delta^{13}C_{DIC}$ values (Hinger et al. 2010) (Figure 2.3). Correlation between $\delta^{13}C_{Donax}$ and $\delta^{18}O_{Donax}$ resulted in the following significant ($p < 0.01$) relationship ($\delta^{13}C_{Donax} = 1.3 + 0.5 * \delta^{18}O_{Donax}$ $r^2=0.52$).

3.3. Edge-sampled minor element ratios

Sr/Ca ratios varied from 1.1 to 2.1 mmol/mol with an average of 1.4 (±0.2). The stepwise forward regression identified shell size as the only significant factor in the relationship: Sr/Ca = 1.1 + (0.02 * shell size) ($r^2 = 0.19$) (Figure 2.7). While seawater temperature was not significantly related to Sr/Ca, the relationship between Sr/Ca and temperature was quantified by RMA regression of paired Sr/Ca ratios and seven-day-temperature, which produced the relationship: T (°C) = -1.51 + 13.85 Sr/Ca

($r^2 = 0.25$, n = 165, $p<0.001$). When only Cohort B is considered, this relationship between temperature and Sr/Ca markedly improves (i.e., T (°C) = 1.12 + 12.13 Sr/Ca, $r^2 = 0.41$, n = 144, $p<0.001$), but still has a relatively low correlation coefficient. For the period of August 2008 to September 2008, when both Cohort B and C were sampled, Cohort B had an average Sr/Ca ratio of 1.82 ± 0.14 (mmol/mol) and the smaller individuals in Cohort C had a lower average of 1.38 ± 0.09 (mmol/mol).

3.4. Minor Elements determined using LA-ICP-MS

Four cohort B specimens collected on 8 July 2008 were sampled with LA-ICP-MS from the umbo to commissure along the maximum growth axis (Figure 2.8). Specimens A and B were 17.1 and 21.9 mm long (anterior-posterior) and were laser-ablated every 300 μm for a total of 47 and 57 ablations, respectively. Specimens C and D were 18.2 and 19.1 mm long (anterior-posterior) and were laser-ablated every 900 μm for a total of 16 and 17 ablations, respectively. In general, laser-ablated shells show greater variability with a higher mean of Sr/Ca compared to the edge-milled samples (Figure 2.7 and 2.8). Laser-ablated shells tended to have highest Sr/Ca values near the umbo, minimum Sr/Ca values in the mid-section, and slightly higher Sr/Ca values near the commissure (Figure 2.8). Laser-ablated Sr/Ca values from the shell commissure of the specimens A-D and edge-milled Sr/Ca values from 8 July 2008 sample population had similar mean values of 1.53 ± 0.37 (n=4) and 1.56 ± 0.11 (n=5) mmol/mol, respectively. Specimen D had higher values from 3-11 mm compared to other shells.

3.4. Sand temperature

A total of 156 sand measurements were made over nine transects including 85 measurements adjacent to *D. gouldii*. Transects on 8/15/11, 9/13/11, and 9/21/11 all occurred in the afternoon between 14:00-17:00. Starting on 9/29/11 through the following day transects where completed every three hours for a 24 hour period. The average of all sand temperature measurements was 2.9 C° warmer than seawater with a maximum difference of 11.7 C°. When only sand measurements associated with living *D. gouldii* were considered, the averaged difference decreased to 1.7° warmer with a maximum difference of 4.4 C° (Figure 2.9).

4. Discussion

4.1 Oxygen:

This study independently assessed the relationship between $\delta^{18}O_{Donax}$ and a suite of environmental parameters, resulting in a *D. gouldii* specific paleotemperature equation that correlates $\delta^{18}O_{Donax}$ to seven-day temperature and $\delta^{18}O_{SW}$, explaining 78% of the variability in $\delta^{18}O_{Donax}$. While this finding is congruent with the current understanding of oxygen isotope thermodynamics (Epstein et al. 1953a), it is necessary to quantify this relationship for the intertidal *D. gouldii* given the variance in published paleotemperature equations and species specific fractionation factors (McConnaughey 1989a; Shanahan et al. 2005). $\delta^{18}O_{Donax}$ clearly tracks the seasonal seawater temperature with more positive $\delta^{18}O_{Donax}$ values when temperatures are cooler and more negative $\delta^{18}O_{Donax}$ when temperatures are warmer (Figure 2.5). The within-collection variability of $\delta^{18}O_{Donax}$ did not follow any obvious seasonal pattern

with high variability observed during the winter (11/28), summer (5/28) and fall (8/21 and 9/19), indicating that within-collection variability is not related to seasonality or seawater temperature (Figure 2.4).

Understanding the ecology of *D. gouldii* is necessary to account for potential basis in $\delta^{18}O_{shell}$ based temperature reconstructions, such as growth shut-downs or temperature differences in micro-habitat niches (Goodwin et al. 2004). If growth shut-down occurred, it would be expected that *D. gouldii* based temperature would under-estimate summer SST and over-estimate winter SST. Based on the constant relationship between $\delta^{18}O_{Donax}$ and $\delta^{18}O_{predicted}$, these data confirm that *D. gouldii* grow year round and do not show marked declines in shell growth. Studies comparing $\delta^{18}O_{shell}$ to $\delta^{18}O_{predicted}$, based on ambient environmental conditions and published paleotemperature equations, have reported average offsets up of over 1‰, or ~4 °C, necessitating the calibration of $\delta^{18}O_{Shell}$ – temperature correlations for species-specific differences in isotope fractionation (Mannino et al. 2008; Ford et al. 2010). While, the hypothesized driver for these differences vary from study to study and are often ad hoc, the pattern remains that calibration studies are necessary to account for species-specific fractionation and to understand how the ecology of the study organism impacts $\delta^{18}O_{shell}$ records.

Seven-day temperature and $\delta^{18}O_{SW}$ explained 78% of the variation in $\delta^{18}O_{Donax}$. For the entire study interval, the average pairwise difference between measured $\delta^{18}O_{Donax}$ and $\delta^{18}O_{predicted}$ was 0.08 ‰, or $\delta^{18}O_{Donax}$ would predict seawater to be ~0.4°C cooler, if converted to temperature. For synthetic aragonite,

paleotemperature equations have an error of ~0.08 ‰ (Kim et al. 2006) and for this study, instrument error for $\delta^{18}O_{Donax}$ was 0.04‰ and 0.06‰ for $\delta^{18}O_{SW}$. Given the variation in synthetic aragonite studies and instrument errors an average difference between predicted and measured $\delta^{18}O_{Donax}$ of 0.08 ‰ is reasonable. *D. gouldii* has potential to be a reliable proxy of mean annual temperature (MAT), provided that $\delta^{18}O_{SW}$ could be constrained.

If *D. gouldii* are living a heterogeneous environment and experiencing different temperatures based on micro-habitat niches these temperatures would be reflected as $\delta^{18}O_{Donax}$ variability within each collection. The within collection $\delta^{18}O_{Donax}$ standard deviation varied from 0.05 to 0.5‰ however, the variance did not follow a seasonal pattern. Collection dates with the highest standard deviations (11/28/07 ± 0.41, 9/19/08 ± 0.54) were bounding by collections with much lower stand deviations (11/15/07 ± 0.07, 12/12/07 ± 0.06, 9/4/08 ± 0.08, 9/29/08 ± 0.10), suggesting that the observed within collection variability could be driven by ephemeral environmental changes rather than seasonal variability.

One mechanism to explain offsets between $\delta^{18}O_{predicted}$ and $\delta^{18}O_{Doanx}$, such as more negative $\delta^{18}O_{Doanx}$ between 11/5/07 and 1/4/08 and more positive $\delta^{18}O_{Doanx}$ 4/1/08 and 5/12/08, is microhabitat variability at the individual level. *D. gouldii* can be dislodged during storm events or by disturbance and transported to a different tidal height, making it nearly impossible to reconstruct the exact chronology of tidal level and subaerial exposure experienced by each *D. gouldii*. Further microhabitat changes such as slight sand depressions and sand bars can alter the amount of time an

individual remains gapped while subaerially exposed. These sources of variably might be reflected in the within collection variability, but based on the agreement between the annual $\delta^{18}O_{Donax}$ and $\delta^{18}O_{predicted}$ appear to not impact the annual temperature record.

Oxygen isotope thermometery has been proposed (Urey 1947) and applied to biogenic carbonates (Epstein et al. 1953) for over 60 years. It is has been generally accepted $\delta^{18}O_{carbonate}$ is related to temperature and $\delta^{18}O_{SW}$, what remains unclear is the precise temperature-$\delta^{18}O_{carbonate}$ relationship for a given locality and species. Estimated fractionation factors differ significantly from synthetic carbonate, theoretical calculations, and natural biological carbonates (Shanahan et al. 2005), often requiring a calibration to be conducted before applying a temperature $\delta^{18}O_{carbonate}$ relationship.

The *D. gouldii* paleotemperature equation from this study predicted more negative $\delta^{18}O_{carbonate}$ with a steeper slope than the aragonite paleotemperature equations from Grossman and Ku (1986) and Bohm et al. (2000). Notably, this offset is not constant, but increases with decreasing temperature. Offsets from $\delta^{18}O_{predicted}$ from the equations has been noted; for example, Mannino et al (2000) found the $\delta^{18}O$ of the intertidal gastropod *Osilinus turbinatus* to be systemically heavier than predicted by the paleotemperature equations presented in Grossman and Ku (1986) and Bohn et al. (2000), whereas this study found $\delta^{18}O_{Donax}$ to be lighter than predicted. Mannion et al. (2008) also found seasonal variability in the degree of offsets, with a higher offset with warmer temperature, compared to this study which found greater deviation at lower temperatures. Using monthly collected *O. turbinatus* Colonese et al.

(2009) found that edge milled $\delta^{18}O$ samples under-estimate warmer seawater temperatures and over-estimate cooler temperatures.

In a similar study, Jones et al. (2004; 2005) sequential milled the outer surface of two north-eastern Florida *Donax variablilis* from commissure to umbo. The researchers then estimated ambient SST by applying the mollusk paleotemperature equation from Grossman and Ku (1986) using $\delta^{18}O_{shell}$ and $\delta^{18}O_{SW}$ values. Visually, the $\delta^{18}O_{D.\ variablilis}$ based SST estimates showed good agreement with nearshore SST, though the study only used two specimens of *D. variablilis* collected that the same. Ecologically *D. variabilis* migrates along the shoreface through tidal cycles (presumably to maximize submersion), whereas *D. gouldii* occupies a relatively fixed middle intertidal position that is regularly subaerially exposed during spring tides.

Calibration of thermodynamic relationship of $\delta^{18}O_{carbonate}$ to seawater temperature is necessary to account for species specific fraction factors and ecological impacts on $\delta^{18}O_{carbonate}$ from growth shutdowns, migrations, and microhabitat variability. As a paleothermometer, *D. gouldii* showed within collection variability but if taken on average, $\delta^{18}O_{Donax}$ was slightly more positive than $\delta^{18}O_{predicted}$. Ecological, $\delta^{18}O_{Donax}$ shows that *D. gouldii* grow throughout the year without major shutdown.

4.2 Carbon:

$\delta^{13}C_{Donax}$ was not correlated with $\delta^{13}C_{DIC}$ (r^2=0.03, p= 0.36) and therefore $\delta^{13}C_{Donax}$ should not be used as a direct proxy for $\delta^{13}C_{DIC}$ or thereby an indirect proxy for upwelling. Average $\delta^{13}C_{Donax}$ was 0.37‰ lighter than average $\delta^{13}C_{DIC}$, considerably less than the previously reported enrichment factor of 2.7‰ for synthetic

aragonite (Romanek et al 1992). While the mechanistic driver of $\delta^{13}C_{carbonate}$ is often not clear, these results will be related to previously published models which attribute observed patterns to either metabolic or kinetic effects. Metabolic carbon can be the source for up to 25-40% of $\delta^{13}C_{aragonite}$, with increasing metabolic contributions for larger/older bivalves (Gillikin et al., 2007). Thus, one test for metabolic effects upon the $\delta^{13}C_{Donax}$ would be progressively lower $\delta^{13}C_{Donax}$ for larger/older specimens and a weak relationship between $\delta^{13}C_{Donax}$ and $\delta^{18}O_{Donax}$ (Gillikin et al., 2007; McConnaughey, 1989a (Lorrain et al. 2004). If kinetic effects dominated $\delta^{13}C_{Donax}$, then a positive relationship between $\delta^{13}C_{Donax}$ and $\delta^{18}O_{Donax}$ would be expected from the preferential incorporation of the lighter isotopes during intervals of rapid extension (McConnaughey, 1989a). The $\delta^{13}C_{Donax}$ age/size relationship for *D. gouldii* appears to be opposite of they hypothesis presented in Lorrain et al (2004) since younger *D. gouldii* specimens within a collection had more negative $\delta^{13}C_{Donax}$ values (Figure 2.7). In this study, a significant positive relationship was found between $\delta^{13}C_{Donax}$ and $\delta^{18}O_{Donax}$ ($p < 0.01$, $r^2=0.52$), consistent with the hypothesis that $\delta^{13}C_{Donax}$ is influenced by kinetic effects. Air temperature was identified by the stepwise forward regressions as a significant parameter to explain $\delta^{13}C_{Donax}$ but no hypotheses which mechanistic links air temperature and $\delta^{13}C_{Donax}$ could be found for this relationship.

4.3 Sr/Ca:

The stepwise forward linear model found a significant relationship between Sr/Ca and shell size however, SST was not significantly related to Sr/Ca. Given that evidence of thermodynamic control on minor element ratios is variable between

speices and possibly locations, for many species among many localities (de Villiers et al., 1994; Gillikin et al., 2005a; Rosenheim et al., 2005; (Klein et al. 1996; Ford et al. 2010). *D. gouldii* Sr/Ca is likely influenced by growth rate, ontogeny effects, and other non-temperature-based controls which should be further investigated.

The influence of thermodynamics and non-temperature effects on Sr/Ca can be obscured by the positive relationship between growth and temperature (Gillikin et al. 2005). Evidence for non-temperature controls on Sr/Ca can be tested in *D. gouldii* by looking for cohort dependant relationship between Sr/Ca and temperature, if cohort assignment, thereby age effects the Sr/Ca-temperature relationship then ontongeny and growth rate could be impacting Sr/Ca. To test if age impacts Sr/Ca, simple linear regressions were preformed between Sr/Ca and seven-day temperature resulting in Sr/Ca being weakly positively correlated ($r^2 = 0.25$) with ambient temperature. However, this relationship greatly improved ($r^2 = 0.41$) when just cohort B was included, suggesting non-temperature effects.

D. gouldii Sr/Ca values from laser ablation also displayed evidence for ontogenetic control, with higher values closer to the umbo, presumably when the young clam is calcifying more rapidly. After this peak Sr/Ca values decrease then rise slightly toward the commissure, representing growth during the spring and summer when clams were collected. While a seasonal signal can be implied by these data, there is very little support of temperature dependence as the clams the Sr/Ca values are asymmetric, with higher values near the umbo.

4.4 Sand Temperature

When subaerially exposed, ***D. gouldii*** were on average, buried in sand 1.7 °C warmer than seawater, however the question remains does $\delta^{18}O_{Donax}$ reflect the temperature of seawater, subaerial exposure, or a combination of both. For $\delta^{18}O_{Donax}$ to record temperature during subaerial exposure, ***D. gouldii*** must be calcifying during exposure. Shell carbonate is precipitated in the extrapallial fluid, between the mantle and existing shell. When ***D. gouldii*** are gapped the mantel can cover commissure allowing calcification to occur, however when they close to prevent desiccation the mantel is retracted, preventing calcification. In the swash zone, ***D. gouldii*** may remain gaped while exposed for short periods between waves, but the temperature in the surfzone is typically close to seawater. Even if ***D. gouldii*** could calcify when subaerially exposed, at the 0.2 m MLLW tidal level they would only be exposed 14% of the time. Given the average temperature difference between subaerially exposed ***D. gouldii*** and seawater is 1.7 °C and 14%, if ***D. gouldii*** were calcifying during exposure, the resulting record would overestimate seawater temperature by 0.24 °C or 0.04 ‰ $\delta^{18}O$.

5. **Conclusion**

This study assessed the utility of biogenic $\delta^{18}O_{carbonate}$ and Sr/Ca as proxies for ambient temperature as well as $\delta^{13}C_{carbonate}$ as a proxy for seawater $\delta^{13}C_{DIC}$ and thereby upwelling intensity. Such baseline calibration studies are needed to assess the robustness of shell-chemistry – environmental relationships in light of potential biases that are systematic (e.g., species level fractionation factors) or episodic (e.g., seasonal

growth shut down, energetic shifts). For *D. gouldii*, growth appears to be relatively constant throughout the year and average $\delta^{18}O_{Donax}$ only slightly underestimates MAT by less than 0.5°C. Such calibrations require robust environmental records that are as close as possible to the study organisms, which can pose a challenge in dynamic soft substrates (e.g., sand, or silt). Despite the close proximity (<300 m) to collected *D. gouldii* and high frequency (10 minute sample interval) of the temperature record for this study it was not sufficient to fully explain the variation seen shell $\delta^{18}O_{Donax}$ as micro-scale habitat differences cause within collection variability.

Non-temperature control of *D. gouldii* Sr/Ca is evidenced by ontogenetic signals and cohort dependent relationship to temperature. While, thermodynamic control of Sr/Ca has been reported in aragonite sclerosponges (Rosenheim et al. 2005a) and corals (McCulloch et al. 1996), this study did not find strong thermodynamic control on Sr/Ca. Previous work on Sr/Ca in bivalves, has been inconclusive, but suggests biological control rather than thermodynamic (Gillikin et al. 2005). *D. gouldii* Sr/Ca appears to be under biological control as evidenced by the highest Sr/Ca values in the youngest portions of the shell and poor correlation with temperature when multiple generations when multiple cohorts are analyzed.

D. gouldii shell $\delta^{13}C$ was not found to track isotopic variation in $\delta^{13}C_{DIC}$ and is most likely influenced by under kinetic effects. Mollusk shell $\delta^{13}C$ typically becomes more negative as individuals age due to increased amount of respired CO_2 being incorporated into the calcification process, however in this study it was found that the smallest clams had the most negative $\delta^{13}C$ (McConnaughey and Gillikin 2008). The

kinetic effect on $\delta^{13}C_{Donax}$ is evidenced by more negative $\delta^{13}C_{Donax}$ in small fast growing individuals and a positive correlation between $\delta^{13}C_{Donax}$ and $\delta^{18}O_{Donax}$.

Despite the possibility of disequilibrium fractionation in intertidal mollusks, they still warrant study because of their known tidal position and availability of well preserved specimens for both natural and archaeological deposits. *D. gouldii* can serve as a useful proxy for MAT and combined analysis of the distinct sub-annual growth increments could also provide detailed seasonal temperature variation. Additionally the prevalence ancient *D. gouldii* from both natural and anthropogenic deposits represents a valuable paleoceanographic resource.

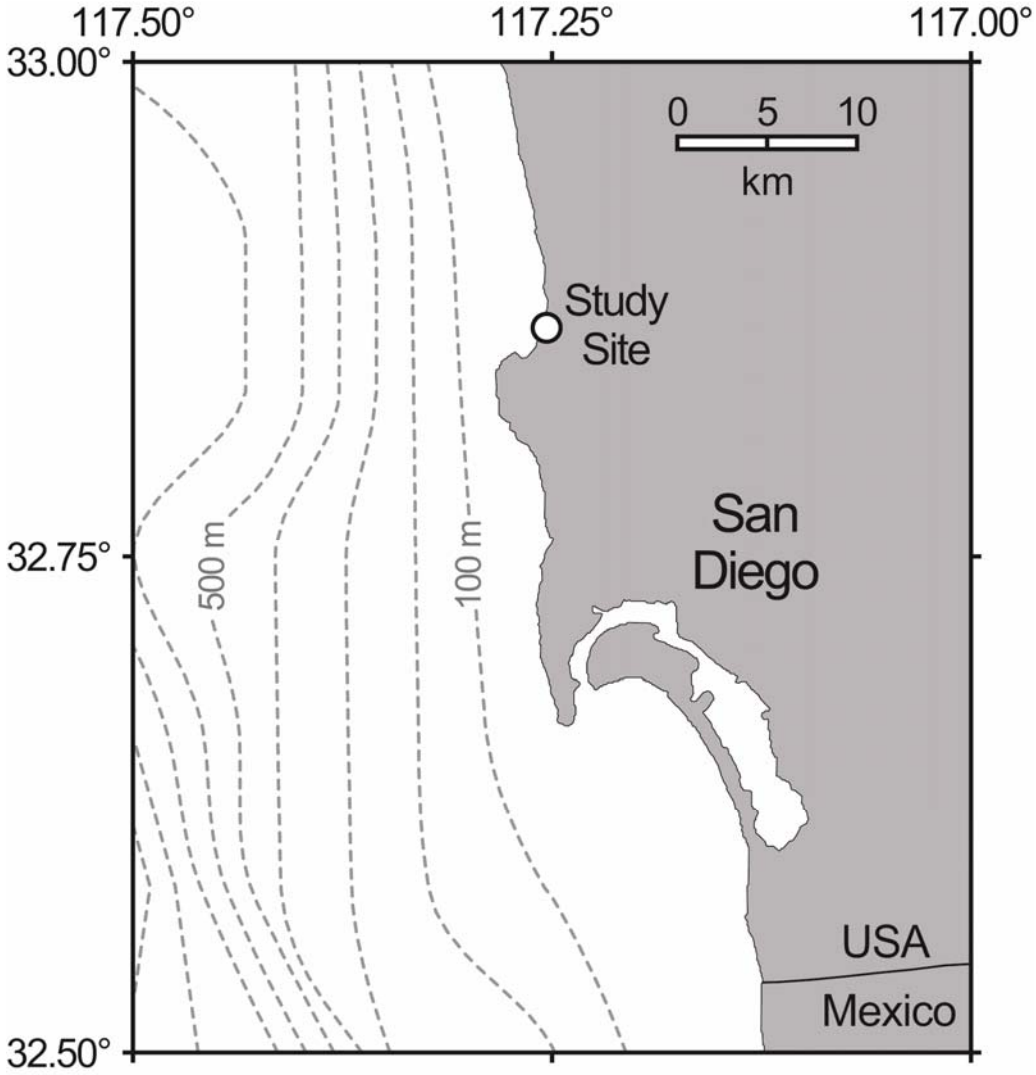

Figure 2.1: Scripps Institution of Oceanography (SIO) is labeled as "study site" *D. gouldii* and seawater were collected just north of SIO pier. Seawater temperature was measured from near the end of the SIO Pier.

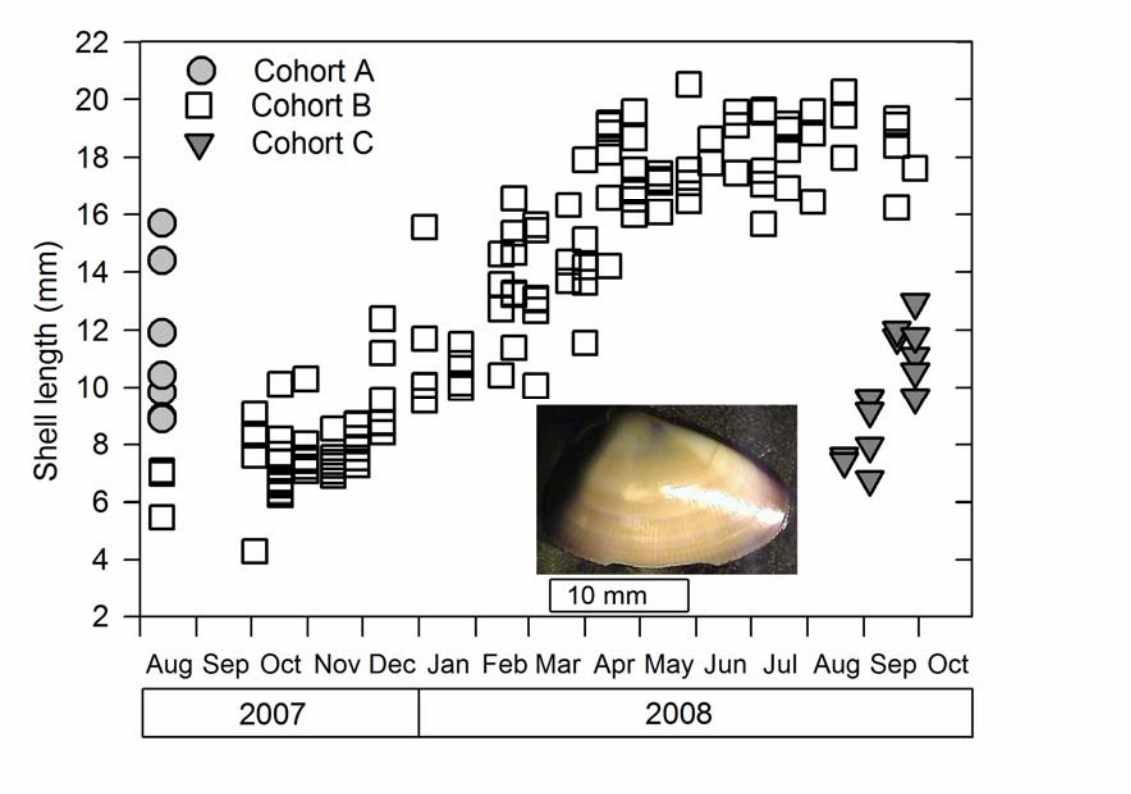

Figure 2.2: Size and cohort for collected *D. gouldii*. Inset is a representative valve that was milled along the commissure for 1,000 μm yielding ~300 μg of powder that split between minor element and stable isotope analysis.

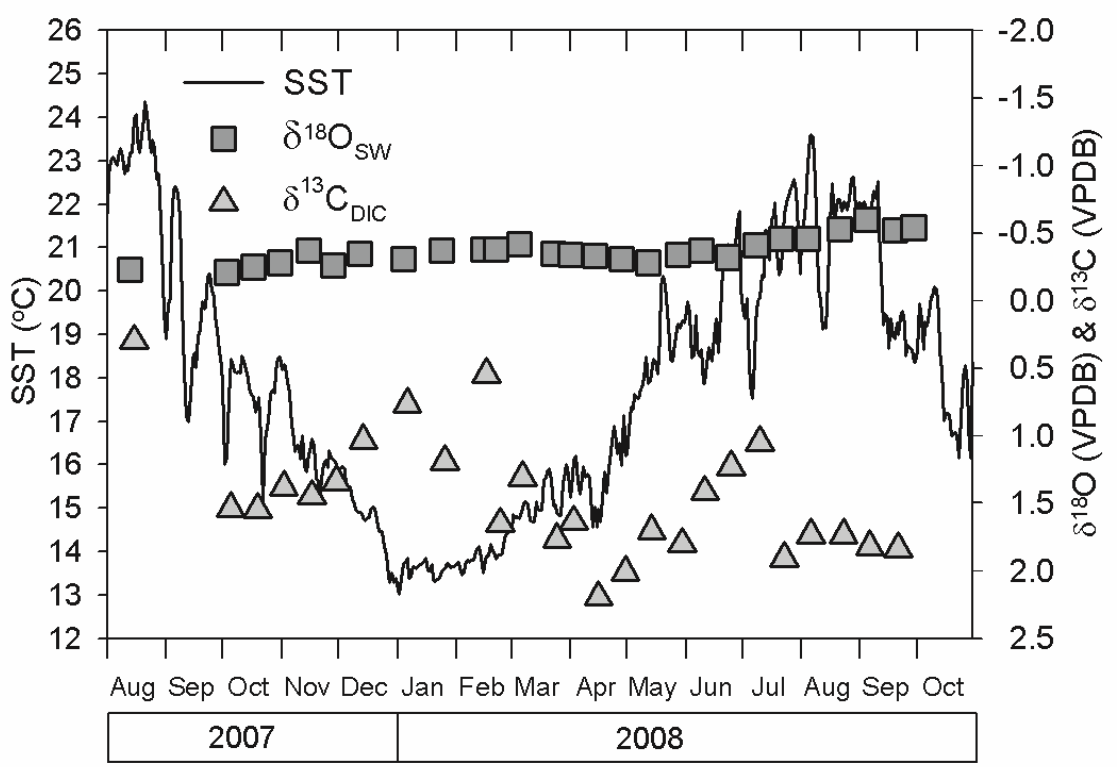

Figure 2.3: Daily averaged sea surface temperature measured from data logger attached to SIO pier from 9/2007-11/2008 and corrected daily sea surface temperature for 8/2007. Seawater $\delta^{18}O_{SW}$ and $\delta^{13}C_{DIC}$ were sampled from the swash-zone every two weeks. Note $\delta^{18}O_{SW}$ is converted from SMOW to VPDB by subtracting 0.27‰.

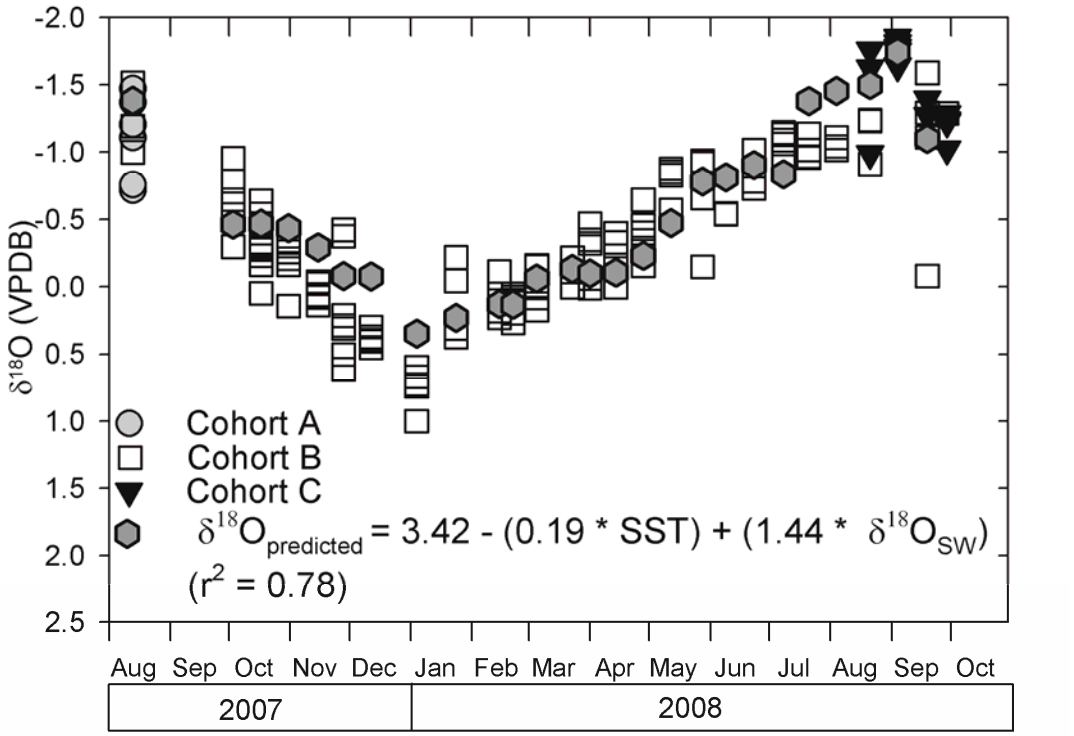

Figure 2.4: $\delta^{18}O_{Donax}$ from all samples plotted with cohort and predicted $\delta^{18}O$ based on results from stepwise forward regression.

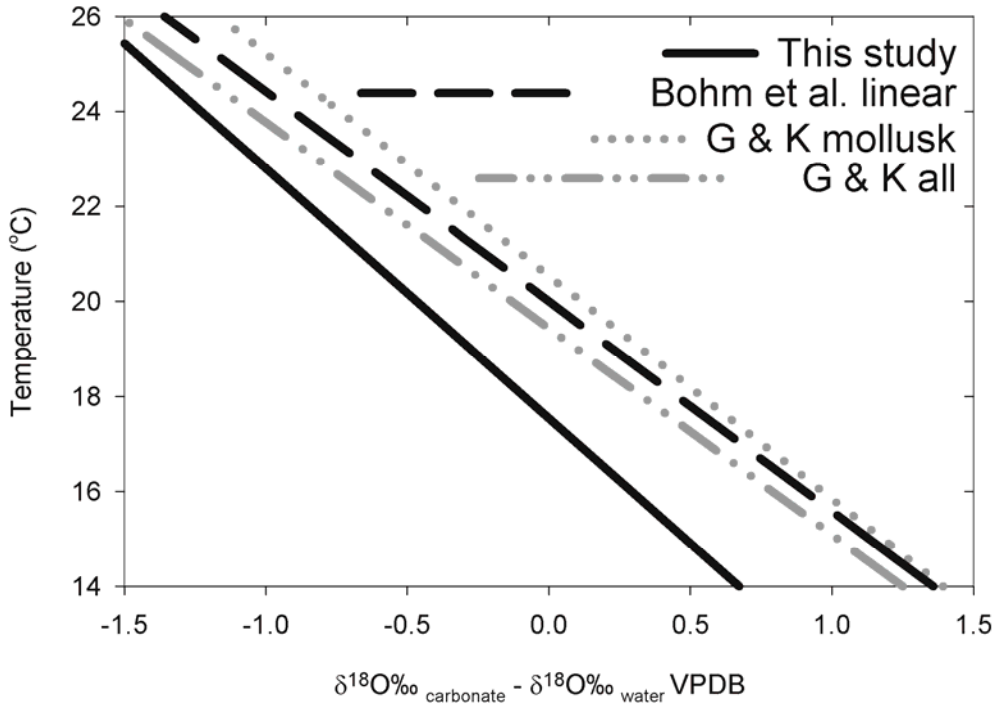

Figure 2.5: *D. gouldii* specific paleotemperature equation plotted with linear equation from Bohm et al. (2000) and the "all" and mollusk equations from Grossman and Ku (1986).

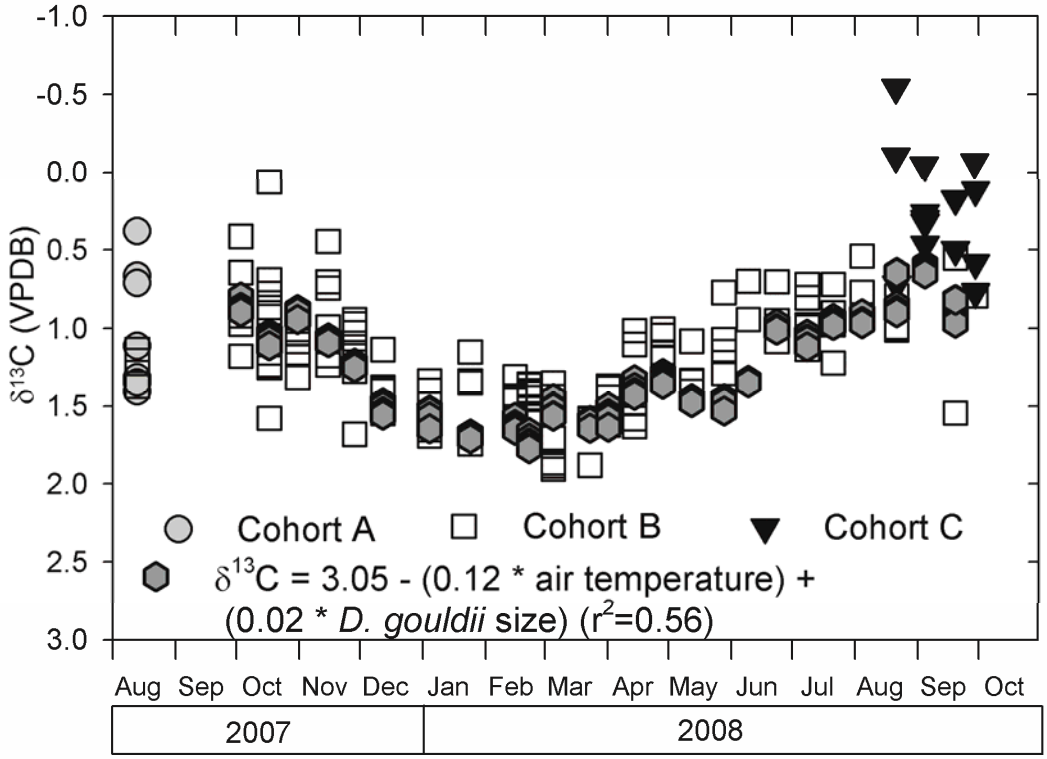

Figure 2.6: Measured $\delta^{13}C_{Donax}$ from all samples and predicted $\delta^{13}C$ based on *D. gouldii* size and air temperature.

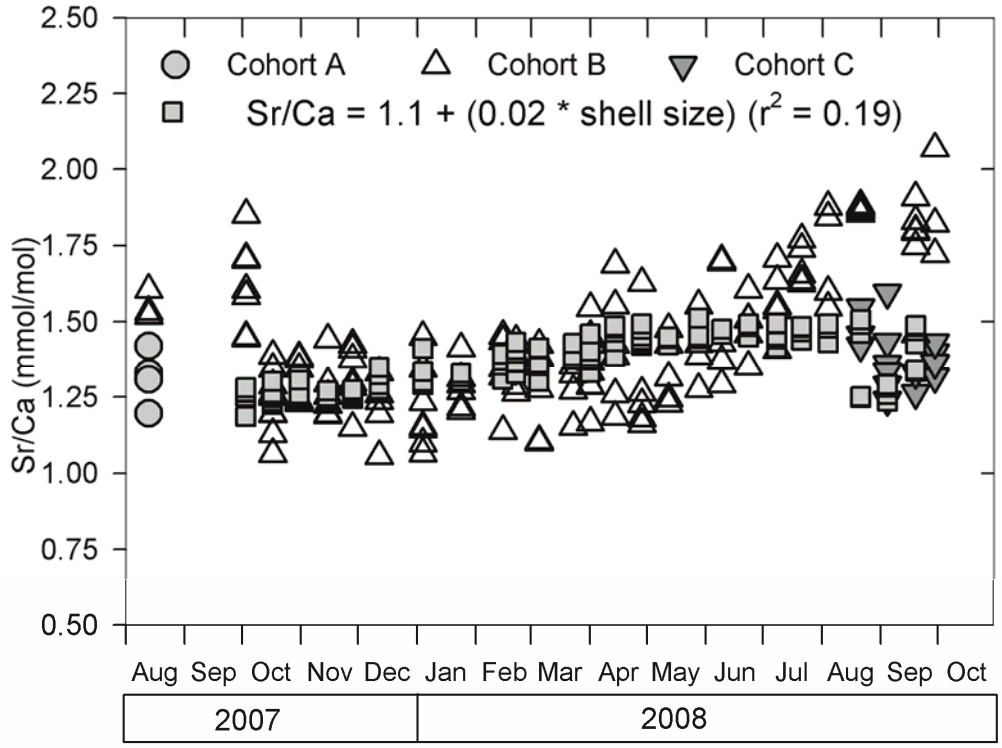

Figure 2.7: *D. gouldii* edge milled Sr/Ca values plotted with cohort and predicted Sr/Ca based on shell size.

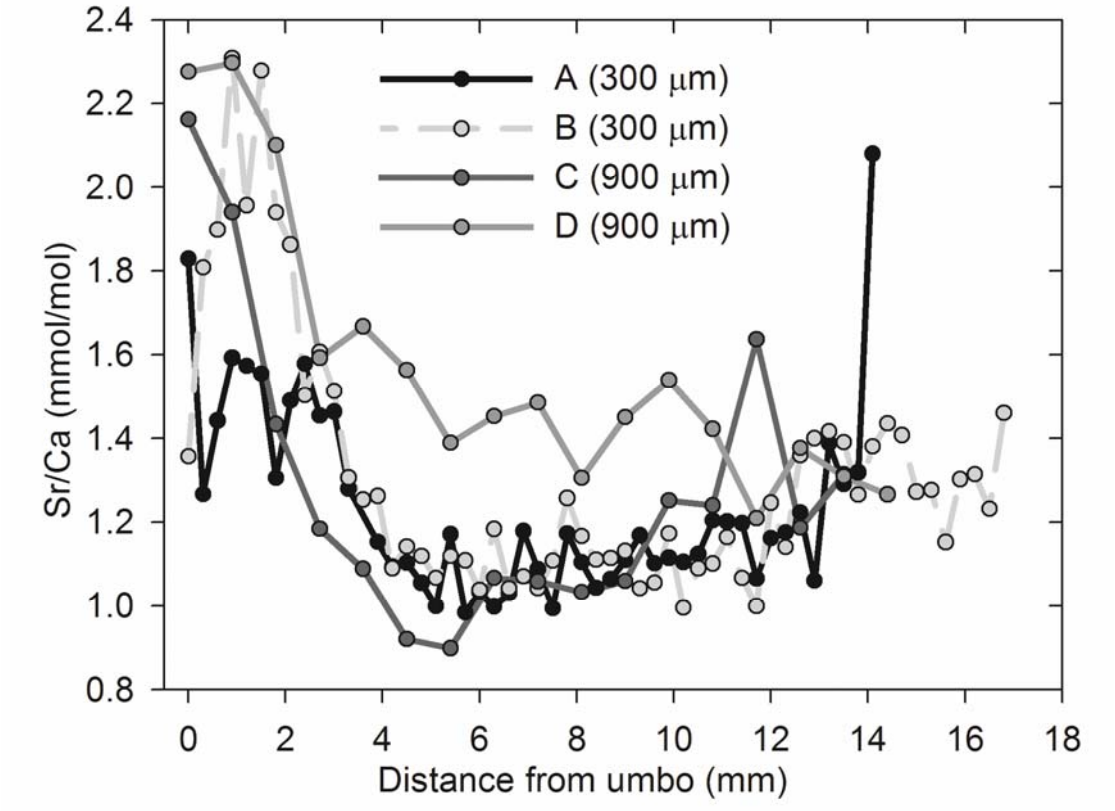

Figure 2.8: Laser ablation ICP-MS determined Sr/Ca profiles from four *D. gouldii* showing evidence for ontogenetic control of Sr/Ca, with high values near the umbo followed by a decrease and slight increase near the commissure.

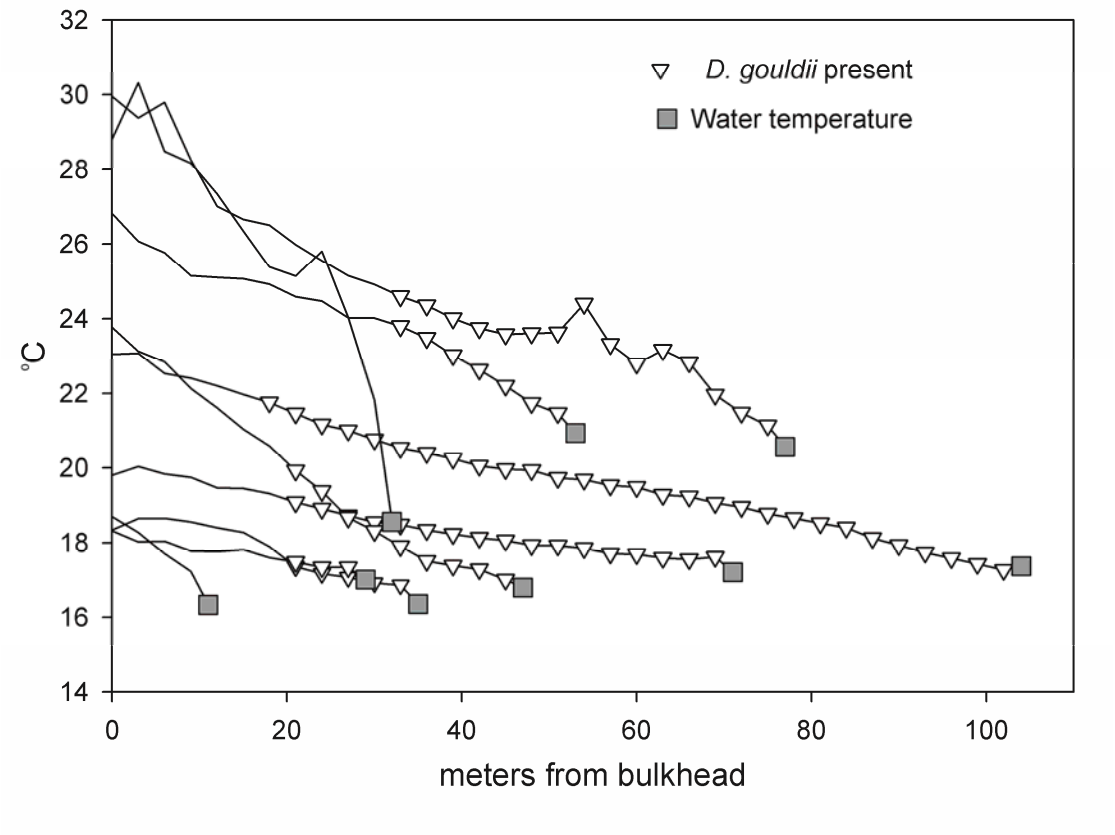

Figure 2.9: Sand temperature transects. All transects start 20 m north of the SIO at the bulkhead then precede ocean-ward with temperature taken every three meters. Locations with *D. gouldii* within ~1.5 m are noted by a triangle. Seawater temperature is plotted at then end of each line with a square.

6. References

Bakun A (1973) Coastal upwelling indices, west coast of North America, 1946-71. In. U.S.Dep. Commer., NOAA Tech. Rep., NMFS SSRF-671, p 103 p

Black BA, Copenheaver CA, Frank DC, Stuckey MJ, Kormanyos RE (2009) Multi-proxy reconstructions of northeastern Pacific sea surface temperature data from trees and Pacific geoduck. Palaeogeography, Palaeoclimatology, Palaeoecology **278**:40-47

Burnham KP, Anderson DR (2002) Model Selection and Multi-Model Inference: a practical information-theoretic approach. Springer

Carpenter SJ (1998) A duct-tape manipulator for polishing thin sections. Journal of Sedimentary Research **68**:515-518

Carre M, Bentaleb I, Fontugne M, Lavallee D (2005) Strong El Nino events during the early Holocene: stable isotope evidence from Peruvian sea shells. The Holocene **15**:42

Cobb KM, Charles CD, Cheng H, Edwards RL (2003) - El Nino/Southern Oscillation and tropical Pacific climate during the last millennium. **- 424**:- 276-- 276

Coe WR (1955) Ecology of the Bean Clam Donax Gouldi on the Coast of Southern California. Ecology **36**:512-514

de Villiers S, Nelson BK, Chivas AR (1995) Biological Controls on Coral Sr/Ca and $d^{18}O$ Reconstructions of Sea Surface Temperatures. Science **269**:1247-1249

de Villiers S, Shen GT, Nelson BK (1994) The -temperature relationship in coralline aragonite: Influence of variability in and skeletal growth parameters. Geochimica et Cosmochimica Acta **58**:197-208

Dietl GP, Flessa KW (2011) Conservation paleobiology: putting the dead to work. Trends in ecology & evolution (Personal edition) **26**:30-37

Ellers O (1995) Behavioral-Control of Swash-riding in the clam *Donax variabilis*. Biological Bulletin:120-127

Epstein S, Buchsbaum R, Lowenstam HA, Urey HC (1953) Revised Carbonate-water isotopic temperature. Geological Society of America Bulletin **64**:1315-1326

Field DB, Baumgartner TR, Charles CD, Ferreira-Bartrina V, Ohman MD (2006) Planktonic Foraminifera of the California Current Reflect 20th-Century Warming. Science **311**:63-66

Ford HL, Schellenberg SA, Becker BJ, Deutschman DL, Dyck KA, Koch PL (2010) Evaluating the skeletal chemistry of Mytilus californianus as a temperature proxy: Effects of microenvironment and ontogeny. Paleoceanography **25**:PA1203

Gallegos DR (2002) Southern California in transition: Late Holocene occupation of southern San Diego County. Catalysts to Complexity: Late Holocene Societies of the California Coast, Perspectives in California Archaeology **6**:27–39

Gillikin DP, Lorrain A, Navez J, Taylor JW, André L, Keppens E, Baeyens W, Dehairs F (2005) Strong biological controls on Sr/Ca ratios in aragonitic marine bivalve shells. Geochem. Geophys. Geosyst. **6**:Q05009

Goodwin DH, Flessa KW, Téllez-Duarte MA, Dettman DL, Schöne BR, Avila-Serrano GA (2004) Detecting time-averaging and spatial mixing using oxygen isotope variation: a case study. Palaeogeography, Palaeoclimatology, Palaeoecology **205**:1-21

Grossman EL, Ku TEHL (1986) Oxygen and carbon isotope fractionation in biogenic aragonite: temperature effects. Chemical Geology **59**:59-74

Hinger E, Santos G, Druffel E, Griffin S (2010) Carbon isotope measurements of surface seawater from a time-series site off Southern California. Radiocarbon:69-89

Jones DS, Quitmyer IR, Andrus CFT (2005) Oxygen isotopic evidence for greater seasonality in Holocene shells of Donax variabilis from Florida. Palaeogeography, Palaeoclimatology, Palaeoecology **228**:96-108

Killingley JS, Berger WH (1979) Stable Isotopes in a Mollusk Shell: Detection of Upwelling Events. Science **205**:186-188

Kim H-J, Miller AJ, McGowan J, Carter ML (2009) Coastal phytoplankton blooms in the Southern California Bight. Progress In Oceanography **82**:137-147

Kim S-T, Hillaire-Marcel C, Mucci A (2006) Mechanisms of equilibrium and kinetic oxygen isotope effects in synthetic aragonite at 25 °C. Geochimica et Cosmochimica Acta **70**:5790-5801

Klein RT, Lohmann KC, Thayer CW (1996) Bivalve skeletons record sea-surface temperature and delta 18 O via Mg/Ca and 18 O/16 O ratios. Geology **24**:415-418

Kroopnick P, Deuser WG, Craig H (1970) Carbon 13 Measurements on Dissolved Inorganic Carbon at the North Pacific (1969) Geosecs Station. In, Journal of Geophysical Research

Lorrain A, Paulet Y-M, Chauvaud L, Dunbar R, Mucciarone D, Fontugne M (2004) [delta]13C variation in scallop shells: Increasing metabolic carbon contribution with body size? Geochimica et Cosmochimica Acta **68**:3509-3519

Mannino M, Thomas K, Leng M, Sloane H (2008) Shell growth and oxygen isotopes in the topshell <i>Osilinus turbinatus : resolving past inshore sea surface temperatures. Geo-Marine Letters **28**:309-325

McConnaughey T (1989a) 13C and 18O isotopic disequilibrium in biological carbonates: I. Patterns. Geochimica et Cosmochimica Acta **53**:151-162

McConnaughey T (1989b) 13C and 18O isotopic disequilibrium in biological carbonates: II. In vitro simulation of kinetic isotope effects. Geochimica et Cosmochimica Acta **53**:163-171

McConnaughey T, Gillikin D (2008) Carbon isotopes in mollusk shell carbonates. Geo-Marine Letters **28**:287-299

McCulloch M, Mortimer G, Esat T, Xianhua L, Pillans B, Chappell J (1996) High resolution windows into early Holocene climate: Sr Ca coral records from the Huon Peninsula. Earth and Planetary Science Letters **138**:169-178

Morris RH, Abbott DP, Haderlie EC (1980) Intertidal Invertebrates of California. Stanford University Press, Stanford

Purton LMA, Shields GA, Brasier MD, Grime GW (1999) Metabolism controls Sr/Ca ratios in fossil aragonitic mollusks. Geology **27**:1083-1086

Rosenheim BE, Swart PK, Thorrold SR (2005a) Minor and trace elements in sclerosponge Ceratoporella nicholsoni: Biogenic aragonite near the inorganic endmember? Palaeogeography, Palaeoclimatology, Palaeoecology **228**:109-129

Rosenheim BE, Swart PK, Thorrold SR (2005b) Minor and trace elements in sclerosponge Ceratoporella nicholsoni: Biogenic aragonite near the inorganic endmember? Looking back over Skeletal Diaries - High-resolution

Environmental Reconstructions from Accretionary Hard Parts of Aquatic Organisms **228**:109-129

Shanahan TM, Pigati JS, Dettman DL, Quade J (2005) Isotopic variability in the aragonite shells of freshwater gastropods living in springs with nearly constant temperature and isotopic composition. Geochimica et Cosmochimica Acta **69**:3949-3966

Sosdian S, Gentry DK, Lear CH, Grossman EL, Hicks D, Rosenthal Y (2006) Strontium to calcium ratios in the marine gastropod Conus ermineus: Growth rate effects and temperature calibration. Geochem. Geophys. Geosyst. **7**:Q11023

Surge D, Walker KJ (2006) Geochemical variation in microstructural shell layers of the southern quahog (Mercenaria campechiensis): Implications for reconstructing seasonality. Palaeogeography, Palaeoclimatology, Palaeoecology **237**:182-190

Urey HC (1947) The thermodynamic properties of isotopic substances. Journal of the Chemical Society (Resumed) **1947**:562-581

Valentine (1960) Habitats and Sources of Pleistocene Mollusks at Torrey Pines Park, California. Ecology **41**:161

Wara MW, Anderson LD, Schellenberg SA, Franks R, Ravelo AC, Delaney ML (2003) Application of a radially viewed inductively coupled plasma-optical emission spectrophotometer to simultaneous measurement of Mg/Ca, Sr/Ca, and Mn/Ca ratios in marine biogenic carbonates. Geochem. Geophys. Geosyst. **4**:8406

Weber JN (1972) Temperature dependence of oxygen-18 concentration in reed coral carbonates. In: P.M.J. W (ed). Journal of Geophysical Research, pp 463-473

Chapter 2, in full, is currently being prepared for submission for publication of the material, Hatch, Marco B.A, Schellenberg, S.A. The dissertation author was the primary investigator and author of this material.

CHAPTER 3

ARTICLE IN PRESS

PALAEO-06071; No of Pages 10

Palaeogeography, Palaeoclimatology, Palaeoecology xxx (2012) xxx–xxx

Contents lists available at SciVerse ScienceDirect

Palaeogeography, Palaeoclimatology, Palaeoecology

journal homepage: www.elsevier.com/locate/palaeo

Ba/Ca variations in the modern intertidal bean clam *Donax gouldii*: An upwelling proxy?

Marco B.A. Hatch [a,*], Stephen A. Schellenberg [b], Melissa L. Carter [a]

[a] Scripps Institution of Oceanography, University of California, San Diego, La Jolla, CA 92093-0208, USA
[b] Department of Geological Sciences, San Diego State University, San Diego, CA 92182-1020, USA

ARTICLE INFO

Article history:
Received 30 April 2011
Received in revised form 8 February 2012
Accepted 8 March 2012
Available online xxxx

Keywords:
Barium
Upwelling
Primary productivity
Cross-dating
Laser ablation

ABSTRACT

The discovery and calibration of high resolution paleoceanographic proxies is necessary to extend historic climate records and to understand regional climate variability. Chemical variations of skeletal remains have emerged as an often reliable recorder of environmental conditions. Specifically, Ba/Ca ratios have been correlated to temperature, salinity, seawater Ba/Ca, and phytoplankton biomass, although, many of these relationships appear taxon- and location-specific. To assess the sub-weekly Ba/Ca variations in the intertidal shallow-burrowing bivalve *Donax gouldii*, specimens were collected from the Southern California Bight, skeletal growth increments were cross-dated based on tidal-driven growth patterns, and skeletal aragonite Ba/Ca was determined using laser ablation inductively coupled plasma mass spectrometry. Cross-dated growth among specimens revealed a simultaneous, large, and transient Ba/Ca peak in all shells. The timing of peak Ba/Ca was compared to a suite of locally measured physical and biological data, including temperature, salinity, density, nitrate, silicate, chlorophyll, diatom abundance, dinoflagellate abundance, and phytoplankton community composition. Based on cross-dated chronologies, Ba/Ca_{shell} is significantly correlated with Chl *a* from six and nine days prior and nutrients (nitrate, phosphate, silicate, and nitrite) from three days prior. In this system diatom abundance was not related to Ba/Ca_{shell}. Transiently higher seawater Ba/Ca resulting from upwelling may be reflected in peak Ba/Ca_{shell}, however the exact mechanisms leading to population wide Ba/Ca peaks remains enigmatic.

1. Introduction

Phytoplankton primary productivity supports a diverse array of marine ecosystems and sustains an important global carbon flux from the atmosphere into the deep ocean through the export production of organic matter (Behrenfeld et al., 2006). As anthropogenic global warming and ocean acidification progressively alter the global ocean system, scientific and policy communities would benefit from a more dynamic understanding of the myriad controls on primary productivity over both time and space (Sarmiento et al., 1998). One avenue for improving this understanding is the reconstruction of spatiotemporal variations during prehistoric climate regimes, and the comparison of such "proxy-based" data to computational models (Jones et al., 2001).

The concentration of barium (Ba) in seawater, marine sediments, and biogenic carbonates has long generated interest in the element's potential as a proxy for upwelling and thereby indirectly primary productivity (Bacon and Edmond, 1972; Lea and Boyle, 1989, 1991; Shaw et al., 1998). In the ocean, Ba typically displays a nutrient-type distribution with low concentrations in the mixed layer and increasing concentrations with depth due to remineralization and respiration (Chan et al., 1977). Higher bulk sediment Ba concentrations are common under regions of higher primary productivity (Goldberg and Arrhenius, 1958; Bacon and Edmond, 1972; Dehairs et al., 1980), and have been attributed to adsorption of dissolved barium onto iron oxyhydroxide substrates associated with diatom frustules (Sternberg et al., 2005) and direct precipitation of barite (Monnin et al., 1999). The flux of barite is not constant with depth and accumulates at mesopelagic depths, particularly under areas of high productivity (Dehairs et al., 1987, 1992). Higher Ba/Ca ratios within biogenic carbonate skeletons also correspond with higher seawater Ba concentrations; for example, elevated Ba/Ca is measured in the calcitic tests of planktonic foraminifera (Lea and Boyle, 1989) and the aragonitic skeletal layers of scleractinian corals when deeper Ba-rich water is upwelled (Lea et al., 1989; Alibert and Kinsley, 2008).

In bivalves, Ba/Ca_{shell} ratios along shell growth profiles are typically relatively low (i.e., <10 μmol/mol), and many contain population wide synchronous peaks (Stecher et al., 1996; Vander Putten et al., 2000; Gillikin et al., 2006; Barats et al., 2007; Gillikin et al., 2008; Barats et al., 2009; Thébault et al., 2009). Background Ba/Ca_{shell} is broadly consistent with ambient seawater Ba concentrations with a Ba seawater–shell partition coefficients of 0.07–0.18 for both calcite

* Corresponding author.
E-mail address: marco.hatch@gmail.com (M.B.A. Hatch).

0031-0182/$ – see front matter © 2012 Elsevier B.V. All rights reserved.
doi:10.1016/j.palaeo.2012.03.006

Please cite this article as: Hatch, M.B.A., et al., Ba/Ca variations in the modern intertidal bean clam *Donax gouldii*: An upwelling proxy? Palaeogeogr. Palaeoclimatol. Palaeoecol. (2012), doi:10.1016/j.palaeo.2012.03.006

and aragonite (Gillikin et al., 2006, 2008). In the aragonitic *Saxidomus giganteus*, ten years of continuous Ba/Ca_{shell} show remarkably synchronous inter-individual variability, suggesting that Ba/Ca_{shell} is related to some environmental parameter (Gillikin et al., 2008). A common working hypothesis, first proposed by Stecher et al. (1996), attributes such peaks to increased ingestion of Ba-rich phytoplankton (e.g., diatoms (Sternberg et al., 2005)) or suspended barite precipitates with subsequent internal transport via the hemolymph into the extrapallial fluid and thereby the shell structure. This diatom-diet-based hypotheses is supported by Vander Putten et al. (2000), who argued for a positive correlation between ambient chlorophyll *a* (Chl *a*) and Ba/Ca_{shell} in the temperate North Atlantic mussel *Mytilus edulis*, and by Thébault et al. (2009), who demonstrated a significant positive correlation between ambient Chl *a* and Ba/Ca_{shell} in the tropical New Caledonian scallop *Comptopallium radula*. Importantly, both studies assumed that gross Chl *a* concentrations were a sufficient proxy for the often complex variability in phytoplankton biomass and diversity — an assumption that can be problematic given that Chl *a* concentrations do not offer taxonomic identification, vary widely between phytoplankton species and are influenced within species by ambient environmental conditions such as light, temperature, and nutrients (Mullin et al., 1966; Chan, 1980; Cullen, 1982; Geider, 1987). In contrast, Gillikin et al. (2008) found no relationship between Chl *a* and Ba/Ca_{shell} in the temperate North Atlantic scallop *Pecten maximus*.

If Ba/Ca_{shell} does reliably record environmental conditions (e.g., diatom blooms, upwelling), then historic (e.g., museum, archaeological, and geological) shells could be exploited to characterize the frequency with which phytoplankton blooms occur and their constituent taxa. Previous studies have been limited in their ability to precisely date bivalve growth increments (i.e., to quasi-daily-resolution) suffering from uncertainties associated with growth increment back-counting (e.g., missed increments due to growth shutdown, false increments due to disturbance) (Thébault et al., 2009). Such dating errors can be greatly reduced, if not avoided, by utilizing the dendrochronology method of cross-dating, which aligns individual growth increments within and among specimens in the time-domain. Cross-dating, in combination with high sampling resolution via laser ablation techniques and sufficient ambient environmental monitoring of nutrient concentrations and phytoplankton dynamics could provide important constraints on the potential environmental causes of Ba/Ca_{shell} peaks.

The aim of the study is to assess relationships between sub-weekly-to-daily variations in monitored environmental conditions (i.e., phytoplankton dynamics, nutrient measurements, temperature and salinity variations) and Ba/Ca variation in cross-dated *D. gouldii* shells via laser ablation inductively coupled plasma mass spectrometry (LA-ICP-MS). *D. gouldii* is a relatively small (<25 mm) and short-lived (<3 years) aragonitic bivalve that inhabits the swash zone of sandy open coast beaches from Point Conception, California to Acapulco, Mexico (Coe, 1955). This species is an ideal candidate for cross-dating given its distinct sub-annual growth increments. *D. gouldii* shells are common in late Holocene Native American middens (Gallegos, 2002) as well as wave-cut terrace deposits from oxygen isotope stages 5a (~85 ka) and 5e (~125 ka) (Valentine, 1960; Gallegos, 2002).

2. Methods

2.1. Location and oceanographic context

The Southern California Bight is characterized as a seasonally stratified oceanographic regime wherein wind-driven upwelling provides dissolved nutrients to the mixed layer. Along the shallow coastal waters off of the Scripps Institution of Oceanography (SIO) (Fig. 1A), regional wind-driven upwelling indices are poorly

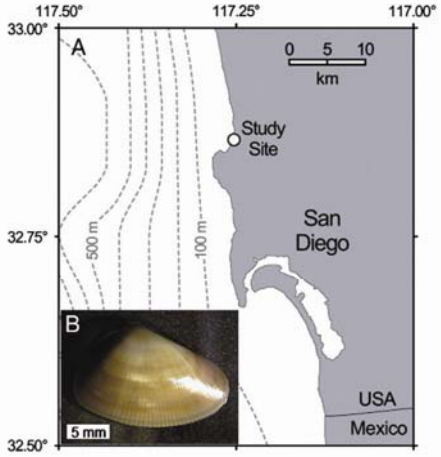

Fig. 1. (A) Map of San Diego County with Scripps Institution of Oceanography pier and beach marked as "Study Site". All environmental data come from the Scripps Institution of Oceanography pier and all *D. gouldii* were collected within 100 m of the pier. (B) Image of adult *D. gouldii* valve.

correlated with local chlorophyll *a* (Chl *a*), sea surface temperature (SST), and sea surface salinity (SSS). In addition, local phytoplankton blooms are significantly correlated in timing, but not magnitude, to phytoplankton blooms at the nearest California Cooperative Fisheries Investigation station (CalCoFI station 93.27; 18 km offshore). However, local blooms are not correlated to the CalCoFI stations farther offshore or to regional upwelling indices (Kim et al., 2009). Based on these observations, Kim et al. (2009) proposed that local dissolved nutrient delivery, and thereby local productivity, were less related to regional wind-driven upwelling and more related to a combination of internal waves, longshore transport, and cross-shore transport. Given the lack of correlation with offshore stations, we chose to focus on local records of ambient environmental conditions from the SIO Pier rather than using offshore buoy- or satellite-derived data.

2.2. Temperature and salinity time-series

Temperature and salinity samples were taken daily from sea surface and five meters water depth at SIO Pier as part of the Shore Station Program (http://shorestation.ucsd.edu). Temperature was measured by immersing a calibrated thermometer in a bucket sample and reading to 0.1 °C. Salinity was determined from a Guildline inductive salinometer (Model 8410) using the algorithms for the 1979 Practical Salinity Scale (UNESCO, 1981). SIO Pier five meter salinity and temperature data were used to calculate seawater density (σ_T).

2.3. Chlorophyll, nutrients and phytoplankton cell counts

Sea surface water samples for Chl *a* and nutrients were collected twice per week (typically Monday and Thursday) and weekly phytoplankton cell counts were done at the SIO pier as part of the Southern California Coastal Ocean Observing System, Harmful Algal Bloom Monitoring Program (http://www.sccoos.org/data/chlorophyll/index.php). Chl *a* values were obtained using standard chlorophyll extraction and analysis procedures outlined by (Venrick and Hayward, 1984) in which seawater was filtered using a ~0.7 μm glass fiber filter and photosynthetic pigments were extracted by soaking in 10 mL of 90% acetone for 24 h before concentration was determined on a calibrated Turner

Please cite this article as: Hatch, M.B.A., et al., Ba/Ca variations in the modern intertidal bean clam *Donax gouldii*: An upwelling proxy? Palaeogeogr. Palaeoclimatol. Palaeoecol. (2012), doi:10.1016/j.palaeo.2012.03.006

10 AU fluorometer. Dissolved nutrient concentrations were collected using acid-washed plastic containers and were filtered through ~0.7 glass fiber filters to remove particulates before being stored frozen at −20 °C. Nutrient analyses (phosphate, silicate, nitrate + nitrite, nitrite, and ammonia) were performed on a Seal Analytical continuous-flow AutoAnalyzer 3 (AA3) following standard methods (Armstrong et al., 1967; Atlas et al., 1971; Hager et al., 1972; Gordon et al., 1992). Abundance of all diatoms and dinoflagellates greater than 5 μm in diameter and other specific taxa related to the harmful algal bloom program (e.g., *Lingulodinium polyedrum*, *Gymnodinium* spp., *Pseudo-nitzchia* spp.) were determined from settling 10–50 ml of seawater preserved with 4% formaldehyde (Utermöhl, 1958; UNESCO, 1981). Cells were identified and tallied to the lowest feasible taxonomic level through a phase-contrast, inverted light microscope at 200×. Sample volume varied between 1.25 ml and 25 ml (1/8 to 1/2 of slide) and detectable cell abundance was between 80 and 800 cells/L, depending on cell size. To increase overlap with the cross-dated Ba/Ca_{shell} data, each nutrient measurement, Chl *a* measurement, and phytoplankton count were assumed to be representative of the day before and after their specific collection.

2.4. Specimens collection and preparation

D. gouldii were collected from the sandy shoreline of the Scripps Coastal Reserve within 100 m from the SIO Pier during lower low tides (e.g., <0.2 m Mean Lower Low Water (MLLW)) from February 2008 to July 2008 (Fig. 1A). Unlike other species of this genus, *D. gouldii* does not markedly migrate with the tidal level, but is consistently most densely distributed between 0.3 and 0.1 m MLLW (Haderlie and Abbott, 1980; Ellers, 1995). Specimens from the following dates were selected for cross-dating: 22 February (n = 2), 23 March (n = 3), 14 April (n = 2), 21 May (n = 2), 9 June (n = 2), and 8 July (n = 8). For each specimen, one valve was thin sectioned by embedding in epoxy (Fig. 1B), cut along the maximum growth axis with a Buehler IsoMet 5000 Linear Precision Saw, and hand-polished with 3M WetorDry Sandpaper (320, 600, 800, and 1000 grit) using a duct-tape manipulator (Carpenter, 1998) to a final thickness of ~100 μm. Four additional specimens were selected from the 8 July collection were thin sectioned to final thickness of ~800 μm for laser ablation.

For digital growth increment measurement, shells were imaged with a Paxcam digital microscope camera (http://www.paxcam.com/) attached to a Leica MZ16 microscope using transmitted-light dark-field illumination at 50× magnification producing 10–20 images per shell. Images were manually mosaiced into a single image using in Adobe Photoshop CS (http://www.adobe.com/). Under these conditions, growth increments within *D. gouldii* are characterized by thin (~6 μm) and light (more transparent) regions bounded by thicker (~30 μm) and darker (more opaque) regions (Fig. 2).

2.5. Cross-dating

Cross-dating ordinates discrete growth increments within and among specimens into a common time-domain. The method is based on the presumption that ambient environmental variability will produce a common and congruent growth-increment pattern among contemporaneous specimens (Yamaguchi, 1991; Black et al., 2005, 2008). For example, at an annual scale, an environmentally favorable year would result in a relatively wide annual growth increment, whereas an environmentally unfavorable year would result in a relatively narrow annual growth increment. Cross-dating utilizes such environmental-induced variation in growth increment widths to align individual samples' time-series of growth-increment widths into a common time-series for the broader population. Individual growth-increment time-series can be incorrectly documented by including false growth increments (e.g., those related to isolated disturbance) or by missing true, but faint, growth increments. Cross-dating effectively identifies such errors as deviations from the population-level growth-increment time-series. Thus, spurious "missing" or "extra" growth increments within an individual can be identified and corrected based on their deviation from prevalent growth-increment pattern. Cross-dating is routinely applied to annual growth increments of trees, rockfish, and long-lived bivalves (Black et al., 2009), and is applied here to growth increments with fortnightly to lunar day periodicity. This study cross-dated *Donax* specimens using two methods: (1) a variation of the traditional "list-year" method and (2) statistical quantification of growth-increment time-series congruence using standard dendrochronology methods.

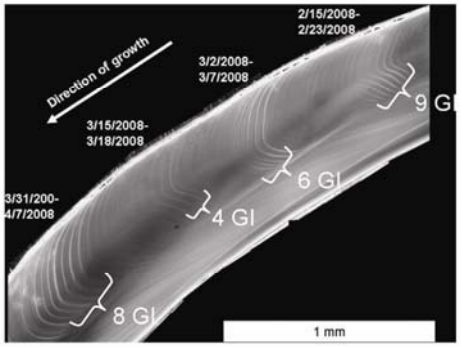

Fig. 2. Image of *D. gouldii* thin section used for crossdating. Four pronounced bundles of growth increments are shown with number of growth increments listed to the right and dates listed to the left. Note in this close-up image with the direction of growth listed, the umbo is to the right and commissure is to the left.

In species with annual growth increments, the "list-year" method requires the initial identification of growth increments which are anomalously wide or narrow and shared among the sample population. These anomalous annual growth increments are then dated by back-counting of annual growth increments from the growth-margin back to the anomalous annual growth increment. If dating of anomalous growth increments is consistent among specimens, then the working hypothesis that these anomalous annual growth-intervals are synchronous among specimens is supported. For an overview of this method as applied to bivalves, see (Black et al., 2008).

For *D. gouldii*, this "list-year" method was modified into a "list-lunar-day" method and applied to randomly selected specimens from each collection date. In thin section, *D. gouldii* shells consisted of intervals of pronounced bundles (PB) of distinct growth increments separated by intervals of poorly resolved growth increments (Fig. 2). These alternations limited assignment of lunar dates by back-counting to the PB immediately adjacent to the shell commissure. For a given collection date, the number of growth increments within the commissure adjacent PB was constant. For example, within their respective commissure-adjacent PBs, all specimens from 9 June consistently contained six growth increments, whereas all specimens from 21 May consistently contained three growth increments (Fig. 3A–B). Based on these consistent patterns, inner PBs in specimens from later collection dates were matched to commissure-adjacent PBs from earlier collections, which then allowed lunar day assignment to each distinct growth increment within each PB within each specimen (Fig. 3).

To quantitatively test cross-dating, a continuous string of growth-increment widths was created by digitally marking each clear growth increment starting from the commissure and working toward the

Please cite this article as: Hatch, M.B.A., et al., Ba/Ca variations in the modern intertidal bean clam *Donax gouldii*: An upwelling proxy? Palaeogeogr. Palaeoclimatol. Palaeoecol. (2012), doi:10.1016/j.palaeo.2012.03.006

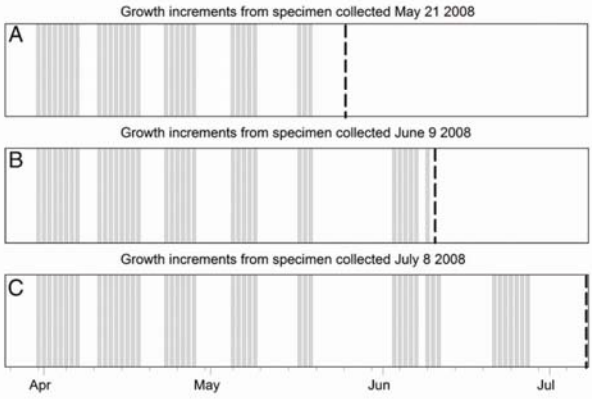

Fig. 3. Graph of dated growth increments from three collections, (A) May 21, 2008, (B) June 9, 2008, and (C) July 8, 2008. All graphs use a vertical bar to represent a growth increment with a dashed bar for the collection date of specimens.

umbo. The resulting growth-increment string consisted of numbered growth increment widths, with sections of poorly resolved growth between each pair of PBs being treated as a single growth increment. Growth increments were marked at the growing edge and measured using the ObjectJ plugin (Vischer, 2011) for ImageJ (Rasband, 1997–2011). Cross-dating was statistically verified using the dendrochronology program COFECHA (available from the International Tree-Ring Data Bank Dendrochronology Program Library; http://www.ltrr.arizona.edu/software.html). The COFECHA program first detrends each chronology to remove ontogenetic effects using a cubic spline with a 50% frequency response of 32 increments. COFECHA then correlates each numbered growth-increment width to the average width for that growth-increment number with low correlations indicating potential cross-dating errors. Finally, the overall agreement of all chronologies is statistically quantified and expressed as a series intercorrelation value, which measures the relative strength of a common signal among all chronologies. The series intercorrelation has been shown to be highly sensitive to dating errors (Black et al., 2008). Once final chronologies had been determined, lunar dates were assigned to each distinct growth increment using methods analogous to those for the "list-lunar-day" cross-dating. Then dating was compared between the both cross-dating methods to verify dating congruence. Finally, lunar days were converted to calendar day by defining a lunar day as 24.8 h.

2.6. Laser ablation for Ba/Ca determination

Ba/Ca variations along the growth profile of four *D. gouldii* specimens selected from the same age class collected on 8 July 2008 were determined using a New Wave UP-213 laser ablation system coupled to a Finnigan MAT Element 2 Sector Inductively Coupled Plasma Mass Spectrometer (ICP-MS) at the University of California, Santa Barbara. Ablation paths followed the central portion of observable growth increments within the prismatic layer, from the umbo to the commissure, and were spaced every 300 μm for specimens A and B and every 900 μm for specimens C and D. *D. gouldii* shells measured 17.1, 21.8, 18.2, 19.2 mm from anterior to posterior for specimens A, B, C, and D, respectively. All ablations were continuous scans, covering 100 μm using a 70 μm spot, taken parallel to growth increments, representing roughly one lunar day of biomineralization. Nuclide concentrations were calibrated against a carbonate-optimized in-house liquid standard for Ba/Ca (342.0 μmol/mol ± 3.4 (1.0% RSD)) (Zacherl et al., 2003). A solid glass (NIST 612) and carbonate (USGS MACS3) standard reference materials were run periodically to check analytical precision or repeatability. Average relative standard deviation for Ba/Ca ($n = 24$) was 6.6% (129.0 μmol/mol ± 8.5) for NIST 612 and 8.5% (47.6 μmol/mol ± 4.1) for USGS MACS3. The laser was operated at a repetition rate of 10 Hz with an RF power of 1200 W. The nebulizer flow rate of argon was 0.8 L min^{-1} and 0.5 ml min^{-1} through the sample chamber.

2.7. Statistical analysis

To increase temporal matches of the weekly to bi-weekly environmental data with the cross-dated Ba/Ca_{shell} data, each environmental datum was assumed to also be representative of the day before and after its specific collection date. In addition, because some temporal lag between environmental conditions and shell chemistry is reasonable and expected based on physiological principles (e.g., for the diet-based Ba/Ca causal mechanism of Stecher et al. (1996)) the dependent Ba/Ca variable was compared to each independent environmental variable from the same date as Ba/Ca_{shell}, three days prior, six days prior, and nine days prior using Pearson Product Moment Correlation Coefficients (PPMCCs).

3. Results

3.1. Cross-dating

Cross-dating was successfully applied to six *D. gouldii* specimens from the 8 July 2008 collection date, resulting in a series intercorrelation value of 0.937 based on the intercomparison of 299 growth increments. This chronology contained nine distinct PBs that contained between four and nine growth increments. The final master cross-dated chronology comprised of all specimens (22 February (n = 2), 23 March (n = 3), 14 April (n = 2), 21 May (n = 2), 9 June (n = 2), and 8 July (n = 8)) had a series intercorrelation of 0.845 based on 702 growth increments.

Using this master cross-dated chronology, the 75 laser ablations for the four specimens from the 8 July 2008 collection were ordinated in the time-domain by referencing the nearest resolvable growth increment or, if the ablation was located within a region of poorly-defined growth increments (i.e., neap tide conditions), by assuming

Please cite this article as: Hatch, M.B.A., et al., Ba/Ca variations in the modern intertidal bean clam *Donax gouldii*: An upwelling proxy? Palaeogeogr. Palaeoclimatol. Palaeoecol. (2012), doi:10.1016/j.palaeo.2012.03.006

a constant daily growth rate between the dated growth increments of the adjacent PBs.

3.2. Shell geochemistry

Ba/Ca_{shell} from 75 laser ablations for the four specimens ranged from 2.0 to 11.3 μmol mol^{-1} with a mean of 3.9 μmol mol^{-1} (±1.7). Based on cross-dating, six of the eight peak values (defined as > 1 SD above the mean) occurred between 28 March 2008 and 3 April 2008 with values ranging from 6.4 to 11.3 μmol mol^{-1} (Fig. 4A). The other two peak Ba/Ca values occurred on 21 May and 1 June with values of 7.5 and 5.7 μmol mol^{-1}, respectively. Pre-peak (11 February–27 March) values averaged 3.6 (±0.7) μmol mol^{-1}, while post-peak (4 April–8 July) values averaged 3.5 (±1.2) μmol mol^{-1} and are more variable. These 75 Ba/Ca determinations cover 147 days of biomineralization (2/11-7/8) averaging one measurement every two days.

3.3. Physical and biological environment

During the study interval, SST varied from 13.2 to 23.7 °C and SSS was relatively constant with a mean of 33.69 PSU (±0.15) (Fig. 4B). Seawater density (σ_T) averaged 24.56 and varied from 22.80 to 25.64 (Fig. 4C). Nitrate and silicate both showed a transient peak on 27 March 2008 of 8.83 and 10.65 μmol/L, respectively (Fig. 5D). Seawater density (σ_T) at five meters was 25.14 on 27 March, the same date increased nitrate was observed, and values of >25.1 are associated with increased levels of nitrate (Parnell et al., 2010). The extended Redfield ratio of nitrate:silicate is roughly 1:1, suggesting that these nutrients were recently brought to the surface mixed layer (Dugdale and Wilkerson, 1998).

The dinoflagellate, *Lingulodiuium polyedrum*, reached peak abundance on 17 March 2008 (80.6×10^3 cells/L) and was responsible for the majority of the aforementioned Chl *a* peak (Fig. 5B). The increase in *L. polyedrum* is also seen in the total count of dinoflagellates, which peaks between 3 March 2008 (136.8×10^3 cells/L) and 24 March 2008 (134.4×10^3 cells/L) (Fig. 5B and C) with an average of 7.3×10^4 cells/L. A second increase in dinoflagellates occurred on 28 April and 12 May 2008, however, *L. polyedrum* remained low (Fig. 5C).

Total diatoms averaged 5.1×10^5 cells/L and peaked three times through the study interval, with a relatively small peak on 31 March 2008 (61.0×10^4 cells/L), a larger peak on 5 May 2008 (21.1×10^5 cells/L), and the largest peak on 2 June 2008 (22.1×10^5 cells/L). The chain-forming diatoms *Chaetocerous* spp. and *Leptocylindrus* spp. visually dominated the 31 March and 5 May peaks (Carter, pers. Ob.) and the 2 June peak was dominated by small, narrow cells of *Pseudo-nitzschia* spp. (*delicatissima* group, frustule width <3 μm, length <50 μm) (Fig. 5C).

Chl *a* varied from 1.5 to 11.6 mg m^{-3} with the highest value on 17 March 2008 followed by a steady decline to 3.4 mg m^{-3} on 3 April 2008 (Fig. 5B). Chl *a* had a second smaller peak on 28 April of 7.2 mg m^{-3}. Over the entire study interval, Chl *a* and dinoflagellates were strongly correlated ($r^2=0.72$, $p<0.0001$), whereas Chl *a* was weakly correlated with diatoms ($r^2=0.07$, $p=0.29$) and total cell count ($r^2=0.15$, $p=0.11$).

3.4. Correlations between environmental variables to Ba/Ca_{shell}

The Pearson Product Moment Correlation Coefficients (PPMCCs) method was used to test correlations between Ba/Ca_{shell} and fifteen environmental variables from the same day as Ba/Ca_{shell} , three days prior, six days prior and nine days prior (Table 1). Of the sixty correlations performed, the six found to be significant ($p<0.01$) are nitrate, nitrite phosphate, silicate from three days prior and Chl *a* from six and nine days prior (Table 1).

4. Discussion

4.1. Cross-dating

Dendronchronlogy methods designed to date annual growth increments are here successfully modified and applied to lunar day

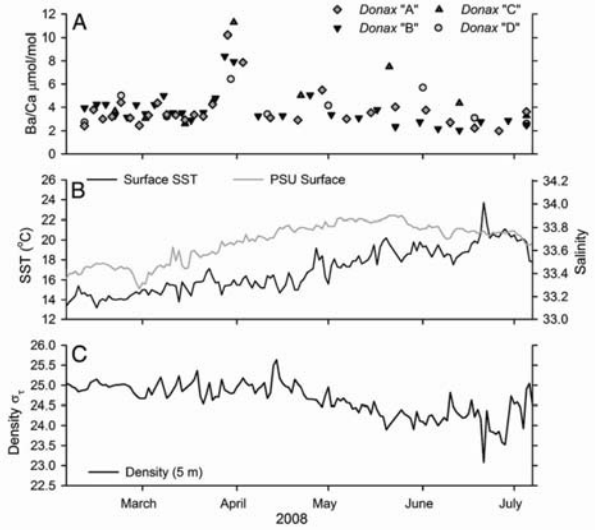

Fig. 4. (A) Ba/Ca determinations of four *D. gouldii* shells collected on 8 July 2008 orientated in time by cross-dating. *D. goudlii* shells displayed a common peak in Ba/Ca from 28 March 2008 and 3 April 2008, reaching values of up to 11.29 μmol mol^{-1}. Non-peak Ba/Ca values averaged 3.47 μmol mol^{-1}. (B) Temperature and salinity from daily measurement made at SIO pier by the Shorestation Program. (C) Seawater density as determined from temperature and salinity.

Please cite this article as: Hatch, M.B.A., et al., Ba/Ca variations in the modern intertidal bean clam *Donax gouldii*: An upwelling proxy? Palaeogeogr. Palaeoclimatol. Palaeoecol. (2012), doi:10.1016/j.palaeo.2012.03.006

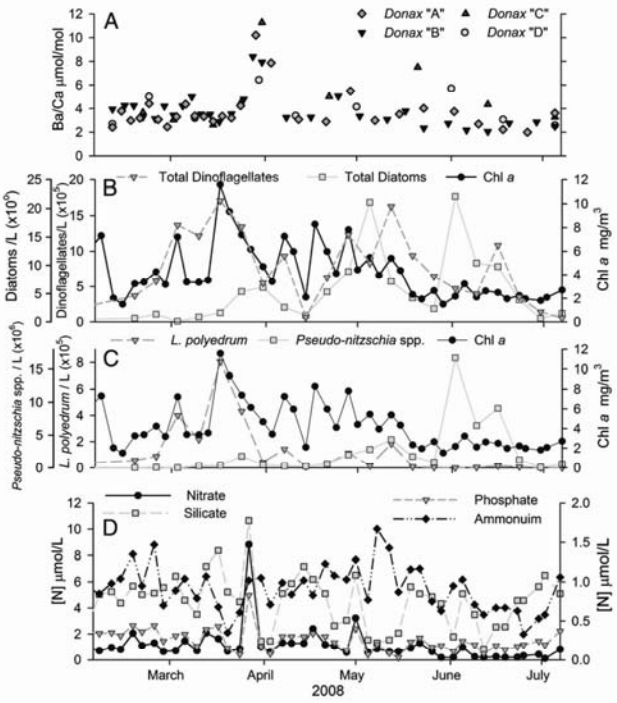

Fig. 5. (A) Ba/Ca determination of four *D. gouldii* shells collected on 8 July 2008. (B)Total diatom and dinoflagellate counts, total dinoflagellates peaked twice, once in March and once in May. While total diatoms had three peaks the largest in early June. Dinoflagellates were primarily responsible for the Chl *a* peak seen in late March. Note diatoms and dinoflagellates are on separate axis. (C) Counts of *L. polyedrum* dinoflagellates and *Pseudo-nitzschia* spp. diatoms with Chl *a* plotted against the right y-axis. (D) Concentrations of nitrate and silicate on the left y-axis and phosphate and ammonium on the right y-axis.

growth increments. The resulting master cross-dated chronology created from 29 specimens collected between 22 February and 8 July 2008 including 702 growth increments had a series intercorrelation value of 0.845. Although a standard threshold value to assess the strength of series intercorrelation values has not been established, values greater than 0.70 are considered high and have been observed in other bivalves (Black et al., 2008).

As a comparison between cross-dating and dating based on assumed constant linear growth, a "constant-growth" date for peak Ba/Ca was determined by linearly dating shells between the collection date (8 July) and the last cross-dated growth increment (11 February). As determined by cross-dating, the large Ba/Ca peak occurred between 28 March and 3 April, whereas the constant-growth-based approach placed this peak between 5 April and 1 May. Thus, if constant growth was used to date growth increments, shell-environmental correlations would be off by more than a month, and peaks in Ba/Ca_{shell} would not be synchronous.

While no quantitative sub-annual study comparing growth-increment back-counting to cross-dating could be found, Black et al. (2008) compared cross-date-determined ages to back-count-determined ages for 432 geoduck bivalves (*Panopea abrupta*) from British Columbia, Canada finding that ages agreed for only 21% of the samples. For the remaining specimens, cross-date-determined ages were younger than the back-count determined age in 72% of the shells and 21% of the shells had older cross-dated-determined ages than the back-counting-determined ages.

Even in shells with clear sub-annual banding, the ability to reliably date growth increments by back-counting is limited due to growth irregularities from to disturbance and shutdown, e.g., Schöne et al. (2002). Additionally, back-counting does not provide a statistical

Table 1
Pearson product moment correlation coefficients for cross-dated Ba/Ca and environmental variables, significant ($p<0.01$) correlations are in bold and number of sets used in parentheses. Offset refers to the number of days *Donax* Ba/Ca date were moved back in time.

Offset	0 day	−3 day	−6 day	−9 day
Chlorophyll *a*	0.07 (62)	0.23 (67)	**0.41 (60)**	**0.54 (62)**
Nitrate	0.30 (62)	**0.68 (67)**	0.27 (60)	0.06 (62)
Phosphate	0.00 (62)	**0.50 (67)**	−0.13 (60)	−0.11 (62)
Silicate	−0.18 (62)	**0.42 (67)**	0.15 (60)	0.17 (62)
Nitrite	0.04 (62)	**0.46 (67)**	0.03 (60)	−0.09 (62)
Ammonium	0.13 (62)	0.10 (67)	−0.17 (60)	−0.10 (62)
Total diatoms	0.28 (27)	−0.17 (30)	0.21 (30)	−0.23 (21)
Pseudo-nitzschia spp.	0.05 (27)	−0.31 (30)	0.38 (30)	−0.30 (21)
Total dinoflagellates	−0.24 (27)	0.14 (30)	0.39 (30)	0.32 (21)
L. polyedrum	−0.26 (27)	0.15 (30)	0.44 (30)	0.35 (21)
SST	−0.12 (73)	−0.09 (75)	0.00 (75)	−0.10 (75)
Salinity	0.07 (73)	0.04 (75)	0.05 (75)	−0.05 (75)
Density (bottom)	0.15 (73)	0.09 (74)	0.14 (73)	0.19 (75)

Please cite this article as: Hatch, M.B.A., et al., Ba/Ca variations in the modern intertidal bean clam *Donax gouldii*: An upwelling proxy? Palaeogeogr. Palaeoclimatol. Palaeoecol. (2012), doi:10.1016/j.palaeo.2012.03.006

framework to relate growth increments between shells from the same collection nor does it allow for shells with different collection times to be correlated. In contrast, cross-dating allows shell chronologies to span areas of growth shutdown and irregularities with an exact date assigned to growth increments. Cross-dating growth increments provides a dating based on an exogenous environmental rhythm compared with matching instrumental seawater temperature to shell based temperature which can be prone to time-averaging and seawater $\delta^{18}O$ variations (Goodwin et al., 2004).

4.2. Relationship among chlorophyll a and phytoplankton

Phytoplankton community data are necessary to interpret Chl *a* measurements with respect to species composition and abundance. In coastal San Diego, phytoplankton blooms are commonly dominated by diatoms and/or dinoflagellates (Allen, 1920). Over a majority of the study period, diatoms were roughly seven times more abundant than dinoflagellates, however, peaks in Chl *a* resulted from increased dinoflagellates, including the increase in Chl *a* during 17 March–7 April which was driven by an increase in the dinoflagellate *L. polyedrum*. The phytoplankton community data show two peaks in dinoflagellate abundance roughly equal in size. The first peak occurred in mid-March, coinciding with a large Chl *a* peak, was dominated by *L. polyedrum*. The second peak occured in late April to early May, dominated by *Akashiwo sanguinea, Prorocentrum* spp., and *Ceratium* spp., and did not coincide with a large Chl *a* peak. Diatom cell abundance through the study interval showed three peaks, with the first two peaks (24 March and 5 May) dominated by *Chaetocerous* spp. and *Leptocylindrus* spp. and the third much larger peak (2 June) dominated by *Pseudo-nitzchia* spp. within the delicatissima group. None of these three diatom cell abundance peaks coincided with a marked increase in Chl *a*. However, the first diatom peak coincided with the largest influx of nitrate (8.83 μmol/L) and silicate (10.65 μmol/L) during the study interval, indicating that this water parcel recently arrived to the euphotic zone, and the second diatom peak occurred with the second highest influx of nitrate (3.22 μmol/L). Thus, weekly-resolution phytoplankton assemblages are influenced by nutrient input, but are poorly related to the available bi-weekly-resolution Chl *a* concentration. Prior studies at this location have also found increased diatom abundance associated with the influx of nitrate near the coast (Kamykowski, 1974; Goodman et al., 1984) and negative sea surface temperature anomalies prior to nutrient peaks (Allen, 1920).

Chl *a* concentration and phytoplankton cell abundance are two parameters used to estimate phytoplankton biomass. Chl *a* is used to estimate phytoplankton biomass based on assumptions to the amount of Chl *a* per cell and size of cells, whereas cell counts directly enumerate the abundance of cells per liter. Chl *a* based biomass estimates can vary independently of actual biomass due to size of cell, health, life stage, and taxonomy of the cells, as well as current growing conditions including light and nutrients. Therefore different growing conditions and stages as well as changes in plankton communities can alter these estimates of biomass. Based on size-fractionated chlorophyll measurements from the SIO Pier (unpublished M. Carter), on average 67% of the chlorophyll biomass consists of phytoplankton greater than 3 μm. Due to variability in phytoplankton species composition, the hypothesis that increased chlorophyll concentration is driven by increased diatom abundance is not valid in this area. Increases in chlorophyll concentration may also be due to increased abundance of dinoflagellates or picoplankton which may not be related to upwelling events.

In the study region, local productivity and nutrient delivery is controlled by local events (e.g., internal waves, tidal bores, and longshore transport) rather than regional wind-driven upwelling. Thus, any attempt to use regional datasets (e.g., CalCOFI, satellite-derived SST, Chl *a*) would lead to an erroneous correlation of these data to local shell-derived patterns. Without local records, calibrating shell based signals to environmental variability can lead to false correlations.

4.3. Relation of Ba/Ca_{shell} to phytoplankton

Ba/Ca_{shell} was significantly correlated to the Chl *a* from six and nine days prior; a finding consistent with other studies of bivalves To test the degree to which these correlations were driven by peak values, the two highest Chl *a* measurements (11.6 and 9.3 mg/m^3) were removed from the analysis and both correlations remained significant. Ba/Ca_{shell}–Chl *a* correlation is not dependent on one co-occurring peak but appear to remain significant for the entire study period.

The dinoflagellate *L. polyedrum* was highly abundant just prior to peak Ba/Ca_{shell} (Fig. 5) however, no significant relationship between *L. polyedrum* abundance and Ba/Ca_{shell} was found. Total dinoflagellate abundance showed two large peaks, one about a week before peak Ba/Ca_{shell} and one six weeks after (Fig. 5B). Diatom cell abundance and Ba/Ca_{shell} were not significantly correlated; diatoms were found in high abundance on 28 April, 12 May, 2 June, and 9 June, but none of these dates were associated with markedly elevated Ba/Ca values (Fig. 5B).

4.4. Relation of Ba/Ca_{shell} to physical environment

Ba/Ca_{shell} was significantly positively correlated with nitrate, phosphate, silicate, and nitrite from three days prior. Nitrogen and phosphate are two important macronutrients necessary for phytoplankton growth. Nitrate, nitrite, and phosphate have a nutrient-type vertical profile with low concentration in surface water and increased concentration below the mixed layer. High concentrations of nitrate in surface waters, as seen in late March, suggests recently upwelled water. At depth, silicate and nitrate occur in a nearly 1:1 ratio, but in the mixed layer nitrate is quickly scavenged. Using this 1:1 relationship, silicate can be used as proxy for the nitrate content of water before it advected into the mixed layer and can be used to date the relative age of upwelled water (Dugdale and Wilkerson, 1998). For example, the peak in nitrate in late March is nearly equal in concentration to silicate, indicating that the water parcel was recently upwelled. If the water parcel was upwelled a relatively longer time ago, then it would be expected that silicate would remain high and nitrate would be low. Recently upwelled water would also contain relatively higher concentrations of other elements not quantified in this study (e.g. barium) compared to other surface waters. Ammonium was not significantly correlated with Ba/Ca_{shell}. The oxidation of ammonium to nitrite occurs in surface waters and is typically associated with recycled productivity.

In this study, *D. gouldii* were collected from a well-mixed sandy-beach environment far from any freshwater point-source and salinity was relativity constant throughout the study interval with no major deviations during intervals of elevated Ba/Ca_{shell}. The nearest rainfall measured at the SIO pier occurred two weeks (16 March) before the elevated Ba/Ca_{shell} with 0.31 cm of precipitation in a day,. During peak Ba/Ca_{shell}, factors which would result in increased ground water discharge (seismic activity or upland precipitation) remained constant. Thus, a freshwater-related mechanism (via an assumed inverse relationship between salinity and seawater Ba/Ca ratios; e.g., Gillikin et al. (2006)) cannot be invoked to explain the observed Ba/Ca_{shell} peaks. Temperature has been reported to be positively related to Ba/Ca_{shell} in larval oysters (Carson, 2010) and negatively related to Ba/Ca_{shell} in larval gastropods (Zacherl et al., 2003). In this study, temperature is weakly negatively correlated with Ba/Ca_{shell} and no temperature deviation coincided with the observed major Ba/Ca peak.

In coastal San Diego, seawater density can be used as a proxy for nitrate, although the dynamics tend to be non-linear (Parnell et al.,

Please cite this article as: Hatch, M.B.A., et al., Ba/Ca variations in the modern intertidal bean clam *Donax gouldii*: An upwelling proxy? Palaeogeogr. Palaeoclimatol. Palaeoecol. (2012), doi:10.1016/j.palaeo.2012.03.006

2010). Typically the nutricline is at densities around 25.1 σ, with <25.1 σ_T water being nitrate-poor and >25.1 σ_T being nitrate-rich. The late March peak in nitrate and silicate occurs at the same time seawater density is >25.1 σ, suggesting that this nutrient peak was due to upwelling rather than runoff- or groundwater-related nutrient input (Fig. 3C).

The question remains whether the peaks in Ba/Ca_{shell} are related to changes in phytoplankton communities or to changes in nutrient concentrations, driven by upwelling, or to a yet to be determined driver not quantified in these data.

4.5. Potential mechanisms to explain Ba/Ca peaks

Ba/Ca variations in biogenic carbonates have been attributed to a plethora of environmental and biological factors including proximity to riverine and groundwater supply (Shaw et al., 1998; Carroll et al., 2009), seawater temperature (Zacherl et al., 2003, 2009; Carson, 2010), gonad development and spawning (Gillikin et al., 2006), seawater Ba/Ca concentrations (Lea et al., 1989), and diatom abundance (Thébault et al., 2009). The inverse relationship between salinity and Ba/Ca seawater is reflected in Ba/Ca_{shell}, for example, Gillikin et al. (2006) found a negative relationship between salinity and background Ba/Ca_{shell} in estuarine-reared *Mytilus edulis* shells. Based on environmental data, we find no support for either a salinity- or temperature-based mechanism for the observed Ba/Ca_{shell} peak. Elevated bivalve Ba/Ca has also been hypothesized to result from internal remobilization of Ba from tissues to skeletal carbonate during spawning (Gillikin et al., 2006). In *D. gouldii*, specimens with shell lengths of less than 9 mm typically do not have differentiated gametes and specimens over 9 mm could be part of the spawning population (Winter and Hatch, 2010). To assess the shell lengths for the four specimens when the major Ba/Ca peak was observed, a *D. gouldii* shell height:length relationship was calculated (height = 0.65 × length − 0.045, $r^2 = 0.98$) based on 47 specimens ranging in length from 5.25 to 20.8 mm. Using this relationship and the analyzed thin sections, the length of the analyzed shells A–D during their observed Ba/Ca peaks were estimated at 13.3, 12.4, 11.8, and 13.6 mm, respectively. Based on these data, the *D. gouldii* specimens would have had differentiated gonads and could have spawned. However, *D. gouldii* are serial broadcast spawners (Haderlie and Abbott, 1980) and likely would have spawned multiple times during the represented four months of life. Thus, if spawning was responsible for elevated Ba/Ca values, multiple elevated Ba/Ca values or at least a step-wise increase in "background" Ba/Ca values would be expected, and no such pattern was observed. Therefore, similar to Gillikin et al. (2008), we reject a spawning-related mechanism for the observed Ba/Ca_{shell} peak.

The remaining hypotheses to explain Ba/Ca peaks in biogenic carbonates are (1) increased consumption of barium-rich particles such as diatoms, and (2) ambient increases in seawater Ba/Ca. The diatom-ingestion hypothesis invokes a mechanism where filter-feeding bivalves digest barite or barite-rich particles then digested Ba is transported via extrapallial fluid to calcification sites and is incorporated in the shell carbonate (Stecher et al., 1996). Prior studies using Chl *a*, as a proxy for diatom abundance, found that Chl *a* peaks and coinciding Ba/Ca_{shell} peaks frequently co-occur (Vander Putten et al., 2000; Thébault et al., 2009). In *Mytilus edulis*, broad and marked Ba/Ca_{shell} peaks (~30 μmol/mol) have been observed lasting ~20 days and coincide with intervals of high Chl *a* (Vander Putten et al., 2000). However, the relationship between Chl *a* and Ba/Ca_{shell} is not linear and Chl *a* peaks occur without corresponding Ba/Ca_{shell} peaks (Vander Putten et al., 2000). Thébault et al. (2009) present compelling data where a large Chl *a* peak occurs a week before a large Ba/Ca_{shell} peak in the tropical scallop *Comptopallium radula*; the authors assume that this Chl *a* peak is due to a diatom bloom and that the Ba/Ca_{shell} peak resulted from ingestion of these Ba-rich diatom frustules. However, the data also contain a smaller Ba/Ca_{shell} peak that preceded the aforementioned Chl *a* peak by ~14 days as well as a Chl *a* peak not associated with a Ba/Ca_{shell} peak. The authors attribute the occurrence of a Ba/Ca_{shell} peak before a Chl *a* peak to dating errors resulting from back-counting growth increments, even though this peak occurs near the commissure, where back-counting would be most accurate. In a similar study, Barats et al. (2009) compared the Ba/Ca_{shell} of the North Atlantic scallop *P. maximus* to a suite of environmental parameters, but unlike the previously mentioned studies, they measured seawater particulate and dissolved barium concentrations as well as abundances of the diatom *Chaetoceros* spp. and the dinoflagellate *Gymnodynium* spp. The researchers found that seawater Ba to Ba_{shell} partition coefficients were comparable to previously published values (e.g., D_{Ba} ~0.2), based on average seawater dissolved barium and background (non-peak) Ba/Ca_{shell}, (Gillikin et al., 2006; Gillikin et al., 2008). Episodically elevated Ba/Ca_{shell} peaks coincided with elevated dissolved Ba concentrations, but were much higher than predicted by partition coefficients. These researchers concluded that Ba/Ca_{shell} peaks cannot be attributed to diatom abundance or any relevant paleoproductivity tracer (e.g., Chl *a*).

While markedly coincident peaks in Chl *a* and shell Ba/Ca are visually compelling, the broader often variable and non-linear relationship between Chl *a* and Ba/Ca_{shell} as well as the existence of peaks in one variable without commensurate peaks in the other variable currently limit the utility of Ba/Ca_{shell} as proxy for primary productivity (Gillikin et al., 2008). This study compared high resolution Ba/Ca_{shell} and environmental data in a robust temporal framework, and found significant correlations between Ba/Ca_{shell} and Chl *a* from and six and nine days prior, with Chl *a* from nine days prior showing a higher correlation. While other studies have found a similar correlation between Chl *a* and Ba/Ca_{shell}, these studies attribute their Chl *a* increases to diatoms whereas this study demonstrates that the Chl *a* is not a universal proxy for diatoms and, in fact, Chl *a* is not specific to any taxon or group. Furthermore, the covariance of upwelled nutrients, which presumably included Ba, and the phytoplankton communities which flourish due to increased nutrients, needs to be addressed before any Ba/Ca_{shell}–Chl *a* proxies are utilized. In this system, the Chl *a* peak which occurs six to nine days prior to peak Ba/Ca_{shell} appears primarily due to the relatively large dinoflagellate *L. polyedrum* rather than diatoms (Fig. 5B).

In bivalves, non-peak Ba/Ca_{shell} values are often low (0.2–2.0 μmol/mol; see Table 2 in Barats et al. (2009)), and these values are dependent on seawater Ba with seawater - shell partition coefficients (D_{Ba}) of 0.07–0.18 (Gillikin et al., 2006; Gillikin et al., 2008). However, Ba/Ca_{shell} peaks are frequently attributed to environmental or biological factors. In corals and foraminifera, peak and non-peak Ba/Ca_{shell} values are used as a proxy for seawater Ba/Ca values based on a D_{Ba} of 1.3 and 0.17–0.22, respectively (Lea et al., 1989; Lea and Boyle, 1991). Although seawater Ba concentrations for this study area and interval are not known, Carson (2010) found seawater Ba near the mouth of San Diego Bay to vary from 13.7 to 66.0 nmol/kg from spring to fall during 2006 and 2007. Seawater Ba was also sampled in 1998 as a continuous surface transect from southern Baja Mexico to San Diego and typical averaged 30–35 nmol/kg with deviations down to 13 nmol/kg occurring over small spatial scales (<100 km) (Esser and Volpe, 2002). To place the observed Ba/Ca_{shell} in the context of these regional seawater Ba/Ca values, a D_{Ba} can be estimated using the average non-peak for Ba/Ca_{shell} (i.e., 3.47 μmol/mol) and "normal" surface Ba concentrations for the area (36 nmol/kg; Esser and Volpe, 2002), which produces a D_{Ba} of 0.95. While this estimated D_{Ba} is higher than previously observed for other aragonitic bivalves, the background shell Ba/Ca ratios are also higher than many other studied species as well. However, abiogenic aragonite has a D_{Ba} of >0.5 (Dietzel et al., 2004; Gaetani and Cohen, 2006) and corals often have a D_{Ba} of ≥1.0 (Lea et al., 1989; Alibert et al., 2003). Using a D_{Ba} of 0.95, the seawater Ba concentration necessary to fully explain observed values in *D. gouldii* would range from

Please cite this article as: Hatch, M.B.A., et al., Ba/Ca variations in the modern intertidal bean clam *Donax gouldii*: An upwelling proxy? Palaeogeogr. Palaeoclimatol. Palaeoecol. (2012), doi:10.1016/j.palaeo.2012.03.006

20.9 to 118.0 nmol/kg. Both regional studies reported values lower than 20.9, but the highest observed seawater Ba concentration was 66.9 nmol/kg (Carson, 2010). Although the barium concentrations measured by Carson (2010) are just over half what would be required to directly explain shell Ba/Ca, these data have a resolution of 2–3 weeks, which might not detect high frequency changes in Ba concentration. Using seawater Ba on data from Carson (2010) and Esser and Volpe (2002), much of the "background" variation observed in Ba/Ca_{shell} can be explained by variations in seawater Ba concentrations. The highest Ba/Ca_{shell} measurement of 11.29 μmol/mol would require a seawater Ba concentration of 118.0 nmol/kg, while such a seawater value has been observed in the deep ocean, it is difficult to evaluate the likelihood of such a value in the surf zone (Chan et al., 1977). In support of the seawater Ba hypothesis, nutrients were high on 27 March just prior to the observed peak in Ba/Ca_{shell} (Fig. 5D), and the nitrate and silicate values were roughly equal, consistent with recent delivery of nutrient rich water to the euphotic zone. Barium, like nitrate, has a nutrient-type profile and is quickly removed from surface waters by primary producers. Therefore, the same upwelling event which resulted in high nitrate values would have, most likely, resulted in high dissolved barium concentrations. This conjecture is difficult to assess without direct measurements of seawater barium, but certainly warrants further investigation.

5. Conclusion

Cross-dating has been successfully applied to lunar day and fortnightly growth increments, which allowed laser-ablated Ba/Ca_{shell} determinations to be precisely dated with less error than either back-counting or assuming constant growth. The dated Ba/Ca_{shell} ablations were then correlated with a robust set of environmental time-series, including temperature, salinity, density, phytoplankton counts, Chl *a*, and dissolved nutrient concentrations. The cross-dated Ba/Ca_{shell} determinations were significantly correlated with nitrate, nitrite, and phosphate concentrations three days prior to Ba/Ca_{shell} determinations with Chl *a* six and nine days prior. While a single driver for population wide synchronous peaks in Ba/Ca_{shell} for bivalves remains enigmatic, this research highlights the methods necessary to create a well-constrained Ba/Ca_{shell} chronology based on high frequency growth increments. Furthermore, these data show that diatom concentration occurs independent of Chl *a*, reinforcing the need for phytoplankton counts to assess the influence of phytoplankton on Ba/Ca_{shell}.

This study supports the hypothesis that Ba/Ca_{shell} peaks are due to environmental forcing, however the exact driver remains unclear. To better understand the nature of such Ba/Ca_{shell} peaks, phytoplankton communities should be well described and seawater Ba/Ca should be monitored. If diet-related hypotheses are to be tested, studies should include measurements of Ba/Ca values in the organisms (e.g., gut, hemolymph).

Acknowledgements

Funding for LA-ICP-MS analysis was supported by NSF IGERT Grant 0333444 and funding for MBAH was provided by the NSF Graduate Research Fellowship Program. This manuscript was greatly improved by reviews from Claire E. Lazareth, Dan Sinclair and David P. Gillikin (guest editor). A special thanks to J.A. McGowan for his helpful insights into the phytoplankton dynamics under the SIO pier in the in Southern California Bight. Funding for the Shore Station program was supported by California Boating and Waterways. Support and for the SCCOOS HAB program by NOAA IOOS through SCCOOS, Grant No. UCSD 20081362. We also thank Mary Hilbern for assistance with the phytoplankton counts and Chl *a* analysis; Susan Becker and Daniel Schuller at Ocean Data Facility, SIO for nutrient analysis.

References

Alibert, C., Kinsley, L., 2008. A 170-year Sr/Ca and Ba/Ca coral record from the western Pacific warm pool: 1. What can we learn from an unusual coral record? Journal of Geophysical Research 113, C04008.
Alibert, C., Kinsley, L., Fallon, S.J., McCulloch, M.T., Berkelmans, R., McAllister, F., 2003. Sources of trace element variability in Great Barrier Reef corals affected by the Burdekin flood plumes. Geochimica et Cosmochimica Acta 67, 231–246.
Allen, W.E., 1920. Quantitative studies on marine phytoplankton at La Jolla in 1919: University of California Publications in Zoology, 22, pp. 329–347.
Armstrong, F.A.J., Stearns, C.A., Strickland, J.D.H., 1967. The measurement of upwelling and subsequent biological processes by means of the Technicon Autoanalyzer and associated equipment. Deep Sea Research 14, 381–389.
Atlas, E.L., Hager, S.W., Gordon, L.I., Park, P.K., 1971. A practical manual for use of the technicon autoanalyzer in seawater nutrient analyses revised. Revised OSU Technical Report, 215. Dept. Oceanography, Oregon State University, Corvallis, OR, p. 49.
Bacon, M.P., Edmond, J.M., 1972. Barium at Geosecs III in the southwest Pacific. Earth and Planetary Science Letters 16, 66–74.
Barats, A., Pécheyran, C., Amouroux, D., Dubascoux, S., Chauvoud, L., Donard, O.F.X., 2007. Matrix-matched quantitative analysis of trace-elements in calcium carbonate shells by laser-ablation ICP-MS: application to the determination of daily scale profiles in scallop shell (*Pecten maximus*). Analytical and Bioanalytical Chemistry 387, 1131.
Barats, A., Amouroux, D., Chauvaud, L., Pécheyran, C., Lorrain, A., Thébault, J., Church, T.M., Donard, O.F.X., 2009. High frequency Barium profiles in shells of the Great Scallop *Pecten maximus*: a methodical long-term and multi-site survey in Western Europe. Biogeosciences 6, 157–170.
Behrenfeld, M.J., O'Malley, R.T., Siegel, D.A., McClain, C.R., Sarmiento, J.L., Feldman, G.C., Milligan, A.J., Falkowski, P.G., Letelier, R.M., Boss, E.S., 2006. Climate-driven trends in contemporary ocean productivity. Nature 444, 752–755.
Black. B.A.. Boehlert. G.W., Yoklavich. M.M., 2005. Using tree-ring crossdating techniques to validate annual growth increments in long-lived fishes. Canadian Journal of Fisheries and Aquatic Sciences 62, 2277–2284.
Black, B.A., Gillespie, D.C., MacLellan, S.E., Hand, C.M., 2008. Establishing highly accurate production-age data using the tree-ring technique of crossdating: a case study for Pacific geoduck (*Panopea abrupta*). Canadian Journal of Fisheries and Aquatic Sciences 65, 2572–2578.
Black, B.A., Copenheaver, C.A., Frank, D.C., Stuckey, M.J., Kormanyos, R.E., 2009. Multi-proxy reconstructions of northeastern Pacific sea surface temperature data from trees and Pacific geoduck. Palaeogeography, Palaeoclimatology, Palaeoecology 278, 40–47.
Carpenter, S.J., 1998. A duct-tape manipulator for polishing thin sections. Journal of Sedimentary Research 68, 515–518.
Carroll, M.L., Johnson, B.J., Henkes, G.A., McMahon, K.W., Voronkov, A., Ambrose Jr., W.G., Denisenko, S.G., 2009. Bivalves as indicators of environmental variation and potential anthropogenic impacts in the southern Barents Sea. Marine Pollution Bulletin 59, 193–206.
Carson, H.S., 2010. Population connectivity of the Olympia oyster in southern California. Limnology and Oceanography 55, 134–148.
Chan, A.T., 1980. Comparative physiological study of marine diatoms and dinoflagellates in relation to irradiance and cell size. II. Relationship between photosynthesis, growth, and carbon/chlorophyll *a* ratio. Journal of Phycology 16, 428–432.
Chan, L.H., Drummond, D., Edmond, J.M., Grant, B., 1977. On the barium data from the Atlantic GEOSECS expedition. Deep Sea Research 24, 613–649.
Coe, W.R., 1955. Ecology of the Bean Clam *Donax gouldii* on the Coast of Southern California. Ecology 36, 512–514.
Cullen, J.J., 1982. The deep chlorophyll maximum: comparing vertical profiles of chlorophyll *a*. Canadian Journal of Fisheries and Aquatic Sciences 39, 791–803.
Dehairs, F., Chesselet, R., Jedwab, J., 1980. Discrete suspended particles of barite and the barium cycle in the open ocean. Earth and Planetary Science Letters 49 (2), 528–550.
Dehairs, F., Lambert, C., Chesselet, R., Risler, N., 1987. The biological production of marine suspended barite and the barium cycle in the Western Mediterranean Sea. Biogeochemistry 4 (2), 119–140.
Dehairs, F., Baeyens, W., Goeyens, L., 1992. Accumulation of suspended barite at mesopelagic depths and export production in the Southern Ocean. Science 258, 1332–1335.
Dietzel, M., Gussone, N., Eisenhauer, A., 2004. Co-precipitation of Sr2+ and Ba2+ with aragonite by membrane diffusion of CO2 between 10 and 50 °C. Chemical Geology 203, 139–151.
Dugdale, R.C., Wilkerson, F.P., 1998. Silicate regulation of new production in the equatorial Pacific upwelling. Nature 391, 270–273.
Ellers, O., 1995. Behavioral-control of swash-riding in the clam *Donax variabilis*. The Biological Bulletin 189, 120–127.
Esser, B.K., Volpe, A.M., 2002. At-sea high-resolution chemical mapping: extreme barium depletion in North Pacific surface water. Marine Chemistry 79, 67–79.
Gaetani, G.A., Cohen, A.L., 2006. Element partitioning during precipitation of aragonite from seawater: a framework for understanding paleoproxies. Geochimica et Cosmochimica Acta 70, 4617–4634.
Gallegos, D.R., 2002. Southern California in transition: Late Holocene occupation of southern San Diego County. Catalysts to complexity: Late Holocene Societies of the California Coast: Perspectives in California Archaeology, 6, pp. 27–39.
Geider, R.J., 1987. Light and temperature dependence of the carbon to chlorophyll *a* ratio in microalgae and cyanobacteria: implications for physiology and growth of phytoplankton. New Phytologist 106, 1–34.
Gillikin, D.P., Dehairs, F., Lorrain, A., Steenmans, D., Baeyens, W., André, L., 2006. Barium uptake into the shells of the common mussel (*Mytilus edulis*) and the potential for

Please cite this article as: Hatch, M.B.A., et al., Ba/Ca variations in the modern intertidal bean clam *Donax gouldii*: An upwelling proxy? Palaeogeogr. Palaeoclimatol. Palaeoecol. (2012), doi:10.1016/j.palaeo.2012.03.006

estuarine paleo-chemistry reconstruction. Geochimica et Cosmochimica Acta 70, 395–407.
Gillikin, D.P., Lorrain, A., Paulet, Y.M., André, L., Dehairs, F., 2008. Synchronous barium peaks in high-resolution profiles of calcite and aragonite marine bivalve shells. Geo-Marine Letters 28, 351–358.
Goldberg, E.D., Arrhenius, G.O.S., 1958. Chemistry of Pacific pelagic sediments. Geochimica et Cosmochimica Acta 13, 153–212.
Goodman, D., Eppley, R.W., Reid, F.M.H., 1984. Summer phytoplankton assemblages and their environmental correlates in the Southern California Bight. Journal of Marine Research 42, 1019–1049.
Goodwin, D.H., Flessa, K.W., Téllez-Duarte, M.A., Dettman, D.L., Schöne, B.R., Avila-Serrano, G.A., 2004. Detecting time-averaging and spatial mixing using oxygen isotope variation: a case study. Palaeogeography, Palaeoclimatology, Palaeoecology 205, 1–21.
Gordon, L.I., Jennings, J.C., Ross, A.A., Krest, J.M., 1992. A suggested protocol for continuous flow automated analysis of seawater nutrients in the WOCE Hydrographic Program and the Joint Global Ocean Fluxes Study. Grp. Tech Rpt 92-1, OSU College of Oceanography Descr. Chem Oc.
Haderlie, E.C., Abbott, D.P., 1980. Bivalvia: the clams and allies. In: Morris, R.H., Abbott, D.P., Haderlie, E.C. (Eds.), Intertidal Invertebrates of California. Stanford University Press, Stanford, California, pp. 355–411.
Hager, S.W., Atlas, E.L., Gordon, L.I., Mantyla, A.W., Park, P.K., 1972. A comparison at sea of manual and autoanalyzer analyses of phosphate, nitrate, and silicate. Limnology and Oceanography 17, 931–937.
Jones, C.D., Collins, M., Cox, P.M., Spall, S.A., 2001. The carbon cycle response to ENSO: a coupled climate-carbon cycle model study. Journal of Climate 14, 4113–4129.
Kamykowski, D., 1974. Physical and biological characteristics of an upwelling at a station off La Jolla, California during 19711. Estuarine and Coastal Marine Science 2, 425–432.
Kim, H.-J., Miller, A.J., McGowan, J., Carter, M.L., 2009. Coastal phytoplankton blooms in the Southern California Bight. Progress In Oceanography 82, 137–147.
Lea, D.W., Boyle, E.A., 1989. Barium content of benthic foraminifera controlled by bottom-water composition. Nature 338, 751–753.
Lea, D.W., Boyle, E.A., 1991. Barium in planktonic foraminifera. Geochimica et Cosmochimica Acta 55, 3321–3331.
Lea, D.W., Shen, G.T., Boyle, E.A., 1989. Coralline barium records temporal variability in equatorial Pacific upwelling. Nature 340, 373–376.
Monnin, C., Jeandel, C., Cattaldo, T., Dehairs, F., 1999. The marine barite saturation state of the world's oceans. Marine Chemistry 65, 253–261.
Mullin, M.M., Sloan, P.R., Eppley, R.W., 1966. Relationship between carbon content, cell volume, and area in phytoplankton. Limnology and Oceanography 11, 307–311.
Parnell, P., Miller, E., Lennert-Cody, C., Dayton, P., Carter, M., Stebbins, T., 2010. The response of giant kelp (*Macrocystis pyrifera*) in southern California to low-frequency climate forcing. Limnology and Oceanography 55, 2686–2702.
Rasband, W.S., 1997–2011. ImageJ. U. S. National Institutes of Health, Bethesda, Maryland, USA.
Sarmiento, J.L., Hughes, T.M.C., Stouffer, R.J., Manabe, S., 1998. Simulated response of the ocean carbon cycle to anthropogenic climate warming. Nature 393, 245–249.
Schöne, B., Lega, J., Flessa, K., Goodwin, D., Dettman, D., 2002. Reconstructing daily temperatures from growth rates of the intertidal bivalve mollusk *Chione cortezi* (northern Gulf of California, Mexico). Palaeogeography Palaeoclimatology Palaeoecology 131–146.
Shaw, T.J., Moore, W.S., Kloepfer, J., Sochaski, M.A., 1998. The flux of barium to the coastal waters of the southeastern USA: the importance of submarine groundwater discharge. Geochimica et Cosmochimica Acta 62, 3047–3054.
Stecher, H.A., Krantz, D.E., Lord, C.J., Luther, G.W., Bock, K.W., 1996. Profiles of strontium and barium in *Mercenaria mercenaria* and *Spisula solidissima* shells. Geochimica et Cosmochimica Acta 60, 3445–3456.
Sternberg, E., Tang, D., Ho, T.Y., Jeandel, C., Morel, F.M.M., 2005. Barium uptake and adsorption in diatoms. Geochimica et Cosmochimica Acta 69, 2745–2752.
Thébault, J., Chauvaud, L., L'Helguen, S., Clavier, J., Barats, A., Jacquet, S., Pecheyran, C., Amouroux, D., 2009. Barium and molybdenum records in bivalve shells: geochemical proxies for phytoplankton dynamics in coastal environments? Limnology and Oceanography 54, 1002–1014.
UNESCO, 1981. Background papers and supporting data on the Practical Salinity Scale 1978. UNESCO Technical Papers in Marine Science, p. 37.
Utermöhl, H., 1958. Zur Vervollkommnung der quantitativen Phytoplankton-Methodik. Mitteilungen Internationale Vereinigung fuer Theoretische und Angewandte Limnologie 9, 1–38.
Valentine, J.W., 1960. Habitats and sources of Pleistocene mollusks at Torrey Pines Park, California. Ecology 41, 161.
Vander Putten, E., Dehairs, F., Keppens, E., Baeyens, W., 2000. High resolution distribution of trace elements in the calcite shell layer of modern *Mytilus edulis*: environmental and biological controls. Geochimica et Cosmochimica Acta 64, 997–1011.
Venrick, E.L., Hayward, T.L., 1984. Determining chlorophyll on the 1984 CALCOFI surveys. California Cooperador Oceanic Fish Investigation Reports 25, 74–78.
Vischer, N., 2011. ObjectJ. University of Amsterdam.
Winter, R.N., Hatch, M.B.A., 2010. Investigating the parasitism of Southern California bean clams (*Donax gouldii*) by the trematode *Postmonorchis donacis*. Bulletin, Southern California Academy of Sciences, 109, pp. 144–152.
Yamaguchi, D.K., 1991. A simple method for cross-dating increment cores from living trees. Canadian Journal of Forest Research 21, 414–416.
Zacherl, D.C., Paradis, G., Lea, D.W., 2003. Barium and strontium uptake into larval protoconchs and statoliths of the marine neogastropod *Kelletia kelletii*. Geochimica et Cosmochimica Acta 67, 4091–4099.
Zacherl, D.C., Morgan, S.G., Swearer, S.E., Warner, R.R., 2009. A shell of its former self: can *Ostrea lurida* Carpenter 1864 larval shells reveal information about a recruit's birth location? Journal of Shellfish Research 28, 23–32.

Please cite this article as: Hatch, M.B.A., et al., Ba/Ca variations in the modern intertidal bean clam *Donax gouldii*: An upwelling proxy? Palaeogeogr. Palaeoclimatol. Palaeoecol. (2012), doi:10.1016/j.palaeo.2012.03.006

Chapter 3, in full, is a reprint of the material as it appears in Palaeogeography, Palaeoclimatology, Palaeoecology 2012. Hatch, Marco B.A, Schellenberg, S.A., Carter, M.L. The dissertation author was the primary investigator and author of this paper.

CHAPTER 4

Growth increment formation and minimum temperature threshold in *Chione undatella*

by Marco B.A. Hatch

Abstract

Growth increments in the accretionary parts of living and fossil organisms can be used to reconstruct environmental conditions. In bivalves, growth increments are related to growth slow down. These bands, commonly referred to as "winter bands", can be formed during winter and/or summer depending on local conditions and the bivalve's thermal limits. Prior to utilizing growth increments in fossil shells, the timing and periodicity of growth increments formations should be determined in modern specimens. Presented here are results from a mark-recapture study of *C. undatella* in Mission Bay (San Diego, California). Based on $\delta^{18}O$ values of shell growth during the outplanted period, total variability in $\delta^{18}O$ is less than expected, based on environmental conditions, with winter seawater temperature under-represented and annual growth increment formation occurring during winter. Shell extension is greatly reduced after the first year of life and continues to slow as the animal ages. *C. undatella* have winter shutdown with reduced increment widths and lengthening winter shutdown during successive years of growth.

1. Introduction

Growth increments of bivalves have been used to study life history, ecology, and seawater temperature. The influence of temperature on growth has been recognized for nearly 80 years (Davenport 1938). More recently, seawater temperature has been correlated with the growth increment widths in long-lived geoduck bivalves, allowing long biological time-series to be created and related to decades of oceanographic conditions (Black et al. 2009). While such long-lived species can produce useful records for historic periods, it is often hard to obtain a suitable sample size of pre-historic remains, either in archaeological or geological deposits. Additionally, such long-lived species commonly used for these reconstructions are rarely lagoon dwellers. As a means to extend our knowledge of paleoclimate in the biologically and culturally important Southern California lagoons, another source of environmental and ecological data must be identified.

The lagoon dwelling venus clam, *Chione undatella* is common in modern lagoons, and is dominate in archaeological shell middens, and geological deposits (Valentine 1960; Gallegos 2002). *C. udatella* have long been noted as potential source of paleoecological information (Rosenberg 1973; Peterson 1985). *C. undatella* range from Goleta, USA to Peru (Haderlie and Abbott 1980) and as the case for bivalves, which span a large geographic and temperature range, the season of growth shutdown is variable. For example in temperate systems, winter shutdown may be more common and in the tropics, summer shutdown may be more common. In the congener, *C. cortezi*, from the northern Gulf of California, both summer and winter shutdown is

observed and the duration of these shutdowns increase with age. For *C. undatella*, variation in the growth rate with temperature has been observed but growth rate and pattern are variable along the Gulf of California (Berry and Barker 1975). These observations highlight the need to study the local ecology of biological proxies before making assumptions about how they would have functioned in the past. Further, observational studies can be combined with geochemical evidence to independently interpret bivalve growth patterns. For example, Goodwin et al. (2001) used $\delta^{18}O$ records to determine minimum and maximum temperature of *C. cortezi* growth, finding the growth shutdown in temperatures below 17 °C and above 31 °C. The purpose of this study is to constrain the seasonal growth patterns and address the following: Do *C. undatella* show seasonal shutdown? And if so is that shutdown variable with age? Is there a temperature threshold for *C. undatella* growth?

2. Methods and Location

2.1. Vacation Island study site

This study was carried out on the north west beach of Vacation Island, in Mission Bay, CA (N 32.777373, W 117.241515) (Figure 4.1). Mission Bay is heavily altered bay created from the former “False Bay”, which was a low-lying shallow lagoon and salt marsh system. Current Mission Bay is connected to the ocean by a large armored and dredged channel. The study location is a well-flushed section of the bay. Although, it is reasonable to assume that Mission Bay is subject to warmer seawater temperature in the summer and lower salinity after rain event, compared to the open ocean, this study site is less exposed to those extreme events than the back of Mission Bay (Largier et al. 1997).

2.2. Environmental monitoring

Seawater temperature from 11/24/2007 to 11/18/2008 was recorded every six minutes using HOBO Pendant data loggers attached to a concrete block placed adjacent to study organisms (Figure 4.1). Salinity and seawater samples for $\delta^{18}O$ seawater ($\delta^{18}O_{SW}$) were taken from the sea surface every two weeks from February 2008 through November 2008. $\delta^{18}O_{SW}$ samples were filtered through a 0.22 μm filter (Millex CP), poisoned with 2-3 drops of 10% zephiran chloride, and stored in vials capped with CO_2-impermeable septa (Wheaton 224186). $\delta^{18}O_{SW}$ values were determined using a Gas Bench II headspace sampling interface coupled to a ThermoFinningan Delta Plus XP isotope ratio mass spectrometer (IRMS) at the University of California, Santa Cruz, Stable Isotope Laboratory. $\delta^{18}O_{SW}$ values were determined by equilibrium exchange of the water sample with 0.3% CO_2 gas in a predominantly helium headspace environment. Analytical precision of internationally calibrated in-house standards was better than 0.06‰ for $\delta^{18}O_{SW}$ and values are reported relative to the VPDB international standard.

Predicted $\delta^{18}O$ for aragonite (hereafter $\delta^{18}O_{predicted}$) for each collection date was calculated from the Grossman and Ku (1986) equation of T ($^{\circ}C$) = 21.8 - 4.69 (shell $\delta^{18}O_{VPDB}$ - seawater $\delta^{18}O_{VPDB}$ - 0.28‰) using daily average temperature and average $\delta^{18}O_{SW}$ from 2/2008 to 2/2009 (Figure 4.2).

2.3. Mark-recapture

Thirty *C. undatella* where collected on 11/24/2007 from Vacation Island (Figure 4.1) marked with calcein stain by immersion in 1g/l solution for 12 hours. Once marked each *C. undatella* was individually tagged by attaching a stainless steel washer with epoxy to the left valve and length (umbo to growing margin) was measured. These *C. undatella* were released on Vacation Island on 11/25/2007 at tidal level -0.5 m (MLLW) within 3 m of the temperature logger. Another 20 *C. undatella* were collected on 2/18/2008 marked using the same method and outplanted on 2/19/2008. Of the 50 outplanted clams a total of eight were recovered, three on 2/18/2008, four on 6/5/2008 and one on 11/13/2008 (Table 4.1). The majority of the clams were lost in two major predation events, one due to octopus and another due to a crushing predator, most likely large bat rays.

2.4. Shell Sampling and Chemical Analyses

One valve of each *C. undatella* was thin-sectioned by embedding in epoxy, cutting along the maximum growth axis with a Buehler IsoMet 5000 Linear Precision Saw, and hand-polishing with 3M WetorDry Sandpaper (320, 600, 800, 1000 grit) using a duct-tape manipulator (Carpenter 1998) to a final thickness of ~700 μm. Shells were imaged with a Paxcam digital microscope camera (http://www.paxcam.com/) attached to a Leica MZ16 microscope using transmitted-light dark-field illumination at 50x magnification producing 10-20 images per shell. Multiple images were used to manually create a single mosaic image using in Adobe Photoshop CS

(http://www.adobe.com/). Calcein markings were detected by exciting with 485 nm light and use of a 495-530 nm cutoff filter.

The post-outplant growth was micro-milled and analyzed for $\delta^{18}O_{Chione}$ in four *C. undatella*, all outplanted on 11/25/07, and collected the following dates: shell "A", 2/18/2008 (n=1), shells "B" and "C", 6/5/2008 (n=2), and "D" 11/13/2008 (n=1). The amount of time each $\delta^{18}O_{Chione}$ determination represents was estimated by dividing the number of $\delta^{18}O_{Chione}$ determinations by the number of days the clam was at large. Although, this calculation assumes constant growth and this assumption if frequently incorrect, it allows the relative resolution of $\delta^{18}O_{Chione}$ to be quantified.

A New Wave Micromill was used to sequentially mill from the commuisure to the calcein mark. The distance of each mill depended on the thickness of the shell and the amount of mass needed (some samples where split for minor element ratio analysis which are not presented here) but generally ranged from 50-100 μm. The resulting ~80 -150 μg of the aragonite powder was sent for $\delta^{18}O_{Chione}$ determination at the University of California, Santa Cruz, Stable Isotope Laboratory on a Micromass PRISM or OPTIMA mass spectrometer with common acid bath carbonate preparation system using 100% H_3PO_4 at 90°C. The long-term reproducibility based on in-house standards tied to NBS standards averaged better than ±0.04‰ for $\delta^{18}O$. All values are reported relative to the VPDB standard.

3. Results

3.1 Growth

Of the 50 marked *C. undatella*, eight were recovered that were outplanted on 11/25/2007 and had been at large for between 85-354 days, growing between 180 - 2,490 μm while outplanted. Three *C. undatella* were retrieved on 2/18/2008 and had grown at a rate of 2-5 μm/day. The four collected on 6/5/2008 had a higher growth rate of 5-13 μm/day and the last *C. undatella* collected 11/13/2008 grew at rate of 2 μm/day. In general larger *C. undatella* grew slower than smaller individuals (Figure 4.2) and clams collected in June (192 days outplanted) had a higher growth rate than those collected in February (85 days outplanted).

3.2 Oxygen isotopes

$\delta^{18}O_{Chione}$ from the four sampled shells ranged from -1.66 to 0.38 ‰ and averaged -0.35 ‰ (±0.37; n= 72). The *C. undatella* "A" outplanted on 11/25/2007 and collected on 2/18/2008 had and average $\delta^{18}O_{Chione}$ of -0.34 ‰ (±0.15; n= 10) with each sample representing nine days. *C. undatella* "B" and "C" both outplanted on 11/25/2007 and collected on 6/5/2008, had an average $\delta^{18}O_{Chione}$ of -0.36 ‰ (±0.37; n= 31) and -0.03 ‰ (±0.19; n= 17), respectively, equating to one sample every six days for "B" and one every seventeen days for "C". *C. undatella* "D" was outplanted on 11/25/2007 and collected on 11/13/2008 and had the most negative $\delta^{18}O_{Chione}$ at -0.73 ‰ (±0.31; n= 14) with each sample representing 27 days.

Daily $\delta^{18}O_{predicted}$ values were calculated by using the daily average seawater temperature as recorded that the study site and the average $\delta^{18}O_{SW}$ measured from

2/2008-5/2009 (average = -0.28 ‰; ±0.27; n= 32; min = -1.4; max=0.07) and the mollusk equation from Grossman and Ku (1986). This resulted in an average $\delta^{18}O_{predicted}$ of 1.06 ‰ (±0.15) for 11/25/2007 to 2/18/2008, 0.71 ‰ (±0.43), for 11/25/2007 to 6/5/2008 and 0.26 ‰ (±0.64) for 11/25/2007 to 11/13/2008.

3.3 Comparison of $\delta^{18}O_{Chione}$ to $\delta^{18}O_{predicted}$

The average $\delta^{18}O_{Chione}$ for each shell was more negative than $\delta^{18}O_{predicted}$, with the difference ranging from 1.41 to 0.29 ‰. Shell A collected on 2/18/2008 was on average 1.41 ‰ more negative than predicted, shells B and C, collected on 6/5/2008, were on average 1.07 and 0.29 ‰ more negative than predicted, and shell D, collected on 11/13/2008, was on average 0.73 ‰ more negative than predicted.

3.4 Comparison of measured temperature to C. undatella based temperature

The discrepancy between measured temperature and $\delta^{18}O_{Chione}$ based temperature estimates can be used to indicate growth shutdown. To calculate temperature derived from $\delta^{18}O_{Chione}$, the Grossman and Ku (1986) mollusk equation with average $\delta^{18}O_{SW}$ (-0.28 ‰; ±0.27) was used (Figure 4.2). Shell "D" was the only *C. undatella* to span the entire study period and had an average $\delta^{18}O_{Chione}$-based temperature of 22.7 °C (± 1.5) with a maximum temperature of 27.0 and minimum of 21.3 °C, which was higher than measured average temperature (18.0 °C (sd± 3.0)); the daily average maximum temperature 24.3°C and a minimum of 12.9 °C. However, the high temperature for shell D came from immediately adjacent to the calcein stain,

when temperature would have been near the minimum (~15 °C) and this $\delta^{18}O_{Chione}$ value could be excluded as an outlier. For shells A-C, which did not span the entire study interval, $\delta^{18}O_{Chione}$ based temperature averaged 20.8 °C (±0.7), 19.4 C (± 0.9), and 20.9 C (± 1.7) for shells A-C respectively. The lowest temperature estimate for all shells was 17.4 C.

4. Discussion

This study indicated that *C. undatella* in Southern California have winter growth shutdown and lengthening winter shutdown with age (Figure 4.2). Also working with *C. undatella* Berry and Barker (1975) found evidence for lengthening winter shutdown with age, which results in less growth between winter increments as the clams get older. $\delta^{18}O_{carbonate}$ time-series from bivalves with lengthening winter shutdown will exhibit decreases maximum $\delta^{18}O$, decreases average $\delta^{18}O$, and decreases annual $\delta^{18}O$ amplitude with age (Goodwin et al. 2003). Thus, a temperature record from a multiple-year old *C. undatella* would reasonably track actual temperature for the first year, then in subsequent years it would over-estimate winter temperature, over-estimate annual mean temperature, and under-represent mean annual temperature range, all of which will become exacerbated with age. Goodwin et al. (2001) found *C. cortezi* to show lengthening winter shutdown and decreased growth with age, but unlike *C. undatella, C. cortezi* has both summer and winter growth shutdown.

Goodwin et al. (2001) used $\delta^{18}O$-based temperature to determine that *C. cortezi* from the northern Gulf of California does not grow below ~17 °C or above ~31

°C. This study area had a daily averaged seawater temperature between ~13 and ~24°C, compared to the *C. undatella* based temperature which varied between ~17 and 24°C (excluding the 27°C outlier). $\delta^{18}O$-based temperature reasonably estimated the maximum temperature but the discrepancy between minimum temperatures indicates that *C. udatella* does not grow below 17 °C. However, this is based on daily average temperatures, so it is possible that with a daily average temperature of 17 °C there are parts of the day when temperature is warm enough for growth.

5. Conclusion

Paleotemperature estimates based on $\delta^{18}O_{Chione}$ will be less variable, over-estimate winter temperatures, and on average be warmer than actual temperature. *C. undatella* shell followed the lengthening winter shutdown model represented in Goodwin et al. (2003). The use of $\delta^{18}O$ analysis in bivalves can produce ecological insights such as the temperature of thermally induced growth shutdowns.

Table 4.1: Sample numbers and data collected from each *C. undatella*, letter samples were milled for stable isotopes and number samples were not.

Specimen	Date outplanted	Date recaptured	Size outplanted (mm)	Growth (mm)	Daily growth (µm/day)	# $\delta^{18}O$ samples	Days/ sample
A	11/25/2007	2/18/2008	31.4	0.2	2	10	9
1	11/25/2007	2/18/2008	39.1	0.2	2		
2	11/25/2007	2/18/2008	42.5	0.4	5		
B	11/25/2007	6/5/2008	31.7	1.9	10	31	6
C	11/25/2007	6/5/2008	30.6	2.5	13	17	17
3	11/25/2007	6/5/2008	34.0	0.9	5		
4	11/25/2007	6/5/2008	34.5	1.7	9		
D	11/25/2007	11/13/2008	37.3	0.8	2	14	27

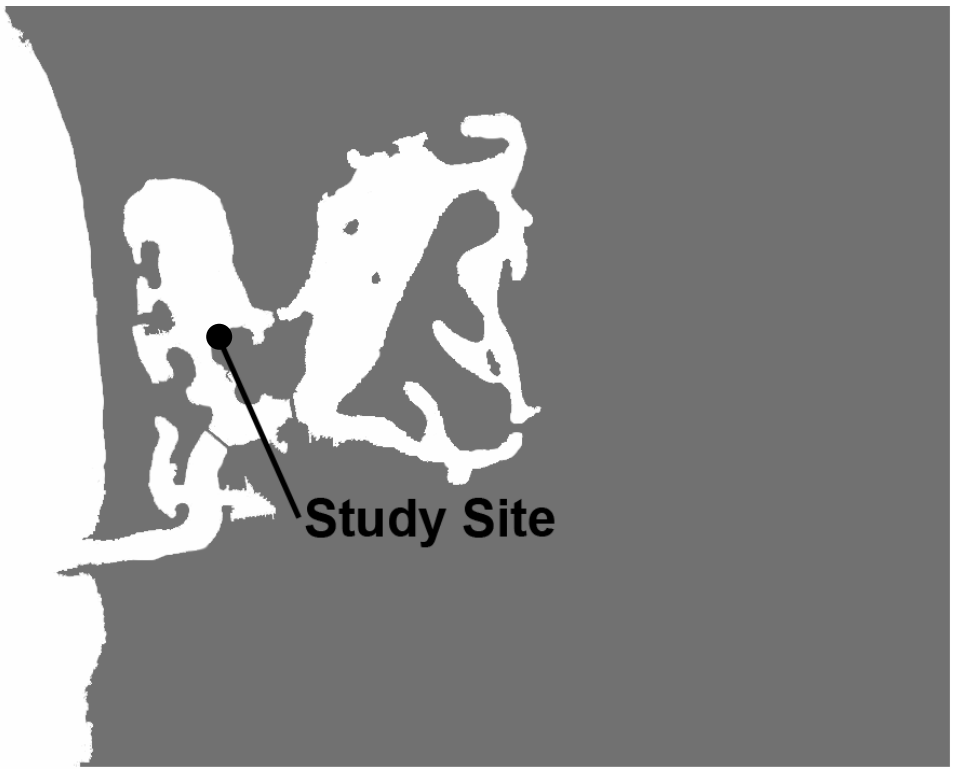

Figure 4.1: Figure on Mission Bay with the Vacation Island study site marked.

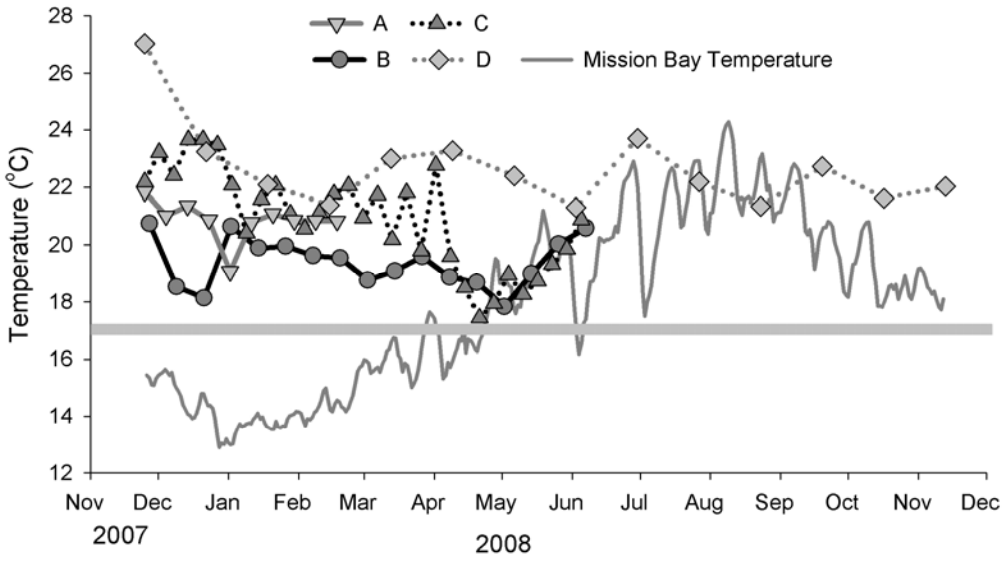

Figure 4.2: Seawater temperature calculated from $\delta^{18}O$ of *C. undatella* A, B, C, and D with measured seawater temperature. To illustrate the minimum *Chione*-based temperature a gray bar is plotted at 17 °C.

References

Berry, W.B.N., Barker, R.M., 1975, Growth increments in fossil and modern bivalves: in Rosenberg, G.D., and Runcorn, S.K., eds., Growth Rhythms and the History of the Earth's Rotation: John Wiley & Sons, New York, p. 9–25.

Black BA, Copenheaver CA, Frank DC, Stuckey MJ, Kormanyos RE (2009) Multi-proxy reconstructions of northeastern Pacific sea surface temperature data from trees and Pacific geoduck. Palaeogeography, Palaeoclimatology, Palaeoecology **278**:40-47

Carpenter SJ (1998) A duct-tape manipulator for polishing thin sections. Journal of Sedimentary Research **68**:515-518

Davenport CB (1938) Growth lines in fossil pectens as indicators of past climates. Journal of Paleontology **12**:514-515

Gallegos DR (2002) Southern California in transition: Late Holocene occupation of southern San Diego County. Catalysts to Complexity: Late Holocene Societies of the California Coast, Perspectives in California Archaeology **6**:27–39

Goodwin DH, Flessa KW, Schone BR, Dettman DL (2001) Cross-Calibration of Daily Growth Increments, Stable Isotope Variation, and Temperature in the Gulf of California Bivalve Mollusk Chione cortezi: Implications for Paleoenvironmental Analysis. Palaios **16**:387-398

Goodwin DH, Schone BR, Dettman DL (2003) Resolution and Fidelity of Oxygen Isotopes as Paleotemperature Proxies in Bivalve Mollusk Shells: Models and Observations. Palaios **18**:110-125

Grossman EL, Ku TEHL (1986) Oxygen and carbon isotope fractionation in biogenic aragonite: temperature effects. Chemical Geology **59**:59-74

Haderlie EC, Abbott DP (1980) Bivalvia: The clams and allies. In: Morris RH, Abbott DP, Haderlie EC (eds) Intertidal Invertebrates of California. Stanford University Press, Stanford, California, pp 355-411

Largier JL, Hollibaugh JT, Smith SV (1997) Seasonally Hypersaline Estuaries in Mediterranean-climate Regions. Estuarine, Coastal and Shelf Science **45**:789-797

Peterson CH (1985) Patterns of Lagoonal Bivalve Mortality After Heavy Sedimentation and Their Paleoecological Significance. Paleobiology **11**:139-153

Rosenberg GD (1973) Calcium Concentration in the Shell of the Bivalve Chione undatella Sowerby. Nature **244**:155-156

Valentine (1960) Habitats and Sources of Pleistocene Mollusks at Torrey Pines Park, California. Ecology **41**:161

Chapter 4, in part, is currently being prepared for submission for publication of the material. Hatch, Marco B.A. The dissertation author was the primary investigator and author of this paper.

CHAPTER 5

Age and growth of archaeological *Chione undatella* from a Southern California Lagoon

by Marco B.A. Hatch

Abstract

The Southern California Bight experienced dramatic environmental changes during the Holocene. One of the most dramatic was the transition from rocky beaches to sandy shores in the middle Holocene. This change is reflected in archaeological shell middens as a shift from rocky intertidal mollusks to sandy shore bivalves. Other changes in archaeological material, such as prey switching within a type of habitat, have both environmental and cultural explanations. Evaluating the relative importance of environmental and cultural drivers of the observed changes in archaeological material is a fundamental question in archaeology. If environmental information can be extracted from shell middens, then a framework can be created to evaluate the relative contributions of cultural and environmental change to faunal shifts in shell middens. One method to gain ecological insights from archaeological material is to use the size, age, and growth rate of archaeological faunal remains as a proxy for environmental changes. The purpose of this study is to evaluate the size and age at harvest and growth rate of *Chione undatella* from shell middens in a Southern California lagoon. Based archaeological collections spanning 6,000 years

a change in the dominate bivalve was observed, with *Argopecten* being dominate in older material and *Chione* being dominate in younger material. Over the observed period the size and age of harvested *Chione undatella* did not significantly change. The increased *Chione* abundance is hypothesized to have resulted from an increase if *Chione* habitat, or alternatively, time averaging in the archaeological material obscured sub-century climate variations.

1. Introduction

Knowledge and understanding of long-term changes in the world's climate is essential for understanding temporal and spatial variability and to predict current climatic forcing. Faced with a short instrumental record, especially for the oceans, other ways of obtaining climatic information must be explored. To maximize the utility of paleoclimatic data, efforts should be focused on periods of known environmental change. Recent research has suggested significant changes in the Holocene littoral communities of the Southern California Bight resulting from climate change, sea level rise, and anthropogenic impacts. (Masters 2006) described the evolution of the Southern California Bight sandy beaches from rocky intertidal, suggesting that when the period and intensity of El Niños changed some 5,000 years before present, the beach substratum changed from rocky to sandy for the Oceanside littoral cell. She hypothesized the rise of sand is due to increased monsoonal rains associated with ENSOs, noting that one year of ENSO rains can bring as much or more sediment to the littoral than 25 years worth of "normal" rain. In the Santa

Clara river for years 1968-1975, 55% of the total sediment transport occurred in two days and 98% of the transport occurred to two months (Inman and Jenkins 1999).

Transformation of rocky and cobble shores to perennial sandy shores shifted the environment from a three dimensional alga-dominated system to a low-rugosity microalgae and infaunal system. Rocky habitats support an array of macroalgae with high primary productivity and ameliorate harsh physical stressors such as high currents and desiccation while also serving as habitat for a diverse suit of taxa. Rocky shores also support a diversity of fauna through high rugosity, by increasing available habitat and providing protection from currents and predators. In contrast, sandy habitats are primarily two dimensional, subject to highly episodic erosion and deposition, and have less primary productivity. The dynamic sandy substrate is dominated by infaunal and epifaunal macroinvertebrates such as clams, sea pens, sand dollars, and polychaetes.

Fluctuating Holocene climate not only changed San Diego's environment but also impacted prehistoric human's dependence on marine resources for subsistence. The shift from rocky habitats to sandy beaches occurred about 4,500 ybp based on ratio of sandy beach to rocky coast marine invertebrates in the shell midden under T-29 and other San Diego sites (Masters and Gallegos 1997). In addition to the reduction in rocky substrate invertebrates around 5,000 ybp, a decrease in kelp forest associated fish has also been noted. One village at Los Peńasquitos Lagoon, Ystagua Village, was dominated by the lagoonal *Chione* and *Argopecten* around 5,000 ybp then had a sudden rise in high-energy beach clam *Donax* around 3,000 ybp (Gallegos 2002). This village was then covered by a meter

of sediment at 1,500 ybp. The midden left by the next occupation, dating to 1,000 ybp, was dominated by rocky coast species *Mytlius* and *Chama*. The number of archaeological sites in San Diego County decreased after 3,300 ybp then rose after 1,500 ybp (Breshini et al. 1996). One hypothesis for the decrease of sites after 3,300 ybp is the closure of many coastal lagoons including Bataquitos lagoon (Gallegos 2002). It has also been hypothesized that the 1,500 ybp event that covered Ystagua Village also opened the closed coastal lagoons and subsequently increased the number of archaeological sites in San Diego County (Gallegos 2002).

While the archaeological record indicates continuous occupation for at least 9,000 years, there is a dramatic decline in site near the coastal and lagoons, around 3,300 ybp. This dramatic change in settlement patterns was also associated with a change in tooling and diet. Before the decline, many sites were associated with ephemeral streams and contained portable tools; after 3,300 ybp there was a shift toward perennial streams and increased use of bedrock milling tools, suggesting an increased use of plant foods (True 1990).

Given the known social and environmental change during the Middle and Late Holocene, it is difficult to attribute observed changes in the extent and content of archaeological materials to either change in environment or human activities. Therefore, methods need to be developed to test the relative contribution of changing environments and human activities as reflected in archaeological material, The purpose of this research is to investigate the following: Are the environmental and social changes reported by archaeologists reflected in the growth rate and size

of harvested *C. undatella*? Do the observed changes in *Chione spp.* shell vary with changes in *C. undatella* growth rates?

2. Methods

2.1. Site

Los Peńasquitos Lagoon is in the northern limit of the city of San Diego and is primarily fed by the Los Peńasquitos creek. The lagoon lies in the Soledad Valley, bordered by the cliffs of the Del Mar Terrace to the north and Torrey Pines State Reserve to the south. Currently, Los Peńasquitos Lagoon is approximately 1 km wide and 5.5 km long. The lagoon is formed behind a barrier bar, which is now kept open with a jetty. Historically the lagoon has opened and closed for years at a time (Miller 1966). The location of the mouth lagoon has also changed, early railroad maps put the opening of the lagoon at the northwest corner of the basin compared the current opening near the mid-point of the lagoon (Miller 1966).

2.2. Archaeological sites:

All archaeological collections curated at the San Diego Archaeological Center from the La Jolla and Del Mar quadrants with at least one kg of *Chione* shell per site were examined for shell amount, condition and completeness of collection. The following sites were selected for this study CA-SDI-4614, CA-SDI-10915 and CA-SDI-4619 (Figure 5.1).

Archaeological *C. undatella* were obtained from three previously excavated archaeological sites with median calibrated ^{14}C dates ranging from 1426 to 6996 ybp (all dates presented hereafter are median calibrated dates see radiocarbon dating

section for more details). All sites are located within the Los Peńasquitos lagoon basin and it is expected that all lagoon-dwelling bivalves were harvested from Los Peńasquitos rather than transported from another lagoon. All units within a given site were excavated in 10 cm layers then recovered material was separated by taxon and weighed. The four major taxa in the sites are listed as *Chione*, *Argopecten*, *Ostrea*, and *Mytilus* and this nomenclature will be used throughout this paper. It is helpful to define the species likely encountered in each genera. These archaeological studies only identify *Chione* to genus level; however, from examining these sites the vast majority of the *Chione* recovered are either *Chione undatella* followed by *Chione californiensis* with very few *Chione fluctifraga* recovered. *Argopecten* refers to *Argopecten aequisulcatus* a small lagoon scallop often associated with eelgrass beds. While this species can swim it is typically found attached to eelgrass beds using byssal threads and will remain attached unless disturbed. *Argopecten aequisulcatus* is found from Santa Barbara (California) to Cabo San Lucas (Baja California) (Haderlie and Abbott 1980) and is currently protected from harvest in California. *Ostrea* refers to *Ostrea lurida,* the Olympia oyster, which lives in lagoons and sheltered bays typically either attached to rocks or forming an oyster reef. Finally, *Mytilus* does not differentiate between *Mytilus californianus* and *Mytilus trossulus*, given that these archaeological sites are from a sheltered area either could be encountered. In general, *Mytilus* abundance is low and not a major component of the overall shell weight.

Site SDI-4614 was a shellfish processing area and was excavated by the Affinis Company in 1989. The three units sampled for *C. undatella* were unit 3, unit

5, and unit 6 with dates ranging from 1426 to 6330 ybp. Unit 3 was excavated to depth of 60cm and dated between 1245 and 3702 ybp with a possible layer reversal evidenced by one younger below later dated in the unit (Table 5.1). This unit was primary composed of *Chione* with its percentage lowest at the bottom of the unit (36% for layer 50-60cm) and increasing to just over 60% at the top of the unit (Figure 5.2). In contrast, *Argopecten* had a higher relative abundance at bottom of the unit (36%) and decreased to ~20% at the top of the unit. *Ostrea lurida* showed a similar pattern to *Argopecten*, with higher relative abundance at the bottom of the unit (15%) and lower abundance on top of the unit (2%). *Mytilus* had its highest relative abundance near the middle of the unit. Unit 5 was excavated to a depth of 70cm and was dated between 1276 and 2677 ybp. The general tend in shell abundance is similar in unit 3 with increasing *Chione* spp and decreasing *Argopecten* from the bottom to the top of the unit (Figure 5.3). *Ostrea* and *Mytilus* abundance didn't show a distinct trend in abundance with depth, and *Ostrea* abundance was between 22 - 13% and 1 - 4% for *Mytilus*. Unit 6 also showed a similar trend to the two units in Site SDI-4614 with increased *Chione* and a decreased *Argopecten* moving from the bottom of the unit to the top (Figure 5.4). The relative abundance of *Ostrea* and *Mytlius* was between 13 – 10 and 1 - 5%, respectively.

Site SDI-10915 unit TU 2 was excavated to a depth of 70 cm with two dates of 5924 and 6124 ybp. TU 2 was primarily comprised of *Chione* with relative abundances between 86 - 99% (Figure 5.5). The remaining shells were primarily *Argopecten* with very small amounts of *Ostrea* (1% for layer 40-50 cm) and no

Mytilus recorded. Site SDI-4619 was excavated to a depth of 110 cm and was dated between 6124 and 7050 ybp. The upper part of this site was dominated by *Argopecten* until layer 60 – 70 cm when *Chione* became more abundant (Figure 5.6). In general *Ostrea* and *Mytilus* were either absent or in low abundance.

2.3. Age and length determination

For growth increment analysis, shells were prepared using two methods. Roughly a third of the shells were thin-sectioned and slide-mounted. The thin sectioned shells were imaged with a Nikon 4500 digital camera attached to Leica MZ16 microscope using transmitted-light dark-field illumination at 50x magnification. The remaining shells were coated in epoxy around the major growth axis, cut with a rock saw, and scanned using an Epson v600 scanner at 6400 dpi. Growth increments were measured from the umbo to the start of winter banding using the ObjectJ plugin (Vischer 2011) for ImageJ (Rasband 1997-2011) (Figure 5.7). Additionally, every *C. undatella* with the major growth axis intact was measured using digital calipers to the nearest 0.1 mm for a total of 566 *C. undatella* measured, from three archeological sites, ranging in age from 1400-7000 ybp.

2.4. Radiocarbon dating

Eight *C. undatella* were radiocarbon dated by the Center for Accelerator Mass Spectrometry at the Lawrence Livermore National Laboratory (LLNL). To minimize error introduced from upwelled carbon with different reservoir ages (Culleton et al. 2006), each sample was taken from over a year's growth from the prismatic layer by hand milling. Nine additional radiocarbon dates from *Chione* already existed for the study sites (Table 5.2), and were determined by Beta

Analytic. These dates are presented in carbon years before present (CYBP) and four of these dates were corrected by Beta Analytic for isotope fractionation using $^{13}C/^{12}C$. To correct the remaining five dates from Beta Analytic 430 years was added to the uncorrected CYBP date (Stuiver and Polach, 1977; Erlandson, 1988). Once all dates had been ^{13}C corrected, they were calibrated with the program CALIB v6.1 (Stiuver et al. 2009) with the marine09 calibration curve (Reimer 2009). Marine upwelling adjustment (delta R) of 236 +/- 80 was used as determined from the Marine Reservoir Correction Database (http://calib.qub.ac.uk/calib/).

2.5. Layer dating

The radiocarbon dates clearly show that these sites had two separate occupations, one from ~1,900 – 3,700 ybp and another from 6,000 - 7,000 ybp. If a layer contained a dated shell, that date was used to date the layer, unless there was reason to question the quality of the site stratigraphy. Layers without a radiocarbon date were assigned a date based on linear extrapolation, provided the upper and lower dated layers came from the same occupation. For layers without a radiocarbon date and bounded by layers from two different occupations, it was not possible to linearly extrapolate between the two layers because the result might be a time period when it is known that the site was not occupied. In this case shells were physically examined for signs of weathering, which is common amongst shells from the earlier occupations. If shells were weathered they were assigned to the earlier occupation; if not they were assigned to the later occupation. Finally if there was reason to doubt the dating of a layer, that layer was excluded.

3. Results

3.1. Radiocarbon dating

The eight samples were radiocarbon dated at LLNL resulting in ^{13}C-corrected dates ranging from 1,930 to 6,145 CYBP (Table 5.2). All seventeen dates were calibrated with ages ranging from 1,245 to 7,050 ybp (Table 5.2). In the sampled sites, there is a gap in dates between 3,700- 6,000 ybp (Figure 5.8). As described in the Methods, these radiocarbon dates were used to classify *C. undatella* shells in 1,000 year bins and layers without radiocarbon dates were dated based on stratigraphy and shell condition (Table 5.1).

3.2. Layer dates

For CA-SDI-4614 unit 3, the following dating were based on radiocarbon dates from LLNL and Beta Analytic. Layer 0-10 was dated to 1,426 ybp at LLNL and binned into the 1,000 – 2,000 range. Layer 10-20 was dated to 3,101 ybp at LLNL and binned into the 3,000 - 4,000 range, as was layer 20-30, dated to 3,702 ybp from Beta Analytic. Layers 30-40, 40-50, and 50-60 where excluded due to a young date of 1,245 ybp from layer 50-60. Unit 5 was dated 1,731 and 2,677 ybp from layers 0-10 and 30-40, respectively. Layers 10-20 and 20-30 were dated based on assumed linear deposition and binned into the 2,000 - 3,000 age. Layers 40-50, 50-60, and 60-70 were excluded and a shell from layer 50-60 was dated at LLNL to 1,276 ybp. Unit 6 was dated with three radiocarbon dates from LLNL and one from Beta Analytic. Layers 0-10 and 10-20 were binned in the 2,000 - 3,000 range with dates from LLNL of 2,900 and 2,894 ybp, receptively. Layer 20-30 was also binned

in the 2,000 - 3,000 range given that both bounding layers where also in the 2,000 - 3,000 range. Layer 30-40 was dated by Beta Analytic to 1,923 ybp and binned in the 2,000 - 3,000 range. Layer 40-50 was also binned in the 2,000 - 3,000 range based on preservation quality of the shells. Layer 50-60 was dated to 6,330 ybp by LLNL and binned into the 6,000 - 7 000 age. In general the shells in this layer and 60-70 were weathered compared to shells in layers above. Layer 60-70 was also binned in the 6,000 - 7,000 range.

Site CA-SDI-10915 was dated with two dates from Beta Analytic and was a multiple occupation site. Layer 30-40 was dated to 2,068 ybp by Beta Analytic and binned into the 2,000 – 3,000 range. Layer 40-50 was not dated and excluded from analysis. Layer 60-70 contained weathered shells and was dated to 5,924 ybp by Beta Analytic and binned into the 6,000 - 7,000 range. Site CA-SDI-4619 layers 70-80 and 80-90 cm were binned in the 6,000 - 7,000 range based on a radiocarbon date from LLNL of 6,124 and shell preservation.

3.3. Harvested shell lengths

The average length of all 566 *C. undatella* was 33.3 mm (SD± 4.3) with a minimum of 16.8 mm and a maximum of 52.4 mm The average length *C. undatella* was not significantly different between the binned time periods (Table 5.3). The average age of harvested *C. undatella* for each binned time period ranged from 5.5 to 4.5 years old (Table 5.3). The time period with youngest harvested age (4.5 years) was 3,000-4,000 ybp and the next youngest average age (4.7 years) was 2,000 - 3,000 ybp. The oldest average age of 5.5 came from binned ages 1,000-2,000.

3.4. Age and growth

One hundred thirty eight *C. undatella* were digitally aged with the shell length at a given age calculated as the linear distance from the peak curvature of the umbo start of the winter growth ring. This measurement was designed to best emulate physical measurement using calipers (Figure 5.7). The extension from year x to year x+1 was calculated as the distance between the two growth increments. For all samples the average length at age1 was 22.5 mm (sd± 3.0, n = 138), age2 28.3 mm (sd± 3.0, n = 136), ages 31.2 mm (sd± 3.3, n = 124), age4 33.0 mm (sd± 3.7, n = 106), and age5 33.6 mm (sd± 3.9, n = 75) (Table 5.4). In general *C. undatella* grew rapidly during their first year of life then subsequently grew much more slowly and by the time they reach age 4+ years extension rates were between 2 and 1 mm per year. Because the growth rate of age 6+ individuals is small, all comparisons are for ages 1 through 5.

When comparing the growth rates and sizes of archaeological *C. undatella*, shells from 3,000 – 4,000 ybp tended to be roughly 2 mm larger than the entire population of sampled shells (Table 5.4). This increased size appeared to be from an larger average size at age1. The growth rates from age2 through age5 were roughly equal to that of the population. However, the difference in mean size at a given age or growth rate was not significantly different from the rest of the population. *C. undatella* shells aged 1,000 – 2,000 ybp were on average about 3 mm smaller than the entire population with a significant difference ($p < 0.05$) for ages one, two and three. However, the sample size for 1,000 – 2,000 ybp was rather small (n=6).

Average age at harvest for bins 2,000 - 3,000 and 6,000 - 7,000 was approximately equal across the entire population.

3.5. Comparison of within unit composition

The relative abundances of *Argopecten* and *Chione* and the size of *C. undatella* within in units 3, 5, and 6 were compared to see if the relative increase in *Chione* utilization is reflected in *C. undatella* size, age or growth rate. In all three units the divergence of *Chione* and *Argopecten* abundance was evident in layer 30-40 cm. In unit 3, the average size of harvested *C. undatella* remained relatively constant between 10-20 cm through 50-60 cm, with lengths between 35.6 and 33.2 mm, and layer 0-10 cm had the smallest average size of 31.8 mm (Figure 5.9). Average size at year one was also similar between layers 10-20cm through 50-60cm with layer 0-10cm having a smaller average size at age one. The age of harvested *C. undatella* did not follow a clear pattern, with layer 20-30 cm having the youngest average age of harvested clams. For unit 3, the relative abundance of *Chione* and *Argopecten* began to diverge at layer 30-40 cm and was widely separated from layer 0-10 cm through 20-30 cm.

The relative abundance of *Argopecten* declined in unit 5 from its peak abundance in layer 50-60 cm to the surface and *Chione* steadily increased from layer 30-40 cm to surface (Figure 5.10). The average age at harvest was varied from 4.2 to 6 years and was highest in layer 0-10 cm and lowest in layer 30-40 cm. Average size at harvest and the average size of one year olds followed a similar

pattern with higher values at layers 10-20, 20-30, and 40-50 cm and lower values at layer 30-40 and 60-70 cm.

For unit 6, the relative abundance of *Chione* and *Argopecten* diverged at layer 30-40 cm with high abundances of *Chione* and low abundance of *Argopecten* (Figure 5.11). The average size of harvested *Chione* remained between 33.3 and 36.0 mm with no clear trend in size. The average age of harvested *Chione* varied from 3.7 to 6 years old with highest age from layer 0-10 cm and the youngest from layer 20-30cm.

5. Discussion

5.1. Radiocarbon dates

Radiocarbon dating clearly showed two distinct occupations of these sites, one from 1245 to 3702 ybp, and the other from 5924 to 6996 ybp (Figure 5.8). This finding is consistent with other dates from Southern San Diego lagoons, which typically have a minimum of dated coastal archaeological sites around 3,500 ybp. However, this study was not an extensive survey of Los Peńasquitos Lagoon archeological sites and should not be used exclusively to date when the lagoon was occupied. Units 3, 5, and 6 all had one shell with younger date at 50-60 cm or 30-40 cm (Table 5.2). The most likely explanation of this is the younger shells were moved by burrowing gophers (Erlandson 1984).

5.2. Comparison of within unit composition

Chione and *Argopecten* diverged around 30-40cm in all units, indicating that all units share a common stratigraphy. Congruent with the observed decline of

Argopecten in Batiguitos Lagoon and San Diego Bay, the decline of *Argopecten* in Los Peñasquitos Lagoon also started around 4,000 ybp. Despite what appears to be a strong evidence for a San Diego County wide pattern of inverse productivity between *Argopecten* and *Chione* at 4,000 ybp there is no detectable difference in *C. undatella* growth rate, age, or size at harvest. The stable size at harvest for *C. undatella* is consistent with *C. undatella* never being over harvested, or at least having been harvested in proportion to their abundance. If this is correct, then increases in *C. undatella* abundance would be indicative of increases in recruitment. If so then the factors which increased recruitment (e.g. an increase in habitat or recruitment) were not detectable as a change in growth rates. If the increase in *C. undatella* was due to increased habitat, it would be expected that there would also be increase in favorable habitat for *Argopecten*, given the overlap in habitat between the two species. Or an alternative hypothesis is that each 10cm thick layer averages shells which accumulated over a few centuries. During these centuries, a lot of climate variations could occur which could smooth out temporal trends between layers.

5.3. Shell patterns through time

C. undatella harvested from Los Peñasquitos Lagoon between 1,200 and 6,000 ybp did not have statistically significant differences in growth rate, age at harvest, or size at harvest. Despite two occupations separated by two thousand years and intense resource utilization between 2,000 and 3,000 ybp, no changes were

observed in the size of *C. undatella* harvested. Nor is there any relationship between the relative abundance of *C. undatella* and the size or age of harvested *C. undatella*.

One of the principle questions in archaeology is the attribution of changes seen in faunal remains to environmental impacts or changes in cultural practices. In Southern California the primary environmental hypothesis explaining a shift from *Argopecten* to *Chione* states that increased lagoon siltation would have favored *Chione* and reduced *Argopecten* abundance (Warren 1964). However, Bull (1981) suggested that the reduction of *Argopecten* and increase in *Chione* is due to the westward expansion of the Uto-Aztecan and Yuman language families bringing with them a preference for acorn harvesting over shellfish gathering. Of these two hypotheses only changing ecological conditions is directly testable. Changes in harvested size and growth rate can be used to determine the relative contribution of overharvest and environmental change on prehistoric ecosystems.

Gallegos (1987) also noted a shift from use of *Argopecten* to *Chione* in archaeological sites around Batiguitos Lagoon (17 km north of Los Peńasquitos). Gallegos posed the hypothesis that *Argopecten* decline around 4,000 was directly linked to siltation and environmental decline, with the stated mechanism for declining *Argopecten* and increasing *Chione* is that *Argopecten* require a well-flushed lagoon whereas *Chione* are better adapted to mud and sand flats. However, a similar pattern and timing of *Argopecten* decline and increasing *Chione* is seen in San Diego Bay, which is not believed to have closed or have been impounded to the degree that smaller lagoons, such as Batiquitos would have been (Pignolo 2005). Given the similar pattern of decreasing *Argopecten* and increasing *Chione* in two

systems with a different history of closure and silation, other mechanisms should be evaluated for the decline in *Argopecten* and increase in *Chione.*

Additionally, simply looking at the relative proportion of *Chione* and *Argopecten* and attributing changes to siltation is overly simplistic because there are three commonly encountered species of *Chione* (*C. undatella*, *C. californiensis*, and *C. fluctifraga*), each with a different habitat requirement. *C. undatella* is primarily found near the mouth of bays, in well-flushed sandy areas, or near and in eelgrass beds. *C. fluctifraga* is most often found in the back-bay areas such as mud and sand flats. *C. californiensis* occupies an intermediate niche and is found in small numbers in both habitats. Therefore, a better faunal proxy for siltation and closures of lagoon would be an increase in *C. fluctifraga* relative to total *Chione*. However, this might only detect changes in lagoon sediment type and relative flushing rather than siltation rate. Peterson (1985) found that *C. undatella* suffered high mortality after major siltation events because they have short siphons and are not very mobile. The ability of the *C. calforniensis* or *C. fluctifraga* to survive heavy sedimentation has not been evaluated, but given the similarly sized siphons and poor mobility, it is reasonable to assume they would also suffer high mortality from heavy sedimentation. Given that *C. undatella* is often the most common *Chione* found in archaeological sites and that there is a large overlap in the habitat of *C. undatella* and *Argopecten* habitat, it is questionable if the relative abundance of *C. undatella* and *Argopecten* can be used as a proxy for changes in habitat.

Another hypothesis that could explain the reduction in *Argopecten* is the episodic nature of *Aropecten* recruitment, perhaps related to temperature.

Argopecten densities are highly variable, with densities from 140 - 600 scallops/m^2 to 19 scallops/m^2 from any year to the next (Dyke 1987). Dyke (1987) suggests the high density population was due an abnormally high recruitment resulting from warmer conditions.

The reduction in *Argopecten* and increase in *Chione* seen in San Diego County archaeological sites occurred around 4,000 ybp in most bays and lagoons. The 4,000 ybp reversal also coincides with a transition from a warm period to a cool period, based on oxygen isotopes and foraminifera species assemblages in Santa Barbara Basin cores (Kennett et al. 2007). While this study is not able to mechanistically link colder temperatures in the Santa Barbara Basin to reduced *Argopecten* recruitment in San Diego County bays and lagoons, these data present an interesting relationship. While not quantitative, years 2010 and 2011 were both relativity cool years and trawl surveys from Mission bay have noted a decline in *Argopecten* in Mission Bay (P. Zerofski, pers. comm.) Additionally, in spring 2012 large numbers of newly recruited *Chione* have been noted in certain areas of Mission Bay. It is clear that the inverse relationship between *Argopecten-Chione* abundance is complex. To understand it, the habitat requirements of *Argopecten* and *C. undatella*, *C. californiensis*, and *C. fluctifraga* need to be better quantified. Additionally, the relationship between oceanographic conditions and population growth for these species needs to be understood. Finally, *Chione* needs to be identified to the species level in archaeological studies.

Table 5.1: Table of sites, units, layers, and *C. undatella* with median calibrated ^{14}C date and binned age. "Whole shells measured" refers to the number of whole shells measured using fixed calipers. Growth increment analysis refers to the number of shells thin sectioned and aged. Median calibrated radiocarbon date and binned age calculated as stated in methods.

Site number	Unit	Layer	Whole shells measured	Growth increment analysis	Median calibrated radiocarbon date	Binned age
CA-SDI-4614	Unit 6	0-10	7	4	2900	2000-3000
CA-SDI-4614	Unit 6	10-20	15	9	2894	2000-3000
CA-SDI-4614	Unit 6	20-30	38	10		2000-3000
CA-SDI-4614	Unit 6	30-40	33	10	1923	2000-3000
CA-SDI-4614	Unit 6	40-50	15	7		2000-3000
CA-SDI-4614	Unit 6	50-60	6	4	6330	6000-7000
CA-SDI-4614	Unit 6	60-70	1	1		6000-7000
CA-SDI-4614	Unit 5	0-10	2	2	1731	1000-2000
CA-SDI-4614	Unit 5	10-20	37	8		2000-3000
CA-SDI-4614	Unit 5	20-30	23	8		2000-3000
CA-SDI-4614	Unit 5	30-40	15	5	2677	2000-3000

Table 5.1: Table of sites, continued

Site number	Unit	Layer	Whole shells measured	Growth increment analysis	Median calibrated radiocarbon date	Binned age
CA-SDI-4614	Unit 5	40-50	14	8		excluded
CA-SDI-4614	Unit 5	50-60	7	4	1276	excluded
CA-SDI-4614	Unit 5	60-70	3	2		excluded
CA-SDI-4614	Unit 3	0-10	3	3	1426	1000-2000
CA-SDI-4614	Unit 3	10-20	9	6	3101	3000-4000
CA-SDI-4614	Unit 3	20-30	15	6	3702	3000-4000
CA-SDI-4614	Unit 3	30-40	13	6		excluded
CA-SDI-4614	Unit 3	40-50	8	6		excluded
CA-SDI-4614	Unit 3	50-60	5	5	1245	excluded
CA-SDI-10915	TU-2	30-40	179	10	2068	2000-3000
CA-SDI-10915	TU-2	40-50	71	4		excluded
CA-SDI-10915	TU-2	60-70	12	6	5924	6000-7000
CA-SDI-4619	TU-3	70-80	9	5	6124	6000-7000
CA-SDI-4619	TU-3	80-90	6	3		6000-7000

Table 5.2: Radiocarbon dates included in this study, samples starting with LLNL were analyzed at Center for Accelerator Mass Spectrometry at the Lawrence Livermore National Laboratory and samples starting Beta were analyzed at Beta Analytic. Dates listed under the ^{14}C age are not ^{13}C corrected and italicized dates were ^{13}C corrected using a 430 year correction.

Site	Unit	Level (cm)	Lab Number	^{14}C age (years BP)	± 1σ	Calibrated ages	
						2σ ranges	median
SDI-4614	3	0-10	LLNL-156521	2110	30	1259- 1618	1426
SDI-4614	3	10-20	LLNL-156522	3505	30	2869- 3323	3101
SDI-4614	3	20-30	Beta-32368	4000	60	3443- 3959	3702
SDI-4614	3	50-60	LLNL-156523	1930	30	1047- 1415	1245
SDI-4614	5	0-10	Beta-32369	2380	70	1477- 1989	1731
SDI-4614	5	30-40	Beta-32370	3160	80	2352- 2932	2677
SDI-4614	5	50-60	LLNL-156520	1960	30	1087- 1470	1276
SDI-4614	6	0-10	LLNL-156517	3345	30	2722- 3131	2900
SDI-4614	6	10-20	LLNL-156518	3340	30	2719- 3125	2894
SDI-4614	6	30-40	Beta-32371	2540	60	1669- 2184	1923
SDI-4614	6	50-60	LLNL-156519	6145	30	6160- 6532	6330
SDI-10915	TU-2	10-20	Beta-31560	*2940*	70	2153- 2698	2429
SDI-10915	TU-2	30-40	Beta-31561	*2660*	80	1805- 2330	2068
SDI-10915	TU-2	60-70	Beta-31562	*5770*	80	5656- 6182	5924
SDI-4619	TU-3	40-50	Beta-31558	*6780*	90	6774- 7295	7050
SDI-4619	TU-3	70-80	LLNL-156524	5955	30	5923- 6288	6124
SDI-4619	TU-3	90-100	Beta-31559	*6730*	100	6725- 7247	6996

Table 5.3: Average age from thin sectioned and aged *C. undatella* and average length as measured with calipers for the entire study populations.

	1000-2000	2000-3000	3000-4000	6000-7000
Average age	5.50	4.68	4.50	5.11
±	1.87	1.82	2.17	1.70
n	6	69	10	19
p	0.33	0.40	0.60	0.41
Average length	34.1	33.1	35.1	34.0
±	4.7	4.2	3.7	4.8
n	6	362	24	54

Table 5.4: Table of samples imaged aged and measured, data displayed for years 1-5. Delta values are the amount of growth for that year, for example age3 delta is the amount of growth between age2 and age3.

		1000-2000 ybp		2000-3000 ybp	
		length	delta	length	delta
age 1	mean	19.04	19.04	22.57	22.57
	stdev	2.73	2.73	3.01	3.01
	n	6	6	69	69
	p	0.004	0.004	0.900	0.900
age 2	mean	25.04	7.48	28.70	7.62
	stdev	1.90	3.43	3.14	2.76
	n	6	6	68	68
	p	0.003	0.918	0.757	0.927
age 3	mean	28.58	4.55	31.66	4.11
	stdev	2.55	2.00	3.64	2.12
	n	6	6	61	61
	p	0.026	0.515	0.758	0.644
age 4	mean	30.48	3.08	33.57	2.56
	stdev	2.53	0.48	4.15	1.29
	n	5	5	52	52
	p	0.064	0.408	0.922	0.487
age 5	mean	31.22	1.68	33.90	1.83
	stdev	3.25	0.69	4.47	0.73
	n	4	4	36	36
	p	0.156	0.523	0.675	0.132

Table 5.4: Table of samples imaged aged and measured, continued.

		3000-4000 ybp		6000-7000 ybp		All	
		length	delta	length	delta	length	delta
age 1	mean	24.02	24.02	22.78	22.78	22.51	22.51
	stdev	2.85	2.85	3.31	3.31	3.02	3.02
	n	10	10	19	19	138	138
	p	0.121	0.121	0.724	0.724		
age 2	mean	30.17	7.85	28.70	7.44	28.28	7.29
	stdev	2.53	3.18	2.87	3.13	3.00	2.84
	n	10	10	19	19	136	136
	p	0.099	0.775	0.908	0.789		
age 3	mean	32.72	3.47	31.73	3.92	31.15	3.94
	stdev	2.89	0.95	2.77	1.76	3.34	1.90
	n	9	9	18	18	124	124
	p	0.295	0.361	0.833	0.778		
age 4	mean	34.60	2.53	34.03	2.75	32.96	2.46
	stdev	4.49	0.97	2.42	1.39	3.73	1.20
	n	5	5	17	17	106	106
	p	0.523	0.844	0.551	0.668		
age 5	mean	35.24	1.80	35.25	2.59	33.60	1.93
	stdev	5.13	0.53	2.54	1.45	3.93	0.91
	n	4	4	11	11	75	75
	p	0.563	0.709	0.298	0.012		

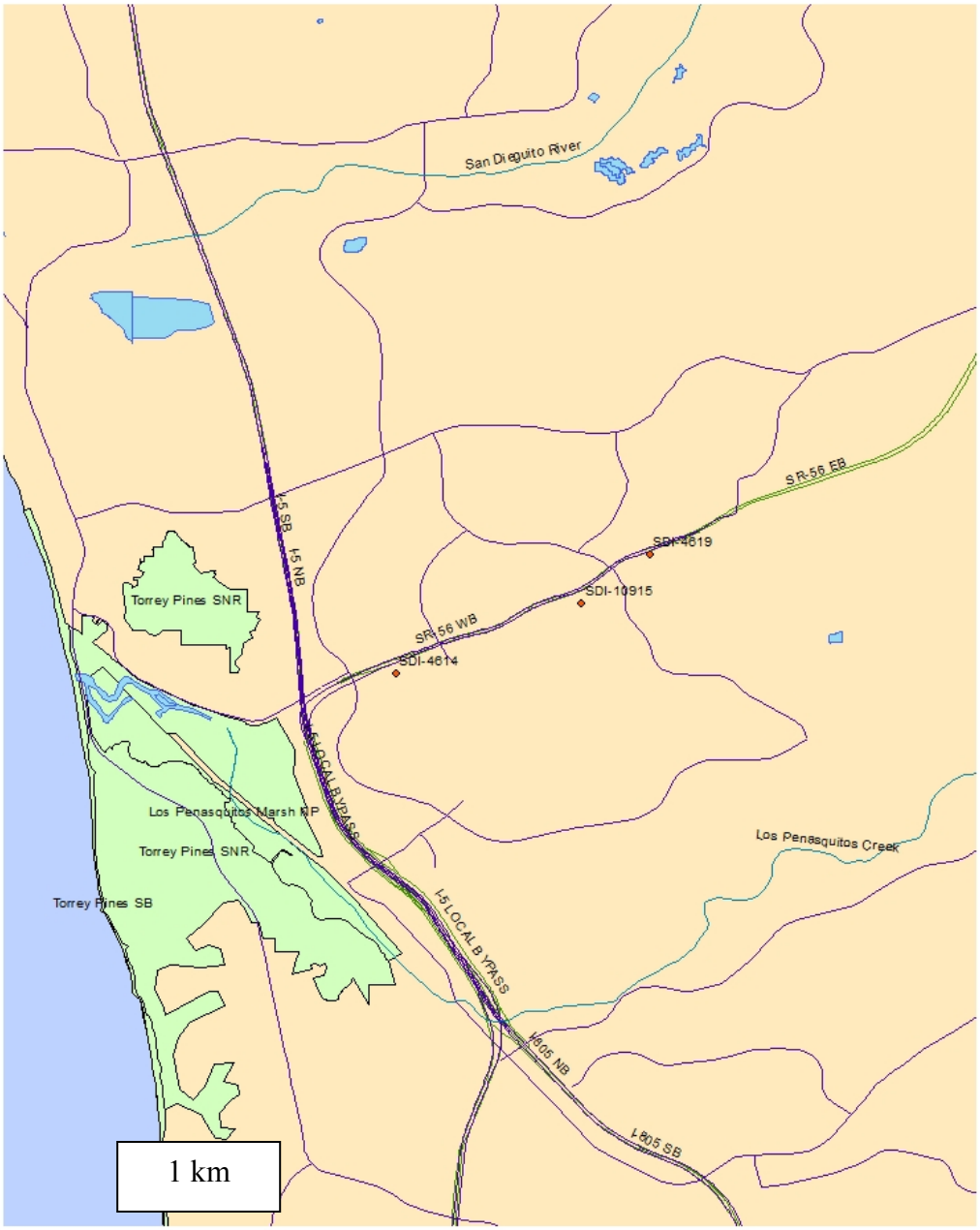

Figure 5.1: Location of study site with archaeological sites listed and scale listed.

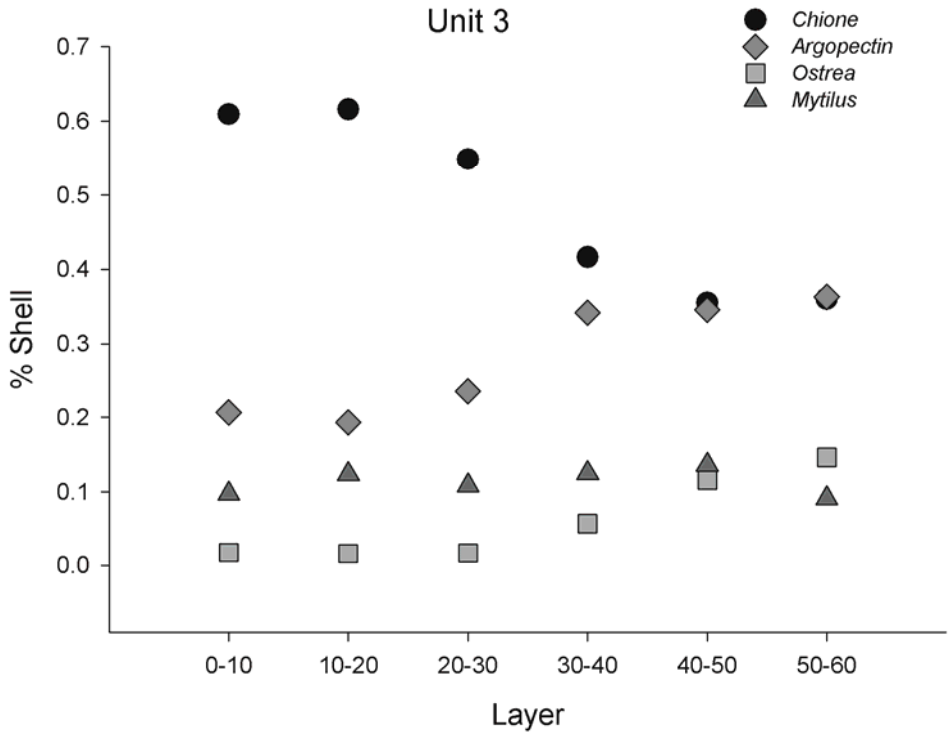

Figure 5.2: Percent shell of the four major faunal remains from unit 3.

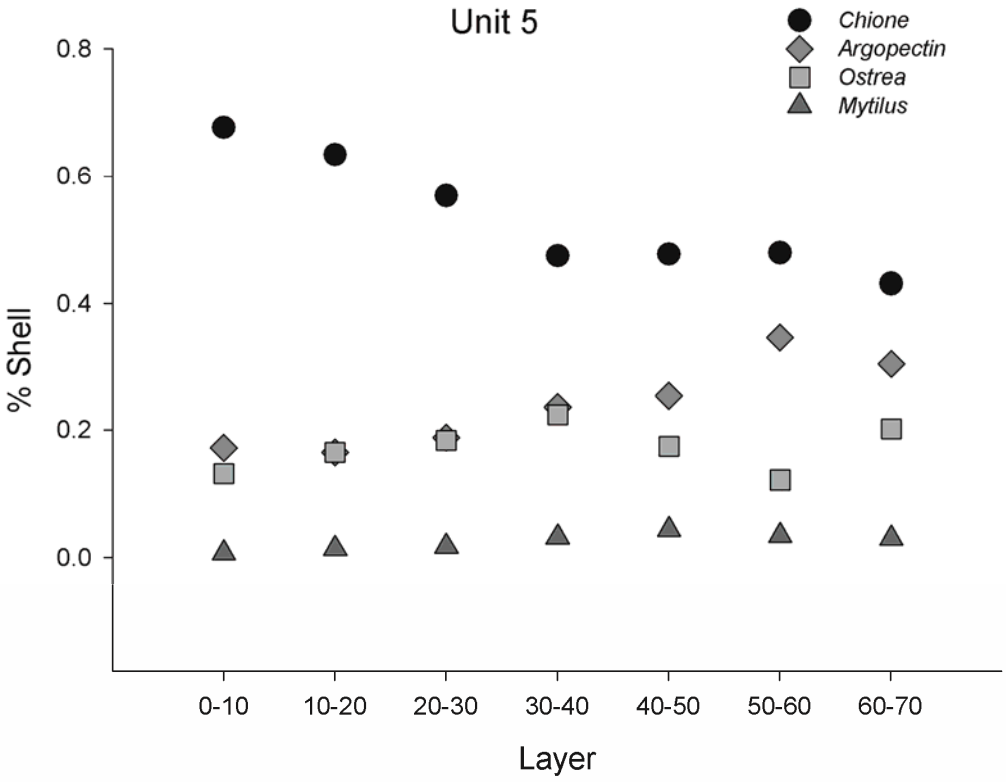

Figure 5.3: Percent shell of the four major faunal remains from unit 5.

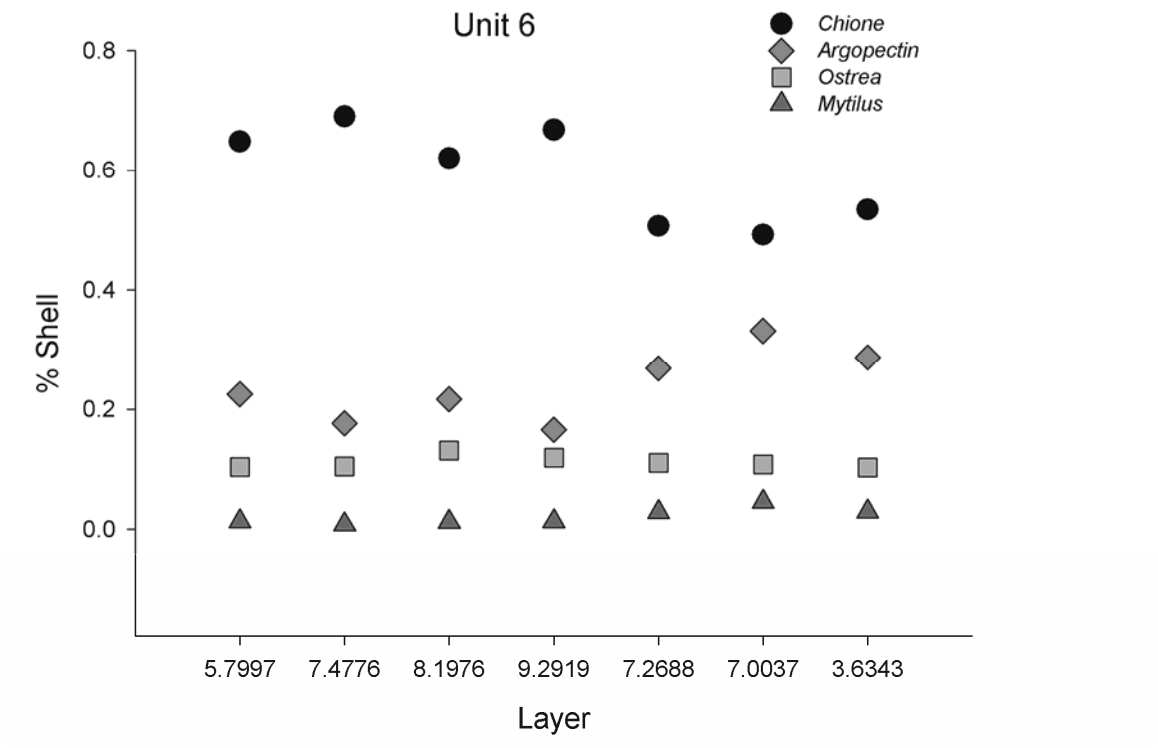

Figure 5.4: Percent shell of the four major faunal remains from unit 6.

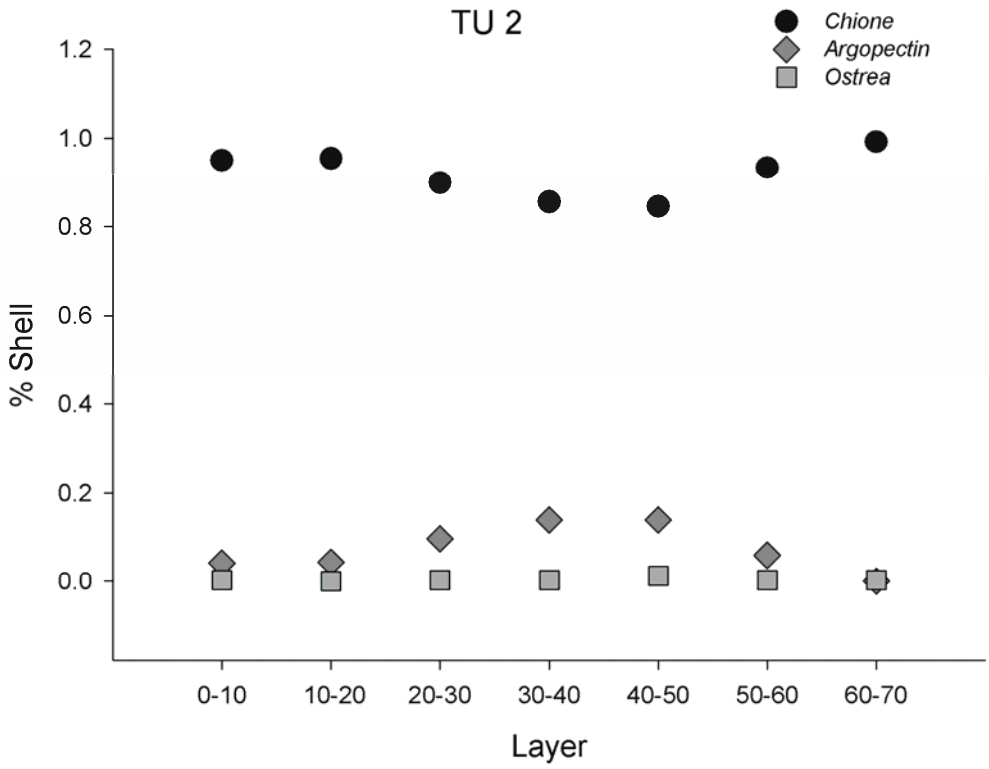

Figure 5.5: Percent shell of the four major faunal remains from TU 2.

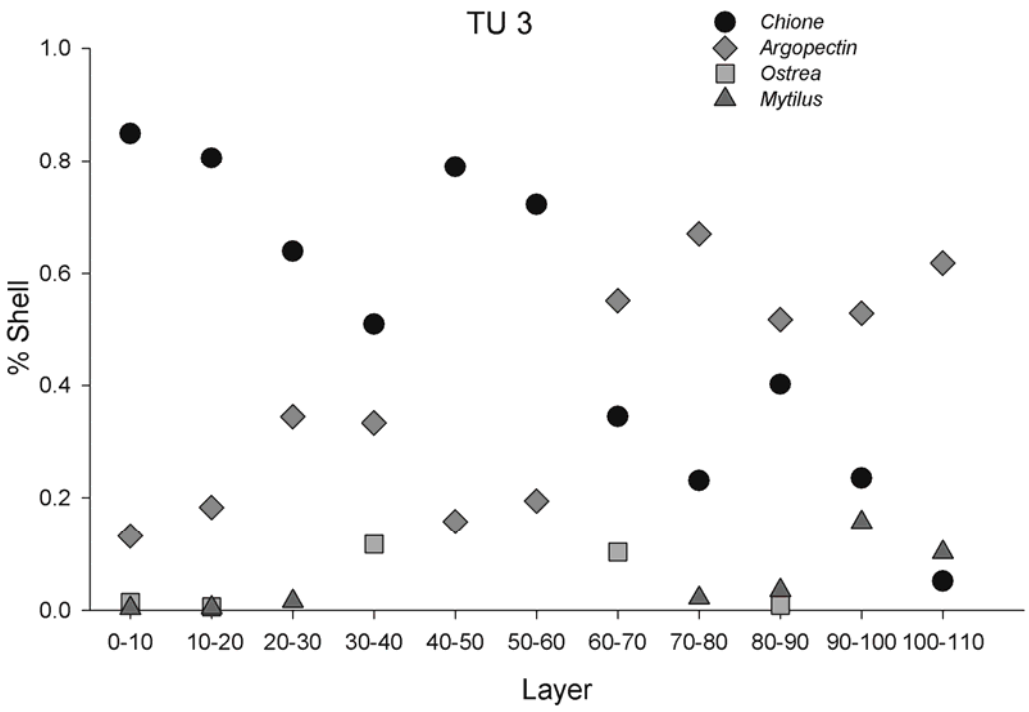

Figure 5.6: Percent shell of the four major faunal remains from TU 3.

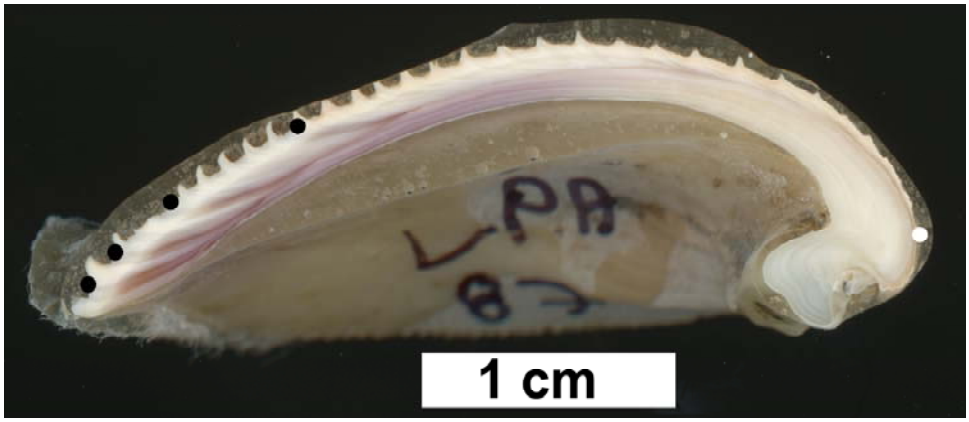

Figure 5.7: Example of scanned shell marked for age analysis. The white dot near the umbo was chosen to best replicate where calipers would have measured the shell from. The black dot are placed at each annul growth increment. Distance at age x was calculated as the linear distance between the white dot and corresponding black dot. Growth between age x and age x+1 was calculated as the distance between the corresponding black dots.

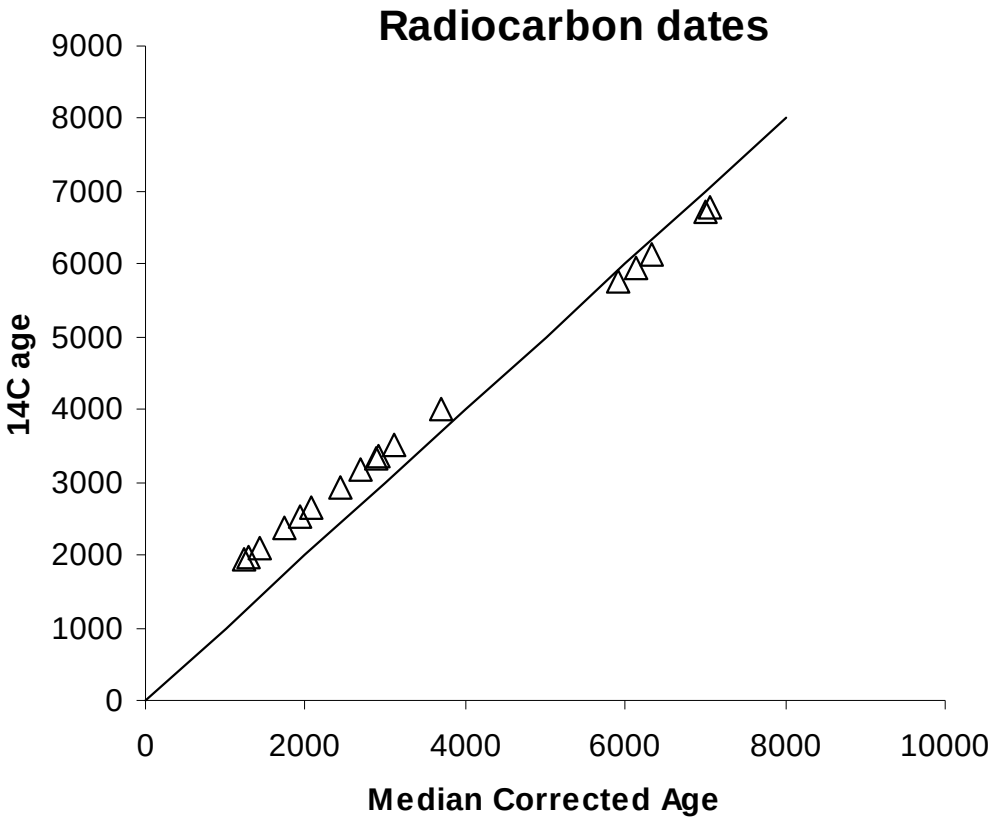

Figure 5.8: Uncorrected radiocarbon age compared to median corrected age as determined by CALIB v6.1 using the parameters described in the methods.

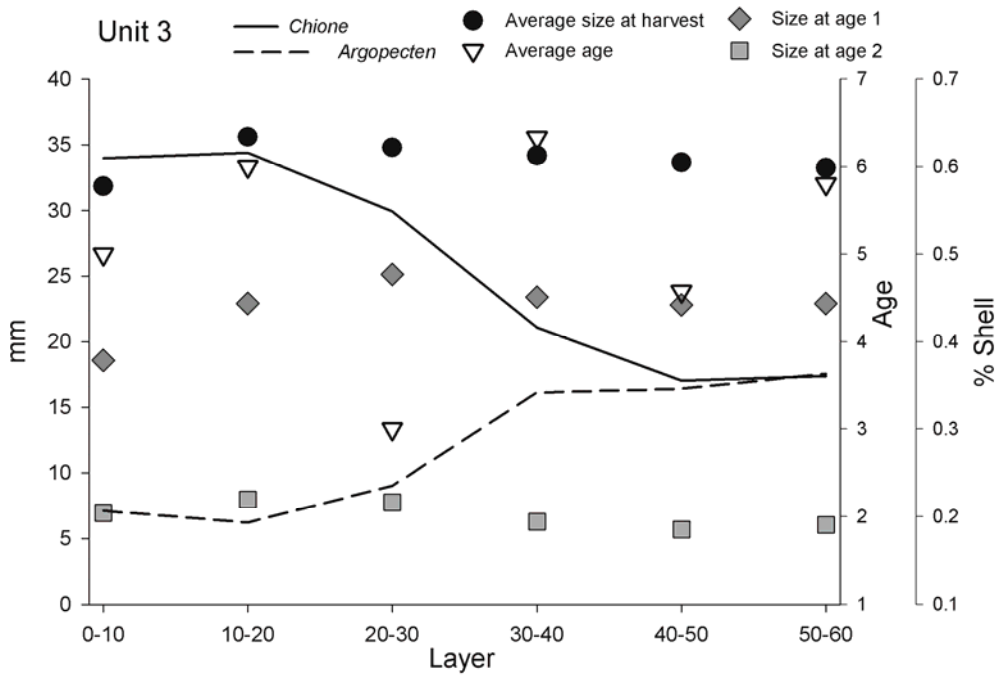

Figure 5.9: Percent *Chione* and *Argopecten* shell compared with the average age, growth rate for years one and two and average size at harvest for *C. undatella.*

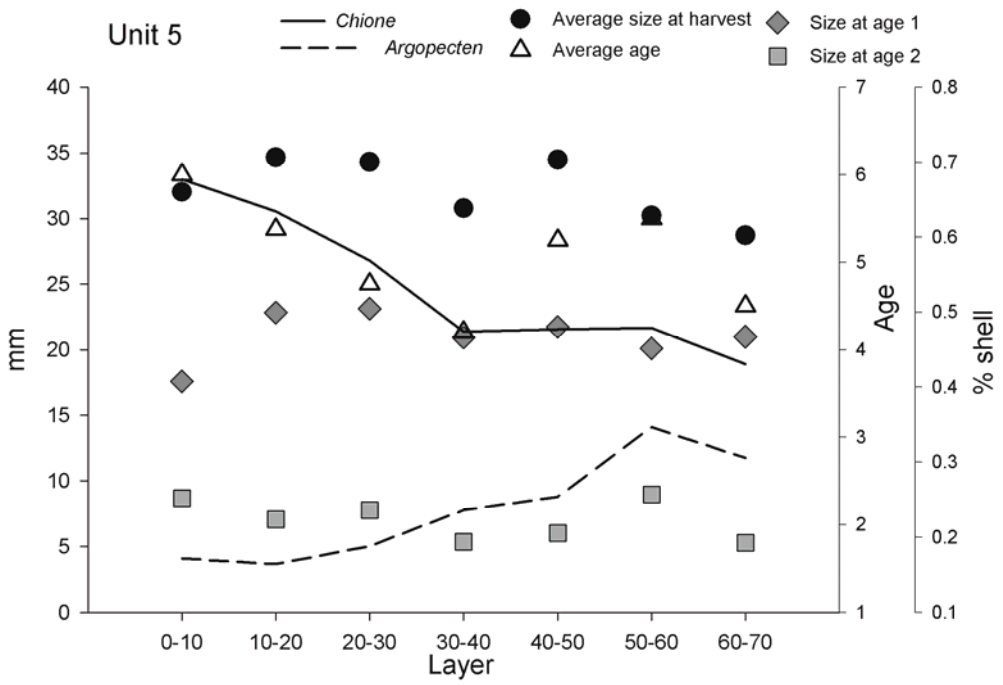

Figure 5.10: Percent *Chione* and *Argopecten* shell compared with the average age, growth rate for years one and two and average size at harvest for *C. undatella.*

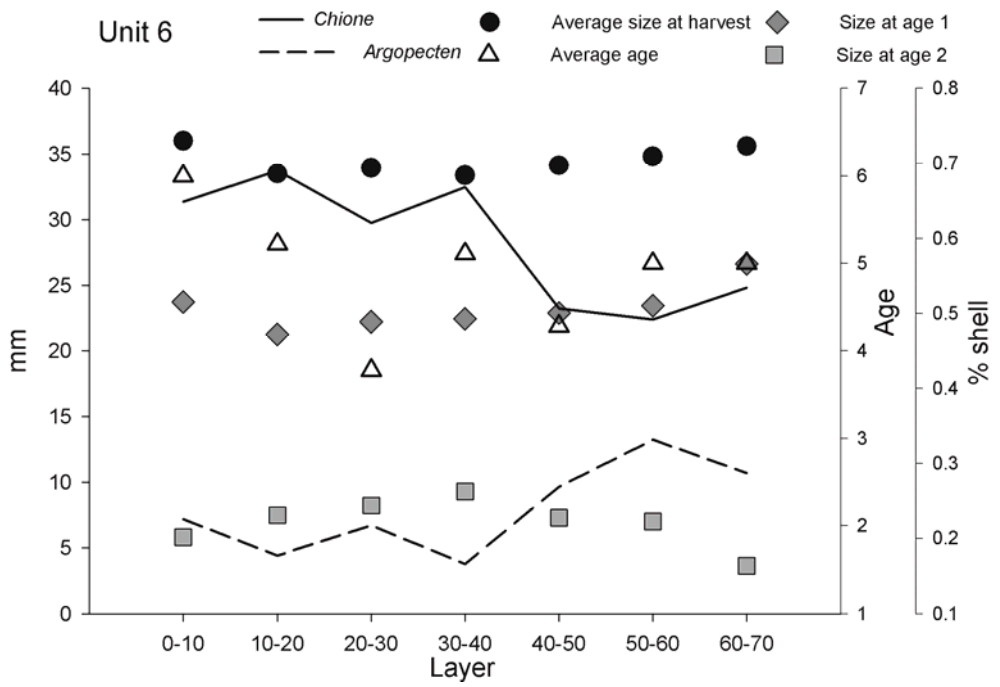

Figure 5.11: Percent *Chione* and *Argopecten* shell compared with the average age, growth rate for years one and two and average size at harvest for *C. undatella.*

References

Breschini, G., Haverstat, T., Erlandson, J. 1996. *California radiocarbon dates.* 8th edition. Salinas: Coyote Press.

Bull, C.S. 1981. Another look at on old lagoon. In *Geologic investigations of the coastal plan*, edited by P.L. Abbott and S. O'Dunn, 25-32. San Diego Association of Geologists.

Culleton, B J. 2006. Intrashell radiocarbon variability in marine mollusks. Radiocarbon, 48(3), 387-400.

Dyke, K.Y. 1987. Population dynamics and the effects of density on growth of the scallop, *Argopecten circularis*. (Master's thesis) San Diego State University, San Diego, CA.

Gallegos, D. 1987 A Review and Synthesis of Environmental and Cultural Material for the Batiquitos Lagoon Region. In San Dieguito - La Jolla: Chronology and Controversy, edited by Dennis Gallegos, pp. 23-34.

Gallegos, D., 2002. Southern California in Transition: Late Holocene Occupation of Southern San Diego County. In: Erlandson, J.M., Jones, T.J. (Eds.), Catalysts to Complexity: Late Holocene Socities of the California Coast. Institute of Archaeology, University of California Los Angeles, pp. 27 – 39.

Erlandson, J.M., 1988. Cultural evolution and paleogeography on the Santa Barbara coast: a 9600-year 14C record from southern California. Radiocarbon 30 (1), 25–39.

Erlandson J.M. 1984. A Case Study in Faunalturbation: Delineating the Effects of the Burrowing Pocket Gopher on the Distribution of Archaeological Materials. American Antiquity 49:785-790

Haderlie E.C., Abbott D.P. 1980. Bivalvia: The clams and allies. In: Morris RH, Abbott DP, Haderlie EC (eds) Intertidal Invertebrates of California. Stanford University Press, Stanford, California, pp 355-411

Inman D.L., Jenkins S.A. 1999. Climate Change and the Episodicity of Sediment Flux of Small California Rivers. The Journal of geology 107:251-270

Kennett D.J., Kennett J.P., Erlandson J.M., Cannariato KG 2007. Human responses to Middle Holocene climate change on California's Channel Islands. Quaternary Science Reviews 26:351-367

Masters P.M. .2006. Holocene sand beaches of southern California: ENSO forcing and coastal processes on millennial scales. Palaeogeography, Palaeoclimatology, and Palaeoecology 232:73-95

Masters, P.M., Gallegos, D., 1997. Environmental change and coastal adaptations in San Diego County during the Middle Holocene. In: Erlandson, J.M., Glassow, M.A. (Eds.), Archaeology of the California Coast During the Middle Holocene. Institute of Archaeology, University of California Los Angeles,pp. 11 – 21.

Miller J.N. 1966. The Present and the Pat Molluscan Faunas and Environments of Four Southern California Coastal Lagoons. In: Scripps Institution of Oceanography. University of California San Diego, La Jolla, p 257

Pigniolo, A.R. 2005. Subsistence, Settlement, and Environmental Change at San Diego Bay. Proceedings of the Society for California Archaeology 18:255-259.

Rasband W.S. 1997-2011 ImageJ. In. U. S. National Institutes of Health, Bethesda, Maryland, USA

Reimer PJ, Baillie MGL, Bard E, Bayliss A, Beck JW, Blackwell PG, Bronk Ramsey C, Buck CE, Burr GS, Edwards RL, Friedrich M, Grootes PM, Guilderson TP, Hajdas I, Heaton TJ, Hogg AG, Hughen KA, Kaiser KF, Kromer B, McCormac FG, Manning SW, Reimer RW, Richards DA, Southon JR, Talamo S, Turney CSM, van der Plicht J, Weyhenmeyer CE. 2009. IntCal09 and Marine09 radiocarbon age calibration curves, 0–50,000 years cal BP. Radiocarbon 51(4):1111–50.

Stuiver, M., Polach, H.A., 1977. Discussion: Reporting of 14-C data. Radiocarbon 19 (3), 355– 363.

Stuiver, M., Reimer, P. J., Reimer, R. W. 2009. CALIB v6.1. http://calib.qub.ac.uk/

True, D.L. 1990. Site Location and water supply: A perspective from northern San Diego County, California. Journal of New World Archaeology 7(4):37-60.

Vischer N. 2011. ObjectJ. In. University of Amsterdam

Warren, C. N. 1964. Culture Change and Continuity on the San Diego Coast. Unpublished Ph.D. dissertation, Department of Anthropology, University of California, Los Angeles.

Chapter 5, in part, is currently being prepared for submission for publication of the material. Hatch, Marco B.A. The dissertation author was the primary investigator and author of this paper.